Alma Mater Studiorum – Università di Bologna

DOTTORATO DI RICERCA IN

Scienze Veterinarie

Ciclo XXIX

Settore Concorsuale di afferenza: 07/H5

Settore Scientifico disciplinare: VET/10 – Clinica ostetrica e ginecologia veterinaria

TITOLO TESI

MODELLING LEIGH SYNDROME IN PIGS.

Presentata da: **Dott.ssa Corinne QUADALTI**

Coordinatore Dottorato **Relatore**

Prof. Arcangelo GENTILE **Prof. Cesare GALLI**

Esame finale anno 2017

TABLE OF CONTENTS

Acknowledgements

L’attività di ricerca presentata in questa tesi è stata svolta presso AVANTEA srl (Cremona), presso la quale sono stata ospite per la maggior parte del dottorato, ed è stata finanziata dal progetto ERC del Prof. Massimo Zeviani e di AVANTEA, MitCare FP7 322424 (Mitochondrial Medicine: developing treatments of OXPHOS-defects in recombinant mammalian models - MitCare FP7 322424).

Il periodo all’estero, svolto presso i laboratori della Mitochondrial Biology Unit dell’MRC (Cambridge), sotto la supervisione del Prof. Massimo Zeviani, è stato finanziato in parte da una borsa Marco Polo (Gennaio – Aprile 2016) e in parte da una Short Term Scientific Mission STSM finanziata da COST Action BM1308, Biomedicine And Molecular Biosciences, Sharing Advances on Large Animal Models - SALAAM (Maggio – Giugno 2016). I miei più sentiti ringraziamenti vanno al Prof. Zeviani per avermi gentilmente accolta ed ospitata presso i suoi laboratori. Grazie anche al Dott. Carlo Viscomi per avermi supportata nell’organizzazione burocratica del mio periodo all’estero.

Un ringraziamento va anche alla Dr. Valeria Tiranti e al suo team (BESTA, Milano) e al Prof. Davide Zani (Università degli studi di Milano) per aver collaborato alla realizzazione del progetto.

Un grazie immenso va al mio tutor, Prof. Cesare Galli, e alla Dr. Giovanna Lazzari, per aver avuto fiducia in me nell’affidarmi questo progetto di ricerca e per l’immancabile sostegno nel corso del suo svolgimento.

Grazie ad Andrea, Irina e al Prof. Franco Lucchini, per avermi insegnato a muovermi nel mondo della ricerca con grande pazienza e passione, tante risposte sempre soddisfacenti e altrettante domande fondamentali alla riflessione.

Grazie a Roberto per il supporto tecnico, morale e notturno nel management dei miei bellissimi maialini.

Grazie ad Elisa, Silvia, Gabriella, Paola e Gaia per l'instancabile lavoro di team, i sorrisi di conforto, le pause tè e le indispensabili torte del Lunedì.

E ora, i miei ringraziamenti si rivolgono ai colleghi oltre manica. Grazie a Dario, per aver fornito un fondamentale contributo al progetto disegnando il vettore di targeting, svolgendo le trasfezioni con CRISPR/Cas9 e contribuendo in modo essenziale alla caratterizzazione del modello, fornendo le relative immagini necessarie alla stesura di questa tesi. E grazie per avermi seguita con pazienza e sempre il buon umore nel mio periodo a Cambridge, mostrando tutto il buon cuore che sotto sotto anche un ottimo scienziato può conservare.

La caratterizzazione istologica e immunoistochimica di tessuti muscolari e intestinali è stata svolta dal Dr. Raffaele Cerutti presso l'MRC di Cambridge, che ha gentilmente fornito le immagini relative presenti in questa tesi. Grazie Raffaele, per avermi introdotto nell'ignoto mondo dell'istologia con attenzione e inquantificabile sapienza ed essere stato un esempio da seguire per l'insaziabile sete di conoscenza per la scienza a 360 gradi. Grazie poi per essermi stato vicino ed avermi supportata nei momenti di sconforto, rivelandoti un prezioso ed inaspettato amico.

Many thanks to Manu, Erika, Gabriele, Sara, Anil and to all the Mitochondrial Biology Unit of the MRC (MRC Mitochondrial Biology Unit, Wellcome Trust / MRC Building, Cambridge Biomedical Campus) for their kind support during my stay.

La caratterizzazione neurologica del modello presentato in questa tesi è stata svolta presso l'IZSTO dal gruppo della Prof. Casalone (Istituto Zooprofilattico Sperimentale del Piemonte, Liguria e Valle d'Aosta, Via Bologna 148, 10154 Torino). In particolare, ringrazio di cuore il Dr. Corona e la Dr.ssa Crociara per aver partecipato con passione agli interminabili

brainstorming che si sono resi necessari, fornendo risultati ed immagini fondamentali per la comprensione del modello.

Niente di tutto ciò sarebbe mai stato possibile senza il sostegno e l'affetto della mia famiglia, che sono qui a ringraziare con tutto il cuore per avermi cresciuta fin da piccola come una mini scienziata senza mai mettere in dubbio l'importanza delle mie passioni e appoggiando ogni mia decisione. E' merito vostro, Mamma, Papà e Nonna, se oggi posso scrivere questa tesi e lo sarà quando Domani potrò continuare a seguire il mio lavoro e la mia passione.

Un ringraziamento speciale va a Luca, da sempre compagno di anima, confessore e spalla.

Grazie a Francesco, mio unico ed insostituibile amico cremonese, compagno di lunghe passeggiate riflessive e solitarie serate da fuorisede.

Grazie ad Anna, per le chiacchiere tra donne e i pomeriggi in piscina.

Grazie a Federico, per esserci stato un po' sì, un po' no e un po' forse, contribuendo in maniera essenziale a rendermi forte ed indipendente, ma consapevole dei miei limiti.

“Stick to a task, 'til it sticks to you.

Beginners are many, finishers are few."

Marjorie Pay Hinckley, Small and Simple Things

Abstract

The terms “neurodegenerative diseases” (NDs) denote a range of conditions affecting primarily the central nervous system (CNS) with a deterioration of specific neuronal populations, consequently determining the clinical phenotype typical of each disease (usually a mixture of motor and cognitive defects). Neurodegenerative diseases, most common are Parkinson’s and Alzheimer’s disease and Multiple Sclerosis, are an increasing phenomenon and affect a relevant number of people in different age ranges. Nevertheless, NDs consist of a heterogeneous group of differentially prevalent pathologies, including rare diseases as Huntington’s disease and Amyotrophic Lateral Sclerosis, and the vast majority of mitochondrial-related NDs (e.g. Leigh Syndrome). However, all NDs cause a reduction of life quality and expectancy in the patients, therefore representing a heavy burden for family members and a financial load on the healthcare system. Currently, efficient therapies are lacking for the vast majority of NDs.

A chance to deepen scientific and medical knowledge of NDs is to generate genetically modified animal models in order to study pathogenesis, prognosis, diagnosis, treatment and possibly prevention (Holm *et al.*, 2016). In this thesis, we present the generation and the descriptive characterization of the first large animal model (swine) of Leigh Syndrome (LS), a well-characterized mitochondrial-derived ND. Leigh syndrome associated with cytochrome C oxidase (COX) deficiency is an early onset, fatal mitochondrial encephalopathy characterized by neurodevelopmental regression and brain stem and basal ganglia lesions, frequently caused by mutations in the Surf1 gene, a nuclear gene that encodes a mitochondrial protein involved in COX assembly.

The animal models of LS generated so far (Drosophila, Zebrafish, Mouse) fail to recapitulate simultaneously the human pathological and biochemical phenotype, which is the main goal of an animal model in order to unveil the mechanisms by which the pathology of interest occurs and therefore pave the way for the discovery of novel therapies. In the last decades, the swine has been increasingly used in biomedical research, mostly thanks to its high similarity to humans, in particular in anatomy, physiology and organogenesis. The project carried out in this thesis consisted in the generation of a putative swine Leigh Syndrome model. To this purpose, we used the most recent genetic engineering technologies in terms of site-specific nucleases, as TALENs and CRISPR/Cas9, associated to a homologous recombination-based (HR) vector, to target swine Surf1 gene and generate an exon-specific double-strand break in order to knock out gene activity and thus reproduce null mutations reported in most human patients. The first problem we

encountered, though, was the absence of a reliable and complete swine Surf1 gene sequence in public databases, as only a few exons were annotated (exon 3 to 5). Therefore, during the course of the project, we sequenced the whole swine Surf1 gene using our cell line of interest as a template to customize our genetic tools and precisely edit swine genome. Knockout (KO) and heterozygous animals were finally generated through Somatic Cell Nuclear Transfer (SCNT), the most well established technique to turn a genome edited somatic cell into live animals in laboratory swine production.

A significant number of KO and heterozygous animals was generated and characterized, from both a clinical and a biochemical point of view, and compared with age-matched wild type individuals. Knockout and heterozygous animals were monitored from birth for the detection of clinical signs attributable to the specific pathology of interest and tissue and organ samples were collected *post-mortem* for the biochemical, molecular and morphological characterizations of our animal model. Surf1 KO piglets exhibit an early onset lethal clinical phenotype characterized by a high perinatal mortality, failure to thrive, muscle weakness and a highly reduced life span due to high susceptibility to general infections and respiratory impairment. On the other hand, Surf1 heterozygous animals were phenotypically normal and completely comparable to wild type individuals, as expected thus ruling out any off target effects of the nucleases. Histochemical analysis on Surf1 KO specimens revealed the presence of isolated COX deficiency in jejunum villi and a reduction of intramuscular fat in skeletal muscle fibers, suggesting an impairment of energy metabolism. Surprisingly, biochemical analysis revealed that, unlike LS patients, Surf1 KO pigs did not develop a severe muscular isolated COX deficit during their short lifespan. In conclusion, we successfully generated a Surf1 KO swine model, which needs to be further analysed as a promising tool to unveil the effective roles of Surf1 protein in metabolic pathways, in particular highlighting the perinatal period as a crucial moment. Thus, this study confirmed that the extremely heterogeneous range of findings and clinical outcomes already found in other Surf1 KO animal models described so far are also present in swine Surf1 model, which is concordant with the wide range of phenotypes recorded in LS patients.

1. Introduction

1.1 Human neuropathology of interest: Leigh Syndrome

Leigh syndrome (LS) (OMIM 256000) is a rare genetic neurometabolic disorder characterized by the progressive degeneration of the CNS. LS is considered the most common clinical paediatric manifestation of a defined mitochondrial disease, affecting 1 per 40,000 live births. The pathology took its name after Denis Leigh, who first described a novel neuropathology in an infant who died of the disease (Leigh, D., 1951). Leigh syndrome is also known as "subacute necrotizing encephalomyelopathy" because of the unique combination of neuropathological features observed in the majority of LS patients. Pathological lesions of classical LS (infantile necrotizing encephalopathy) are bilateral symmetrical lesions in the brainstem and basal ganglia associated with gliosis, capillary proliferation, and vacuolation of the neuropil though neurons are relatively preserved (Leigh, Denis, 1951). Clinical records of LS can be subdivided into three categories, i.e. infantile necrotizing encephalopathy (referred to as classical LS), X-linked infantile necrotizing encephalopathy and adult onset subacute necrotizing encephalopathy (https://rarediseases.org/rare-diseases/leigh-syndrome/). A brief description of these three categories is presented below.

I. Clinical onset of classical LS generally occurs between the ages of three months and 2 years after an initial period of normal development. Late onset has been observed both in adolescence or late childhood and in adulthood, but it is a very rare occurrence (<17%) (Lake *et al.*, 2015). In most children, the first pathognomonic sign is the loss of previously acquired motor skills. In infants, loss of head control and poor sucking ability are often the first symptoms, which can be followed by reduced appetite with vomiting, irritability and possible seizure activity. Delays in reaching developmental milestones (e.g. head control, sitting, crawling, etc) may also occur. Besides, LS infants are often characterized by failure to thrive. If the onset of LS is in childhood, evident symptoms are often dysarthria and ataxia. Previously acquired intellectual skills may diminish and intellectual disability may also occur. Progressive deterioration of CNS associated with LS is characterized by generalized weakness, hypotonia, clumsiness, tremors, spasticity and/or the absence of tendon reflexes; finally, further neurological development is delayed. Abnormally high levels of lactic acid in blood and cerebrospinal fluid are often detected in LS patients, contributing to heart, lungs and/or kidney impairment and failure. Other frequently encountered symptoms of LS patients

are respiratory problems (e.g. apnea, dyspnea, hyperventilation, Cheyne-Stokes), dysphagia, visual problems (e.g. nystagmus, strabismus, ophthalmoplegia, optic atrophy, blindness) and heart problems (e.g. hypertrophic cardiomyopathy, asymmetric septal hypertrophy). Disease affecting the nerves outside of the central nervous system (peripheral neuropathy) may eventually occur, causing progressive weakness of the arms and legs. Other manifestations include microcephaly and hypertrichosis (Santoro *et al.*, 2000; Rahman *et al.*, 2001).

II. Mutations in X chromosome-encoded subunits of MRC enzymes (e.g. pyruvate dehydrogenase) have been reported to be at the basis of a maternal-inherited form of Leigh Syndrome (Matthews *et al.*, 1993). The symptoms of the X-linked infantile form of LS are similar to those of classical Leigh syndrome.

III. The adult-onset form of LS is very rare and its onset is generally during adolescence or early adulthood, often associated with visual impairment (e.g. central scotoma, colour-blindness, bilateral optic atrophy). The CNS degeneration typically associated with LS progression develop slowly in this form of the disorder and late symptoms can be ataxia, spastic paresis clonic jerks, generalized tonic-clonic seizure, and/or varying degrees of dementia (https://rarediseases.org/rare-diseases/leigh-syndrome/).

The abnormalities associated with LS in the pre-natal life can be intrauterine growth retardation, cardiomegaly, oligohydramniosis, microcephaly, enlarged ventricles, intracranial (pseudo)cystis and white matter abnormalities, most of these being non-specific findings.

Generally, the vast majority of LS cases involve infants and the key feature of LS are acute neurological and sometimes systemic events called “decompensation”, usually occurring during an altered immunological state which taxes the body’s energy production (e.g. infections, vaccinations, etc) and associated with psychomotor retardation or regression (Gerards *et al.*, 2016).

Diagnostic criteria for LS include the detection of symptoms typically associated with NDs as bilateral CNS lesions with characteristic neuroimaging (MRI) (Fig.1.1) and/or *post-mortem* neuropathological alterations and mitochondrial dysfunction. In the majority of cases, lactate levels are increased in blood and/or cerebrospinal fluid, although this is not a mandatory finding as at least 25% of cases present normal lactate levels. For this reason, recent diagnostic criteria exclude raised lactate levels as a prerequisite. The results of analysis on muscular biopsies of LS patients can be extremely heterogeneous, presenting lipid accumulation, COX-negative fibres, succinate-dehydrogenase deficiency and abnormal mitochondrial configurations, or, on the other hand, being completely normal. Ragged red fibres are rare in LS patients, whereas in the majority of cases abnormality in the mitochondrial respiratory chain (MRC) enzyme activity are detected, most

frequently isolated complex I or complex IV defects, in particular COX activity is usually less than 20% of that observed in normal fibroblasts, lymphocytes, or muscles biopsies (Gerards *et al.*, 2016).

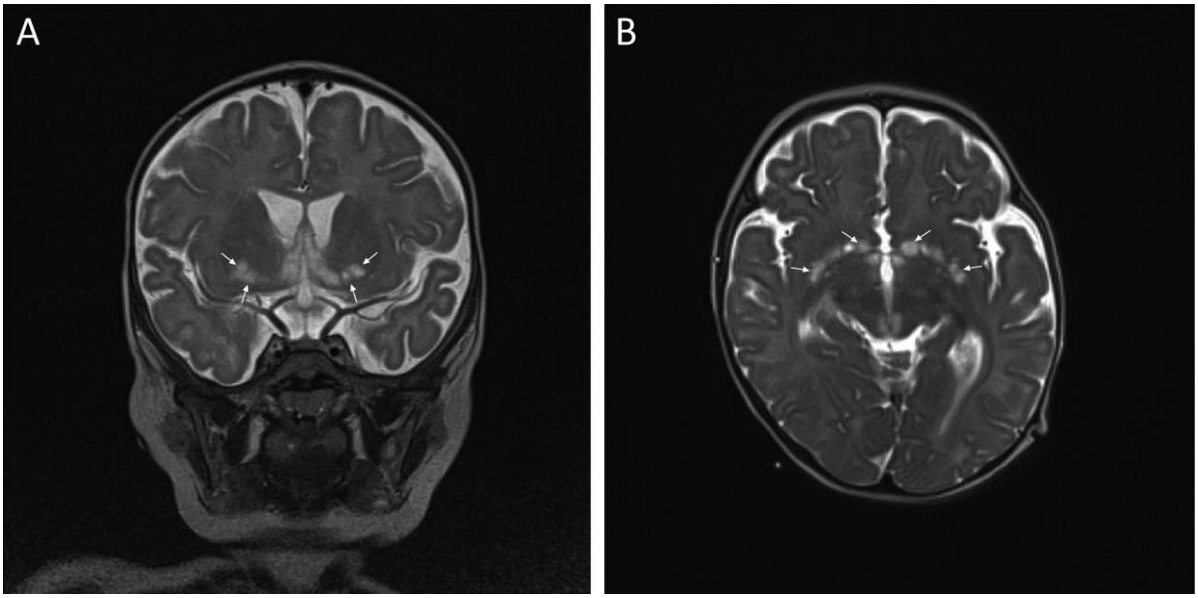

Fig.1.1 Magnetic resonance images (MRI) of a 6-months patient with LS showing bilateral signal intensity in coronal (A) and axial (B) sections of the putamen, nucleus accumbens, and mesencephalon. Figure taken from (Lake *et al.*, 2015).

The variability in the pathological phenotype presentations reflects the extremely heterogeneous genetic background of the pathology. The main genetic cause of LS has been identified in Surf1 gene mutations, reported to be the cause of one third of LS cases (Darin *et al.*, 2003; Sacconi *et al.*, 2003). Nevertheless, even in Surf1-related LS cases, the clinical symptoms can be highly variable. Some LS patients were reported to present with an atypical course, without lactic acidosis or without the unique brain lesions (Rahman *et al.*, 1996; Rahman *et al.*, 2001). Moreover, some Surf1 mutated patients did not present typical LS, but developed different clinical signs e.g. demyelinating Charcot-Marie-Tooth disease (Echaniz-Laguna *et al.*, 2013), villous atrophy, hypetrichosis without the typical brain lesions (Von Kleist-Retzow *et al.*, 2001), or severe renal involvement (Tay *et al.*, 2005). A case of leukodystrophy with systemic COX deficiency was also reported (Rahman S et al 2002). Diabetes, short stature and dysmorphic features have also been reported. However, gene mutations associated with LS onset have been detected in more than 60 mitochondrial and nuclear encoded genes, though still explaining only half of cases (Gerards *et al.*, 2016). Leigh Syndrome can be defined as a distinct mitochondrial oxidative phosphorylation (OXPHOS) syndrome, meaning that the main cause of the

pathology is an impairment in the function of mitochondrial respiration pathway (Koopman *et al.*, 2013). Mutations causing LS have been described in genes coding for subunits of each MRC complex as well as in related assembly factors (Fig.1.2).

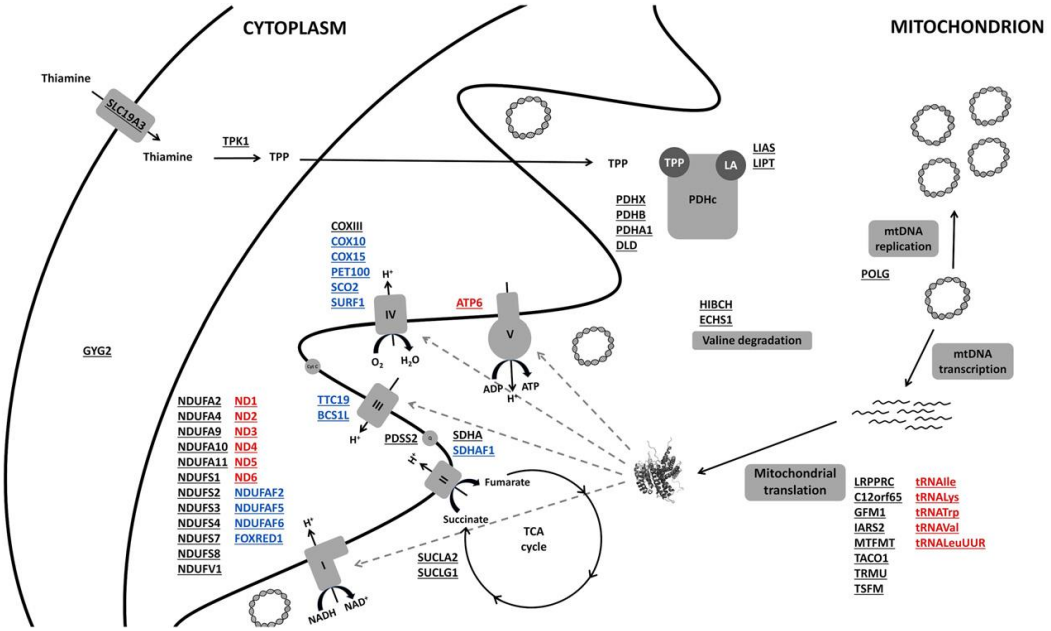

Fig.1.2 Cellular pathways and related genes impaired in LS patients. Genes in which mutations have been identified in patients with LS are underlined. Nuclear encoded proteins are depicted in black, mitochondrial encoded subunits in red and MRC assembly factors in blue. Figure taken from (Gerards *et al.*, 2016).

Briefly, mutations causing LS have been identified as follows:

- Complex I: between 35% and 50% of patients with CI deficiency are diagnosed with LS and it is often a multisystem disease.
- Complex II: CII deficiency is a rare cause of LS and only two mutations have been identified.
- Complex III: LS is caused by mutations in two assembly factors.
- Complex IV: next to CI, CIV mutations are the most common cause of LS, being the main cause of LS in the United Kingdom. Surprisingly, COXIII is the only structural subunit in which mutations have been related to LS; all other mutations affect the assembly factors or proteins involved in the translation of mtDNA-encoded subunits. The most frequently CIV mutated gene (~75%) in LS is the assembly factor SURF1, presenting frequently truncating

mutations resulting in an absence of the functional protein with a consequent decreased formation of complex IV. One third of LS cases are accounted to be caused by mutations in Surf1 gene (Darin *et al.*, 2003; Sacconi *et al.*, 2003).

- Complex V: ATP6 mutations have been described and linked to 5-10% of cases of LS; it is the most common form of maternally inherited LS.
- Multiple complex deficiency: mostly caused by mutations in proteins involved in the mitochondrial translation.

The most frequent pathological finding, however, which remains common among LS patients, is the severe isolated COX deficiency.

1.2 An insight into mitochondria and oxidative phosphorylation

The term “mitochondrial disorders” usually refers to diseases that are caused by disturbances in the mitochondrial oxidative phosphorylation (OXPHOS) system, the final biochemical pathway assigned to produce ATP (Smeitink *et al.*, 2001). Indeed, the most important task of mitochondria is to continuously replenish the cellular ATP storage. The energy required for the ATP synthesis comes from the stepwise oxidation of monosaccharides (glucose, fructose and galactose), fatty acids and amino acids coming from food intake. Monosaccharides oxidation starts in the cytosol with a process called glycolysis, where part of the chemical bond energy is transferred to the electron carrier nicotinamide adenine dinucleotide (NAD^+), reducing it to form NADH, and a small part is used to directly produce ATP. The final product of glycolysis is pyruvate: in the case of glucose, cytosolic oxidation produces two molecules each of pyruvate, ATP and NADH. Pyruvate is also produced from processing of lactose (converted from glucose by mature red blood cells and muscle cells at work) and some amino acids. The oxidation of pyruvate occurs within the mitochondrial matrix, where a series of specific enzymes are located. Fatty acids oxidation is performed completely in the mitochondrial matrix in a stepwise process called β oxidation and the final product is either acetil-CoA (even-numbered fatty acids) or propionyl-CoA (odd-numbered fatty acids). Amino acids oxidation also occurs entirely in the mitochondrial matrix and they are finally processed to pyruvate, acetilCoA or an intermediate of the tricarboxylic acid cycle (TCA) depending on the amino acid type. The products of these partial oxidations (pyruvate, acetil-CoA, propionyl-CoA and intermediates) are further processed in the TCA by the enzymes and electron carriers of the electron transport chain (ETC), located in the inner mitochondrial matrix. This process, called oxidative phosphorylation (OXPHOS), converts the energy stored in the electron carriers in ATP (Fig.1.3).

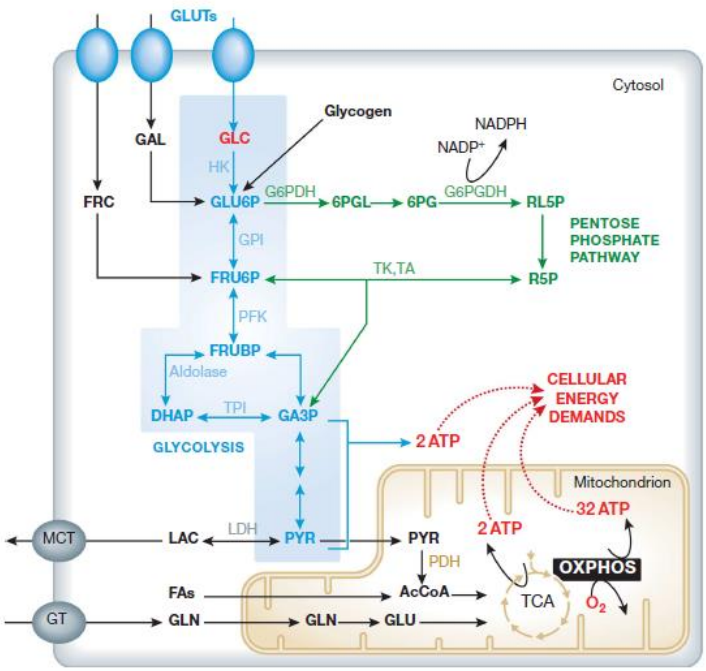

Fig.1.3 Schematic representation of energy metabolism in a mammalian cell. The main energy source, ATP, is generated by the glycolysis pathway (blue), the tricarboxylic acid (TCA) cycle and the OXPHOS system. Figure taken from (Koopman *et al.*, 2013).

The relative proportion of cytosolic and mitochondrial ATP necessary for cellular processes depends on the cell type considered. Neurons, for instance, are high consumers of ATP and they do not have glycogen stores, so they depend totally on the efficient function of mitochondria. The OXPHOS system (Fig.1.4) is composed of five multiprotein enzyme complexes (I-V) and two electron carriers (coenzyme Q_{10} and cytochrome c). Nuclear DNA (nDNA) and mitochondrial DNA (mtDNA) encode for all OXPHOS complexes, except for CII, which is exclusively encoded by nDNA (Fig.1.4). Complex I (NADH:ubiquinone oxidoreductase) is the largest OXPHOS complex, recently proposed to consist of 44 subunits: 7 are encoded by the mtDNA and 37 subunits are encoded by nDNA. The highly conserved core subunits, needed for functioning, are the seven mtDNA-encoded subunits and seven of the nDNA-encoded subunits. There are at least 11 assembly factors involved in the biogenesis of holo-CI. CI oxidizes NADH to NAD^+, transferring the electrons to the electron carrier coenzyme Q_{10} (CoQ_{10}, ubiquinone). Complex II (succinate:ubiquinone oxidoreductase) works in both the OXPHOS system and in the TCA cycle; it oxidizes $FADH_2$ to FAD, transferring electrons to CoQ_{10}. The CII holoenzyme is heterotetrameric, consisting of four subunits all encoded by nDNA and its assembly is assisted by two assembly factors. Complex III (ubiquinol:cytochrome c oxidoreductase) is composed of 11 subunits, only one of which is encoded by mtDNA, and it is

assisted in the assembly by two identified assembly factors. Complex IV (cytochrome c oxidase) consists of 14 subunits, three encoded by mtDNA (COI, CO2, CO3) and the remaining encoded by nDNA; its assembly is assisted by at least 18 assembly factors. CIV transfers electrons to molecular oxygen to form water, and at the same time, the energy released by the electron transport is used to pump protons from the mitochondrial matrix, generating an electric charge and pH difference across the mitochondrial internal membrane. Finally, Complex V (F_0F_1-ATP-synthase) has the fundamental role to couple the energy from the controlled proton backflow to form ATP from ADP and inorganic phosphate. This last complex is composed by 19 subunits, two encoded by mtDNA and the remaining by nDNA, and four nDNA-encoded assembly factor are required in this process.

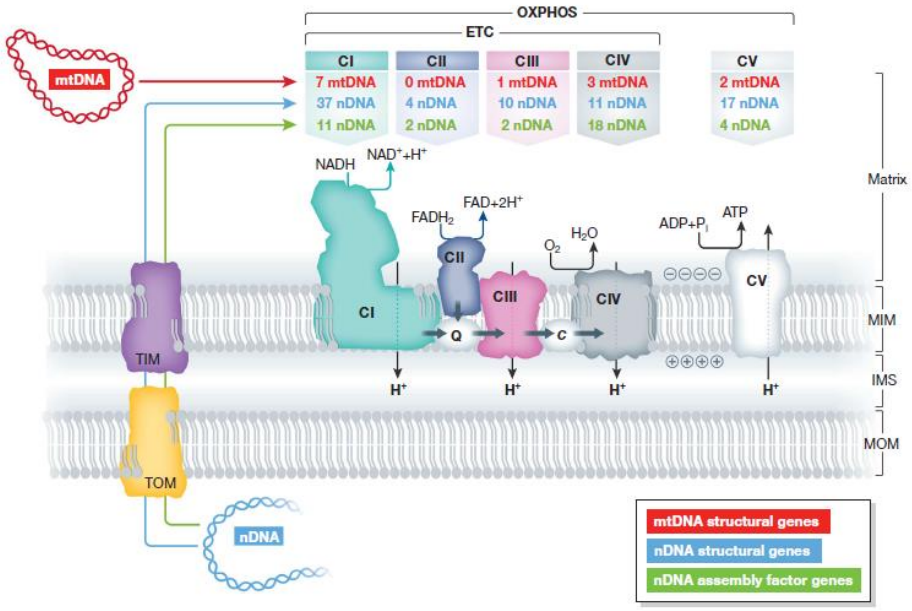

Fig.1.4 Nuclear and/or mitochondrial DNA coding origin and functional interaction of the mitochondrial OXPHOS complexes. The mitochondrial OXPHOS system is composed of five complexes (CI–CV) embedded in the mitochondrial inner membrane (MIM). The genetic origin of complexes subunits can be the mitochondrial DNA (mtDNA, red) and/or the nuclear DNA (nDNA, blue); the same is true for assembly factors (green). Figure taken from (Koopman *et al.*, 2013).

Of the overall quantity of ATP produced, only a small percentage is used for the mitochondria own needs, whereas the great majority of ATP molecules is transferred outside the mitochondria via the adenine nucleotide translocator and used for a wide range of cellular functions (Smeitink *et al.*, 2001). Different studies on bovine heart mitochondria and various rat tissues (heart, kidney, muscle, brain,

liver) suggest that the relative quantity of CoQ_{10} and cytochrome c (cyt-c) vary in a tissue-specific manner, indicating that the brain is more sensitive than liver and kidney, but less sensitive than skeletal muscle and heart tissue. On the other hand, CII, CIII and CIV do not show tissue-specificity. Moreover, experimental evidence of inter-complexes dependency suggest that OXPHOS complexes are not individually embedded in the mitochondrial matrix, but more likely, they are organized in supercomplexes, also known as "respirasomes": for instance, CIII is required to maintain CI and deficiency of CIV reduces CI function. The last identified version of respirasomes suggest the involvement of CI, CIII and CIV in their formation; also CV forms higher oligomeric structures from dimeric units thought to be needed for maintaining of cristae structure (Koopman *et al.*, 2013). The high level of complexity characterizing the OXPHOS system, composed of about 85 proteins encoded partially by the mtDNA and partially by the nDNA, explains the variety of clinical phenotypes associated with genetic defects in oxidative phosphorylation (Smeitink *et al.*, 2001).

1.2.1 The OXPHOS system dual genetic control

The OXPHOS system dual genetic control involves both mitochondrial and nuclear genomes. The human mitochondrial genome was first described 30 years ago, and soon afterwards, some deviations from the universal genetic code were revealed. Moreover, a simplified genetic mechanism is used, so that for translation only 22 transfer RNA (tRNA) are required, instead of the 31 tRNA predicted by Crick's wobble hypothesis. Mitochondrial genome is present in $10^3 – 10^4$ copies in each cell, with two to ten copies per mitochondria. The sequence of mtDNA from unrelated individuals differs by about 0.3%; most individuals have a single mtDNA sequence (homoplasmy) inherited completely from the mother, though some cases of heteroplasmy have been reported. Another important characteristic of the mitochondrial genome is the threshold effect, whereby a critical number of mutated mtDNAs must be present for the OXPHOS system to present dysfunctions. The great majority of OXPHOS proteins are encoded by the nuclear genome (at least 70) and there are nuclear genes also to regulate mitochondrial gene expression. Mitochondria-involved nuclear genes are randomly distributed in the genome and most gene products are ubiquitous, though the predominance is in tissues with a high energy demand. The causes of mitochondrial disorders can be found both in nuclear genome and in mitochondrial DNA. Nuclear gene mutations that affect OXPHOS functions have been classified as follows:

- Defects in genes coding for structural OXPHOS components: in the last two decades, different mutations affecting structural OXPHOS nuclear genes have been described; this

is helpful for diagnosis and to better understand the functional properties of the subunits involved. For instance, the first mutation to be discovered in structural OXPHOS-gene was described in two sisters with LS associated with isolated complex II deficiency and mapped in the flavo-protein gene.

- Faulty intergenomic communication: mtDNA replication, maintenance and integrity rely on several nuclear-encoded factors. The impairment in mt-nDNA intercommunication can potentially cause a quality (e.g. mutations) and/or a quantity (e.g.depletion) drop in mtDNA molecules, therefore influencing MRC enzymes activity (Lamperti e Zeviani, 2009). There are two known diseases in which the primary cause seems to be defective interplay between mitochondrial and nuclear genomes. These diseases are mitochondrial neurogastrointestinal encephalomyopathy syndrome (MNGIE) and autosomal dominant progressive external ophthalmoplegia (adPEO).
- OXPHOS assembly, homeostasis and import defects: no mutations have been mapped in the genes coding for the structural proteins of complex IV. The first mutations characterized in an assembly factor gene have been mutations in the Surf1 (surfeit1) gene in patients with COX-deficient Leigh syndrome. (Smeitink *et al.*, 2001).

Mitochondrial DNA mutations affecting OXPHOS are mainly point mutations and are transmitted maternally. Different kind of mutations, such as deletions, are rarely transmitted from an affected mother to her child. To date, precise epidemiological data about the frequency of known mtDNA mutation is not available. However, mutations in tRNA genes account for ~75% of mtDNA-related diseases. At first, mtDNA mutations were associated only with multi-system syndromes, but recently they have also been observed in patients with tissue-specific disorders and different mutations can be associated with the same clinical phenotype.

1.3 Genetic basis of Leigh Syndrome: Surf1 (surfeit1) gene

The severe, isolated defect of complex IV is the most common biochemical feature associated with Leigh Syndrome. In the 90's, a disease locus has been identified in chromosome 9q34 and further analysis indicated Surf1 as a candidate gene. Surf1 is a nuclear encoded and its product is a protein localized in the MIM, believed to be involved in the assembly of the COX functional complex. The protein is part of the Surf1 family, which includes the homologue yeast protein SHY1 and rickettsial protein RP733. The gene is located in the Surfeit gene cluster, a locus of 60 Kb of DNA. The mouse Surfeit locus has been characterized as the tightest mammalian gene cluster so far described, and it presents some unusual features as overlapping genes and a bidirectional transcriptional promoter. There is no amino acid or DNA sequence homology among the genes of the cluster, the 5' end of each gene is flanked by a CpG-rich island and all genes are ubiquitous expressed in all cell types tested. The genetic organization of the human Surfeit cluster is close to the mouse one, but differs in some details (Fig.1.5). For example, in mouse Surf2 and Surf4 genes overlap by 133 bp in their 3' UTRs, whereas in human they are separated by 302 bp. Besides, the human Surf5 gene is characterized by the presence of an additional intron not present in the mouse homologue. So, Surfeit genes are six sequence-unrelated housekeeping genes, highly conserved in the amino acid sequence of Surfeit homologues from different vertebrates (Duhig *et al.*, 1998).

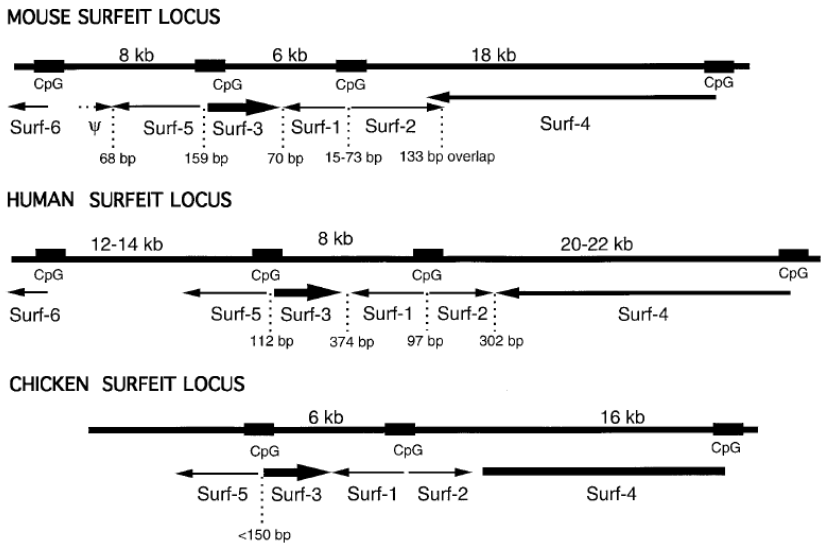

Fig.1.5 Surfeit locus organization in mouse, human, and chicken. The DNA is indicated as a solid line with CpG islands are indicated as black boxes and relative distances are indicated below. The directions of transcription are indicated with arrows (in the chicken the direction has not yet been determined. The mouse Surfeit locus is modified from Garson et al. (1995) and the chicken Surfeit Locus modified from Colombo et al. (1992). Figure taken from (Duhig *et al.*, 1998).

A study by Tiranti et al. demonstrated that in a selected group of patients with defined LS and isolated COX deficiency, Surf1 gene was frequently mutated (Tiranti *et al.*, 1999). The available information on LS pathogenesis were compatible with the hypothesis that the primary cause of cellular metabolism impairment is a critical depletion of ATP, which causes a state of stress in high-consuming cell populations (e.g. neurons). The first symptom of neuronal dysfunction seems to be gliosis, which, if prolonged, may contribute to lesion development and vacuolation of the neuropil. On the other hand, hyperlactacidemia, therefore the local pH changes, can be a cause of increased ROS production and vessel hypertrophy. Nonetheless, the overall neuronal state in LS pathology is relatively conserved, and further studies need to be done in order to understand if cell death is delayed or if a cellular population is more resistant to consequences of energy deprivation then others (Lake *et al.*, 2015).

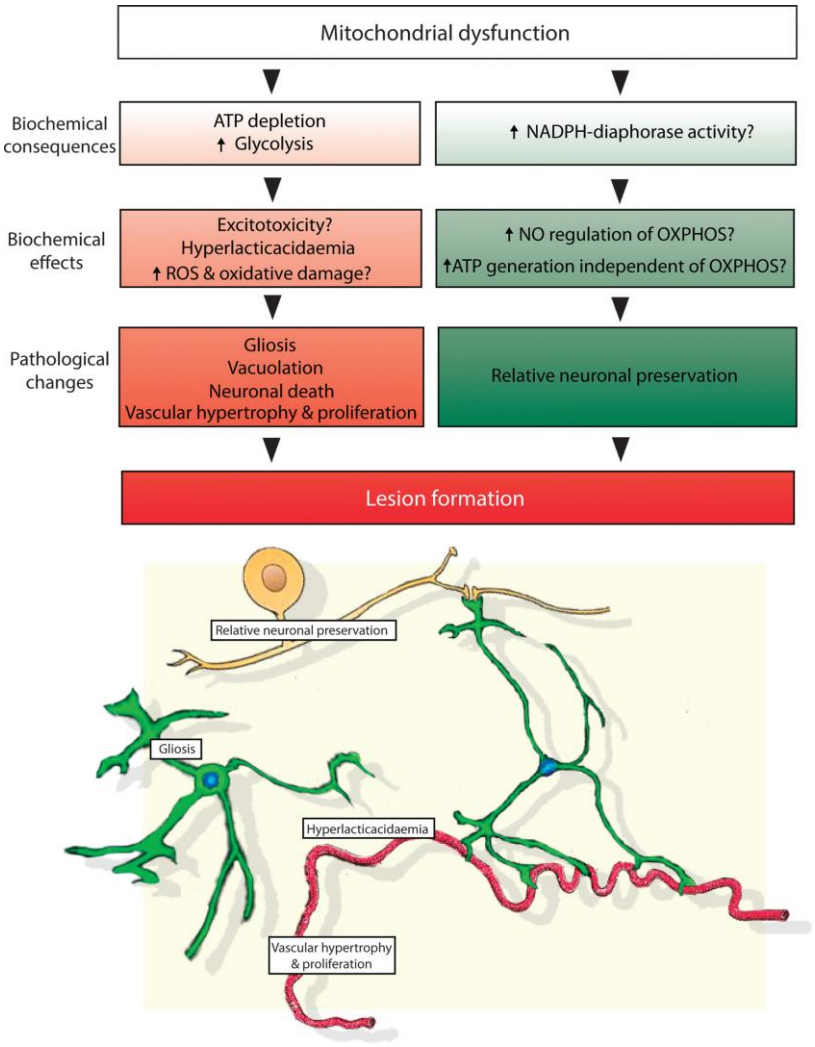

Fig.1.6 Schematic representation of cellular biochemical pathways impairments, consequences and pathogenic pathways leading to LS-characteristic lesions formation. Mitochondrial activity is severely impaired in LS and this has a range of consequences on cellular biochemical pathways that ultimately lead to lesion formation. The depletion of ATP and the consequent increase in glycolysis could directly act on the reduction of neurotransmitter recycling and excitotoxicity, increasing lactate production and hyperlacticacidemia, and promoting excessive production of ROS, the main cause of oxidative damage. These metabolic changes could be the cause of the specific pathologic lesion formation (gliosis, neuronal death, vascular hypertrophy and proliferation, and, ultimately, vacuolation and lesion formation). Figure taken from (Lake *et al.*, 2015).

In most cases, the mutations detected in Surf1 gene were loss-of-function mutation, in particular nonsense mutations, frameshift and splice mutations; in addition, a few silent polymorphisms were detected. No correlation between position, type of mutation and clinical phenotype was observed (Tiranti *et al.*, 1999). In LS patient only two missense mutations in Surf1 gene have been described (Poyau *et al.*, 2000). A case-report was published, reporting an in frame deletion mutation in Surf1 gene that is not specifically associated with LS (Von Kleist-Retzow *et al.*, 2001). In particular, the patient, a female of 1 year of age, was admitted to hospital presenting feeding difficulties and vomiting associated with partial villous atrophy, generalized hypertrichosis, coarse face, strabismus and kyphosis. Moreover, a significant growth retardation was reported, and the patient was hypotonic and unable to walk. Surprisingly, the cerebral CT scan was normal, as were hepatic and cardiac functions. Biochemical analysis showed a markedly reduced COX activity in muscle homogenate and skin fibroblasts, whereas the activity of other complexes were in the normal range. Sequencing analysis revealed two heterozygous mutation in Surf1 gene: a transition G-to-A in position 553 of the cDNA, causing the change of an evolutionarily conserved glycine into a glutamic acid (G180E) in exon 6 and a transversion G-to-C in the intron 6 acceptor splice site (G603-1C). This transversion unmasked a cryptic acceptor in exon 7, resulting in an in frame 6 bp deletion at the start of exon 7 (Von Kleist-Retzow *et al.*, 2001). The conclusion of this work indicate a tissue specific variability in the stability, and therefore in the function, of the Surf1 protein depending on the nature of the mutations. Truncating mutations have been described to disrupt the C-terminal region of the Surf1 protein, necessary for protein stability and function, therefore impairing protein function (Yao e Shoubridge, 1999). The in frame deletion G180E described in the work by Von Kleist-Retzow et al. is predicted to change a charge in a conserved amino acid, therefore probably influencing the membrane insertion of the protein or its interaction with other proteins.

In any case, the striking and conserved isolated COX deficiency detected in LS patients muscle biopsies is believed to be caused by the complete absence of Surf1 protein or its function, even if a residual 10%-20% activity of COX is still present, indicating a redundancy in the function of Surf1 protein.

1.4 Existing animal models for Leigh Syndrome

The increasing knowledge of NDs genetic basis has been fundamental in the last two decades to generate transgenic animal models, mostly rodents, in order to understand the main mechanisms of pathogenesis, disease progression and possible therapy. One crucial point is the characterization of new drugs in term of preclinical efficiency, pharmacology and toxicology to produce a significant slowdown or even stop of the pathology progression.

A successful animal model is able to recapitulate the human disease, both in the symptomatology and in the generation of pathological lesions. Unfortunately, such animal models are still lacking for the majority of NDs, LS among them (Holm *et al.*, 2016). In particular, the most common animal model, the mice, tend to fail in recapitulating the neuronal loss and even in showing phenotypic alterations, probably due to the activation of compensatory mechanisms. The observed phenotype usually is different from the expected one both in models based on neurotoxins application and in models created by directly targeting the identified causative genes. This provides evidence that humans and mice have a significantly diverse vulnerability to the same triggers inducing neurodegeneration (Kreiner, 2015).

1.4.1 Saccharomyces cerevisiae and Surf1 analogue gene SHY1 (Barrientos *et al.*, 2002)

The yeast homologue of the human Surf1 gene is SHY1 gene, which codes for a mitochondrial protein involved in the full expression and functioning of cytochrome c oxidase (COX). The homology between the two genes has been proven by the similarity of the biochemical phenotype of mitochondria from shy1 mutants and Leigh syndrome patients, which suggests a common function of the two gene products, though their precise function is yet not known. A striking common feature between shy1 mutant yeasts and Surf1 deficient patients is that shy1 mutants produce 10-15% of fully assembled and functional COX, unlike other assembly-defective strains that show a complete absence of COX, and LS patients also have 10-30% of normal COX. A possibility is that both Surf1 and shy1 have a redundant function or that their activity simply increase the assembling efficiency of COX. In addition to the low COX content, shy1 mutants show elevated levels of cytochrome c and NADH cytochrome c reductase activity is two times higher than in wild type. To better understand the function of shy1 in yeast, Barrientos et al. investigated from a genetic and biochemical point of view some revertant shy1 mutants and showed that the recovery of the respiratory defect in shy1 revertants is directly related to an increased mitochondrial concentration of COX. Moreover, a yeast strain

defective for MSS51 and shy1 was analysed, and interestingly MSS51 partially supress the COX defect of shy1 mutants. MSS51 is proposed to be a Cox1 (COX subunit) translation factor and Barrientos et al. verified that the two proteins behave as distinct proteins, though do not form complexes even if both are located in the inner mitochondrial membrane. This result indicate that shy1 is directly implicated either in expression or in stability of Cox1 subunit. Further northern analysis excluded a participation of shy1 in the expression of Cox1, as normal levels of fully processed Cox1 mRNA were detected in shy1 mutants, so it is likely to be implicated in Cox1 stability. However, a possibility is that Cox1 expression could be indirectly affected if its translation is coupled to a shy1 protein-dependent downstream assembly event. This type of translational control is termed CES (Control by Epistasy of Synthesis). Besides, another possible explanation for the low expression of Cox1 in the mutant could be an increased protein turnover, coupling the conversion of Cox1 from a protease-labile state to a protected one to an event catalysed by shy1 protein. In Barrientos model, the 15-30% of newly-synthetized Cox1 protein is protease-protected and this fraction is increased in MSS51 revertants (Fig.1.7). Finally, this yeast Leigh syndrome model propose that shy1 protein/Surf1 protein can directly interact with Cox1 subunit or with an assembly intermediate in which Cox1 is one of the interacting partners.

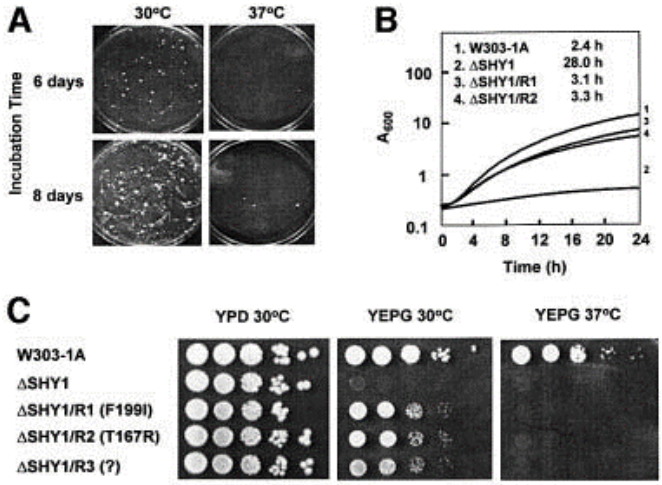

Fig.1.7. **Growth capacity of shy1 mutants and revertants.** A) shy1 null mutant photographed after 6 and 8 days of culture at 30°C or 37°C. B) Growth curve of shy1 mutant and different strains of revertants inoculated in liquid media and incubated at 30°C. Doubling times for different strains are indicated. C) Serial dilutions of the different strains incubated at 30°C or 37°C for 2-3 days. Figure taken from (Barrientos *et al.*, 2002).

1.4.2 Drosophila melanogaster models

The first D. melanogaster Surf1 knockdown (KD) model was described by (Zordan *et al.*, 2006) and was based on the use of transgenic double-stranded RNA interference to obtain post-transcriptional silencing (PTS) of D. melanogaster Surf1 homolog (CG9943). Although Surf1 gene, and presumably its function, are highly conserved between species, interestingly in D. melanogaster the surfeit genes are not organized in cluster as in humans, but are dispersed throughout the genome. Two different models were generated to investigate the egg-to-adult effect of KD in both a systemic KD and a central nervous system-restricted (CNS) KD. The systemic KD model resulted in 100% egg-to-adult lethality, most of the individuals dying as larvae; the observation of 7-day-old larvae showed a sluggish aspect, related with impaired development and smaller dimensions compared with age-matched controls (Fig.1.8). Only a few larvae reached the pupae stage, but they did not progress any further. The systemic KD larvae showed a reduced locomotor activity, but no specific functional or structural defects were detected. Therefore, the altered motor pattern is likely to be caused by defective energy supply due to Surf1 silencing. The systemic silencing of Surf1 is also the most probable cause of the early developmental arrest at larvae-pupae stages, as early larvae stages can progress thanks to a maternal contribution, but KD individuals fail to proceed in successive energy-requiring metamorphosis stages. To bypass the larval lethality of systemic KD model, the expression of dsRNAi was restricted to the CNS. This CNS-restricted KD model showed no lethal effects on egg-to-adult viability and no signs of impairment, but surprisingly individuals showed a significant increase in lifespan compared to controls. Moreover, histological section from the head of CNS-restricted KD individuals showed a significantly reduced COX activity and a parallel strong increase in the SDH levels, indicating an increase in the mitochondrial mass as a compensatory reaction. Finally, a slight abnormality in the visual pattern was measured by the optomotor test paradigm, likely to be due to complex alterations in the eye and CNS involving several visual circuits. In conclusion, this study showed a concordance between human LS Surf1$^{-/-}$ phenotype and Surf1 KD D. melanogaster models because both predominantly affect the brain and, to a lesser extent, the skeletal muscle, and are associated with poor growth and failure to thrive.

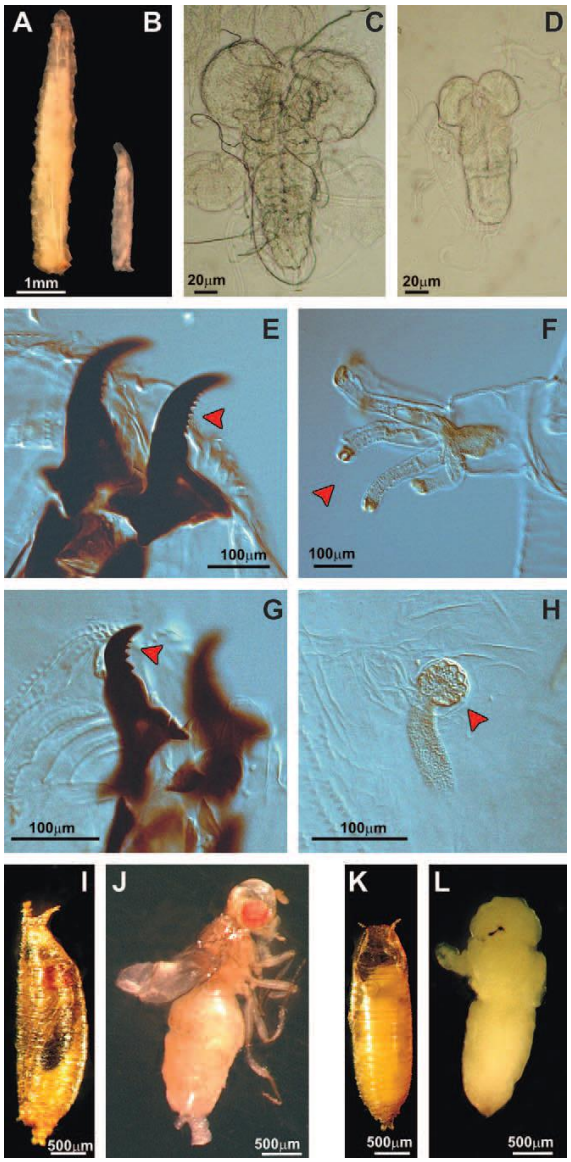

Fig.1.8 Images of Actin5C–GAL4 Surf1 KD individuals at different metamorphosis stages. 7 day-old KD larvae (B) appear drastically smaller than controls (A) and have undersized optic lobes (C is a control brain, D is a brain from Actin5C–GAL4-driven Surf1 KD). KD larvae have present mouth hooks (E) and anterior spiracles (F) (see red arrows), indicating the third instar. On the other hand, in Actin5C–GAL4 Surf1 KD79.1 larvae, cuticular structures are typical of the second instar (G and H); see red arrows. Some KD larvae reach the pupal stage and do not progress any further. Dissection of the dead pupae shows that individuals die at early imago stages. I and J are control pupae, respectively, with and without puparium; K and L are Actin5C–GAL4 Surf1 KD pupae. Figure taken from (Zordan *et al.*, 2006).

A second study was made by Da-Re et al. (Da-Re *et al.*, 2014) to explore the possibility to generate a new Surf1 KD model taking advantage of the GAL/UAS binary system to obtain post-transcriptional silencing of CG9943 (Drosophila homolog of Surf1) and further investigate the biochemical and morphological features of Surf1 KD fly model. In the previous model, two different Surf1 KD models were generated: one systemic model and one CNS-restricted KD model. In this second paper, a third model was developed as a muscle-restricted KD, under the control of *how*^{24b} promoter, which is ubiquitously expressed in embryonic and larval somatic muscle during embryogenesis, late stages of somatic muscle development and during metamorphosis for muscle reorganization. Results confirmed the 100% egg-to-adult lethality in the systemic KD model, in particular at the larval stage. Larvae were smaller, but they possessed mouth hooks (3rd larval stage) indicating that the reduced size was not due to a developmental delay. Interestingly, from a

biochemical point of view a marked decrease in activity of all respiratory complexes and complex V was highlighted (Fig.1.9), instead of the specific deficit in COX activity present in human Surf1 patients. The same generalized deficit in respiratory enzymes activity was observed in the muscle-restricted KO model. Moreover, individuals died during the early stages of pupae metamorphosis, failing to progress beyond pupal stage. In particular, fluorescence microscope images showed how adult muscle did not develop in this model, with the loss of a specific longitudinal fibre in the abdominal segment 4. However, the muscle-restricted KD model showed levels of mtDNA close to controls, assessing that decrease in respiratory enzymes activity is not due to mitochondrial loss. In the CNS-restricted model Da-Re et al. confirmed that there was no negative effects on egg-to-adult development, but interestingly they found that only COX activity was decreased, whereas other MRC complexes and complex V were not affected. These results open the possibility of a more general role of Surf1 in the organization of OXPHOS complexes, in particular at early developmental stages.

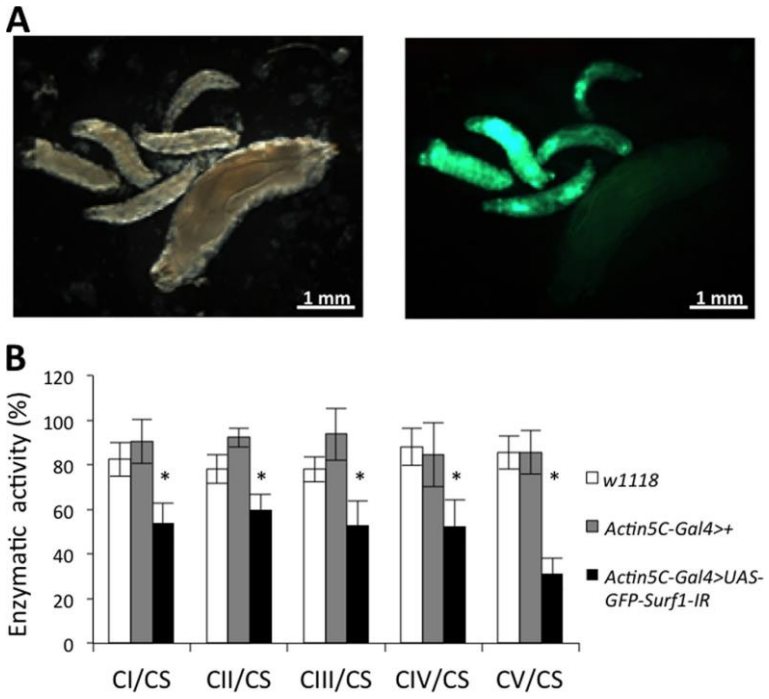

Fig.1.9 Effects on development and MRC biochemistry of ubiquitous Surf1 KD. A) Surf1 KD larvae (GFP positive) were significatively smaller in comparison with stage-matched controls (GFP negative). B) enzymatic activities of MRC complexes (I-IV) and F-ATP synthase (complex V) were measured in w^{1118} (white column), Actin5C-Gal4>+ (gray column), and Actin5C-Gal4>UAS-GFP-Surf1-IR (black column) 3rd instar larvae. Complexes I-V activities were normalized to CS activity. Data plotted are mean S.D. (Student's t test, *, $p<0.005$). Figure taken from (Da-Re *et al.*, 2014).

1.4.3 Early developmental pathology due to cytochrome *c* oxidase deficiency is revealed by a new zebrafish model (Baden *et al.*, 2007)

In this study, Baden et al. used antisense morpholino oligonucleotides (MO) to specifically block expression and sterically inhibit either translation or splicing of the gene of interest. Therefore, they titrated MO to show the range of phenotypes from wild type to complete loss of function of Surf1 gene (COX assembly factor) and CoxVa (COX structural component). In particular, by titrating the injections of MOs they obtained a reduction of COX activity to ~50% of wild type levels, thus impairing normal development but without an immediate lethality. The target of both CoxVa and Surf1 produced the same pathological phenotype, characterized by a shortened rostral-caudal body axis, no or uninflated swim bladder, no or delayed gut development, oedematous and unabsorbed yolk sac at 5 dpf, microphtalmia, no or diminished jaw tissue and abnormal heart shape (Fig.1.10). Moreover, larvae showed severely impaired motility and a serious cardiovascular pathology characterized by significant pericardial edema, bradycardia, ventricular asystole, where edema and bradycardia were progressive, eventually leading to death at ~7 dpf. Further investigations showed a significant increase in apoptosis, especially in the neural tube, with a severe impairment of development of secondary motor neurons, which are more similar to mammalian motor neurons. Based on these findings, Baden et al. conclude that COX deficiency during early development is particularly detrimental to the peripheral nervous system and to cardiac function, resulting in early lethality.

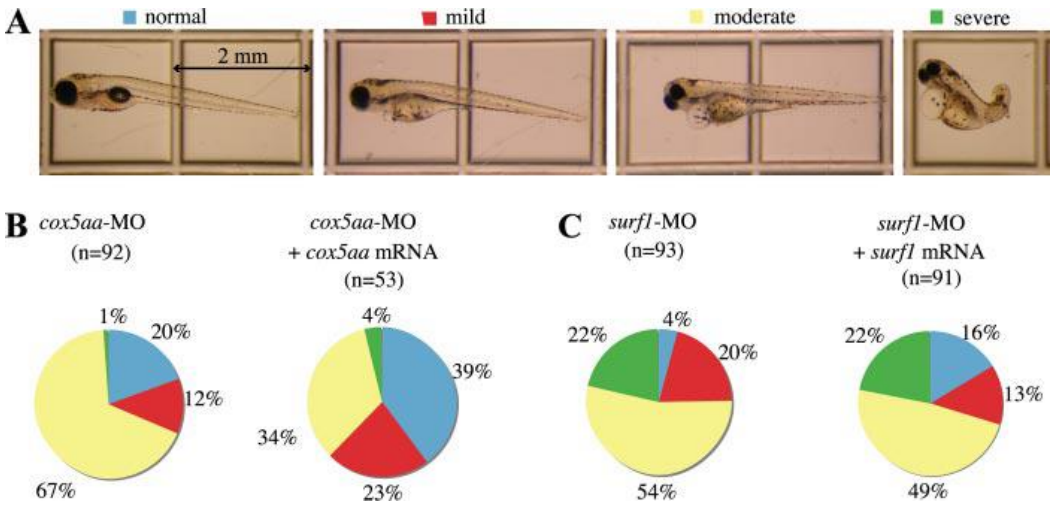

Fig.1.10 RNA resistant to Morpholino (MO) can rescue the COX-deficient phenotype in zebrafish. cox5aa-MO and surf1-MO were co-injected with *in vitro* transcribed target RNA resistant to the respective MO. A) range of COX-deficient phenotypes and relative severity. B) pie charts of phenotypes resulting from 10 ng of cox5aa-MO alone and 10 ng of cox5aa-MO with 4 ng of cox5aamRNA with silent mutations in the MO binding site. C) pie charts of phenotypes resulting from 20 ng of surf1-MO alone and 20 ng of surf1-MO with 0.5 ng of surf1 mRNA. Figure taken from (Baden *et al.*, 2007).

1.4.4 Mus musculus models

In a first study by Agostino et al. (Agostino *et al.*, 2003) a constitutive Surf1 KO mouse was generated through the use of a targeting vector carrying a substitution of murine Surf1 exons 5-7 with a neomycin-resistance (Neo^R) cassette. The resulting murine KO model was characterized by high post-implantation embryonic lethality (~90%) and early-onset mortality of post-natal individuals (~30% died during the first month afterbirth). Interestingly, foetuses where morphologically normal a part from a significant reduction in size compared to littermates controls. Surf1 KO mice were characterized by a significant reduction in muscle strength and motor performance associated with a significant and isolated deficit of COX activity in skeletal muscle and liver and, to a lesser extent, in hearth and brain. Other findings were reduction of histochemical COX reaction and mitochondrial proliferation in skeletal muscle and a slight but significant increase in plasma lactate. In contrast to the human phenotype, this murine Surf1 KO model failed to recapitulate the typical progressive neurological pathological phenotype as no abnormalities in brain morphology were detected, with a consequent absence of overt neurological symptoms. A few years later, the same group of researchers presented a novel murine Surf1 KO model, were the targeting vector only introduced a loxP sequence in murine Surf1 exon 7 and no embryolethality was observed, indicating a possible negative influence

of the Neo^R cassette used in the previous model on neighbouring genes (Dell'agnello *et al.*, 2007). The characterization of this second model confirmed a significant smaller size of Surf1 KO animals compared to control littermates, but this difference progressively disappeared after weaning. No pathological phenotype was observed in KO animals in terms of neurological symptoms, reaction to stimuli, behaviour, cognitive ability and fertility. Only a mild decrease in motor skills resulted from the rotarod test. Histochemically, the specific reduction of COX activity was confirmed in all tissues analysed, where COX activity resulted 30%-50% of controls (Fig.1.11). In addition, blood lactate was slightly but significantly higher than controls. Both COX activity and blood lactate were altered to a lesser extent than human patients. Surprisingly, Surf1 KO mice showed an increased longevity compared to controls and further analysis showed a protection against Ca^{2+}-related excitotoxic brain damage. The results concerning increased lifespan, protection against excitotoxic insults and increased blood lactate levels are confirmed in a study by Lin et al. (Lin *et al.*, 2013), where in addition increased brain glucose metabolism, cerebral blood flow and enhanced memory are described. Finally, no difference was found in reactive oxygen species (ROS) generation, membrane potential and ATP production in Surf1 KO mice; markers of mitochondrial biogenesis (PGC-1α and VDAC) resulted increased in both skeletal muscle and heart, with the induction of mitochondrial stress pathways that can account for a protective effect on cellular homeostasis (Pulliam *et al.*, 2014). In conclusion, this $Surf1^{lox}$ KO model was characterized by mild biochemical phenotype, associated with an apparently null clinical phenotype, suggesting that, in spite of the ubiquitous expression and high evolutionary conservation of Surf1 protein, its function in COX assembly is either ancillary or redundant, so it can be partly rescued by species-specific unknown compensatory mechanisms (Dell'agnello *et al.*, 2007).

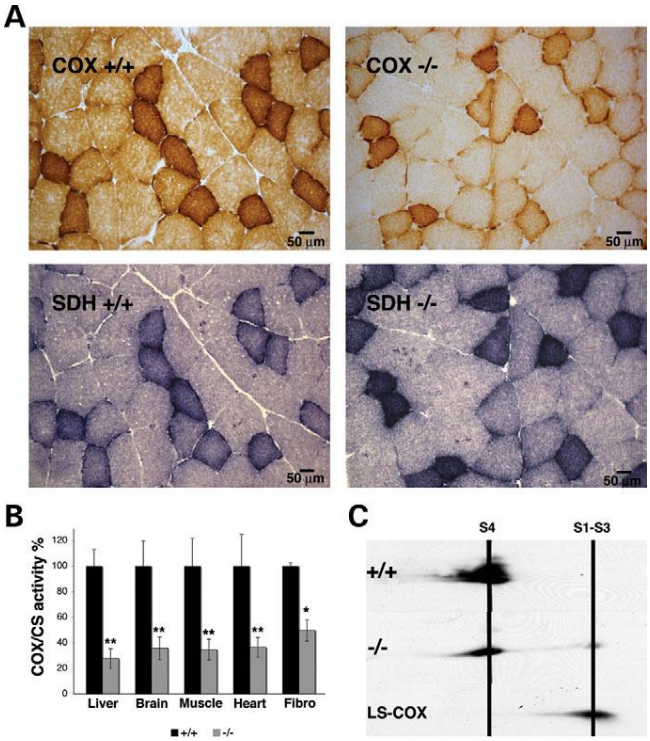

Fig.1.11 Histochemical and biochemical characterization of Surf1^{loxP} KO mice. A) Serial quadriceps sections of from 5-month-old Surf1^{loxP} KO versus controls. Several fibres in the Surf1^{loxP} KO muscle are characterized by a reduction of COX and an increase in SDH reaction, compared to controls muscle. B) COX/CS activities of 3-month-old Surf1loxP KO mice (n = 10) compared to control littermates (n = 10) taken as 100%. *P < 0.01; ** P < 10^{-5}. C) Western blot analysis of 2D-BNE on isolated mitochondria from KO and control animals and from fibroblasts of an LS patient, using an anti-COXI antibody. S4 indicates mature, fully assembled COX; S1–S3 indicate early assembly intermediates. Figure taken from (Dell'agnello *et al.*, 2007).

1.5 The swine as animal model for human diseases and biomedical applications

The failure of small animal models, in particular rodents, to mimic the main features of several human diseases is prompting the generation of large animal models. Over the last 20 years, swine have been increasingly used as general surgical models, for both training and research, for toxicologic testing of pharmaceuticals and as animal models in biomedical research programs. The pig had an increasingly high commercial demand, favouring the development of a vast species-specific knowledge and genetic information and thus allowing the breeding of "laboratory pigs", the use of which can present a great advantage over primates and other non-rodents animal models, for ethical and economic reasons (Fig.1.12).

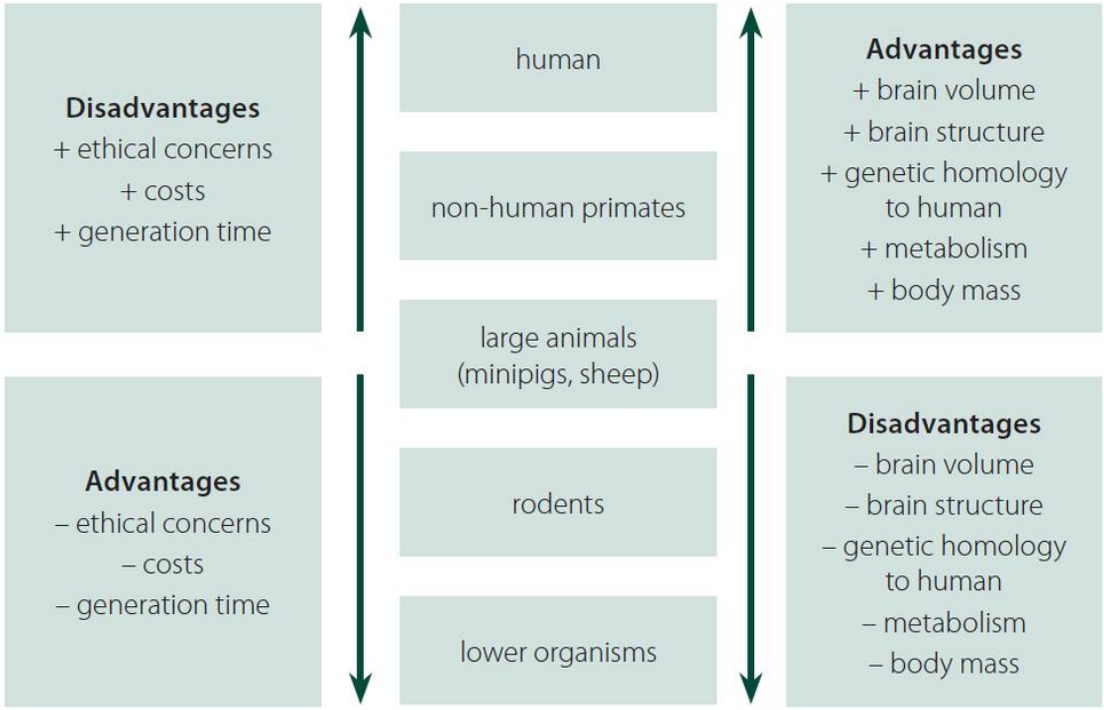

Fig.1.12 Pros and cons in the use of different animal species in research. Figure taken from (http://www.csnn.eu/en/?confirm_rules=1).

Both domestic and miniature swine breeds (commonly known as minipig) are commonly used, where the two differ mainly in the growth rate and size at sexual maturity, whereas anatomic and physiologic characteristics are conserved. As for minipig breeds, since the late 1940s they have been crossed in order to specifically select suitable animals for biomedical research purposes (Gutierrez *et al.*, 2015). On the other hand, some breeds, like Yucatan pigs, are naturally occurring stocks. In any case, miniature breeds are in no way to be considered as transgenic or genetically modified animals. It is nonetheless fundamental to highlight that commercial breeds available today come from a strong selection among the centuries with the aim to increase the commercial-related features (large litters, muscle mass production, etc) of animals.

The pig share a number of anatomic and physiologic characteristics with humans that make it a better model compared with other animals commonly used: it has a long life span (12-15 years), it is relatively easy to breed and produce large litters, and with a gestation period of 114 days on average; puberty occurs at around 6-8 months in commercial breeds and 10-12 months in miniature swine breeds. From an anatomical point of view, the most cited swine systems known to be suitable models are the cardiovascular system (Fig.1.13), the urinary system, the integumentary system and the digestive system.

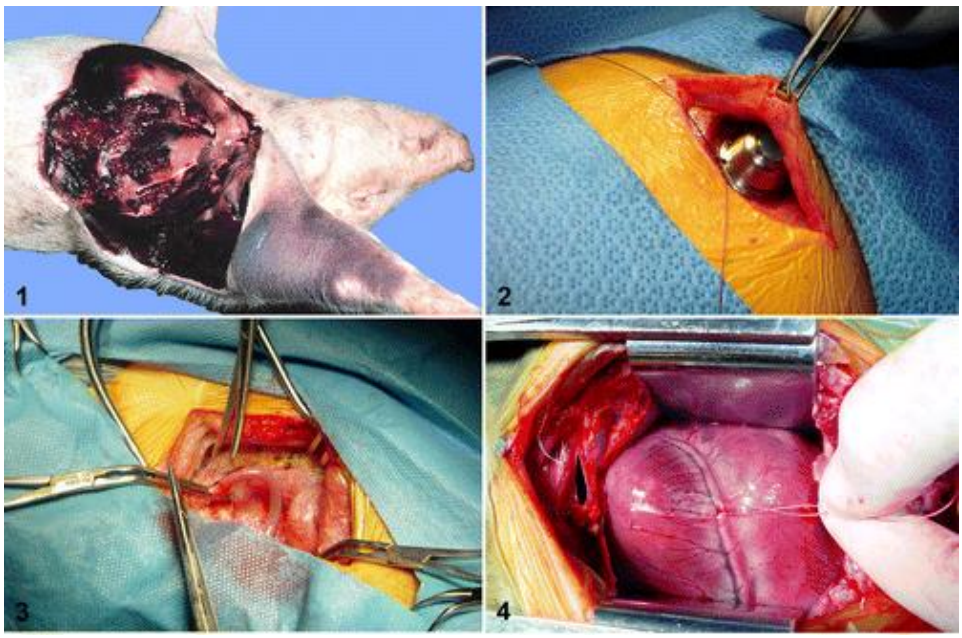

Fig.1.13 Examples of the successful use of pig in biomedical research. 1) Gross necropsy of pig with idiopathic thrombocytopenia syndrome and multiorgan hemorrhage. 2) Surgical model demonstrating implantation of a vascular access port. 3) Arterial graft being implanted in a carotid artery. 4) Coronary occlusion by ligation of the left anterior descending coronary artery to produce an acute infarct. Figure taken from (Swindle *et al.*, 2012).

The swine central nervous system (CNS), and the brain in particular, have been rapidly evolving as a model system for humans given both the size and the anatomic characteristics: it is a relatively large gyrencephalic brain, white matter predominant with similar developmental peaks as human brain, which facilitates the study of specific pathological lesions (Fig.1.14). The internal carotid arteries provide most of the blood supply to the brain and blood flow characteristics are also similar, however pigs have a *rete mirabile*. In particular, the potential of pig models in paediatric neurological research was recognized fifty years ago due to the similarities in the extent of peak brain growth at the time of birth, the gross anatomy (gyral pattern and the distribution of grey and white matter) and the growth pattern of neonatal porcine brain to that of human infants. Moreover, similarities in the gross anatomy of pig brain to that of human brain has also been demonstrated for the hippocampus, a limbic structure, as well as for subcortical and diencephalic nuclei and brainstem structures.

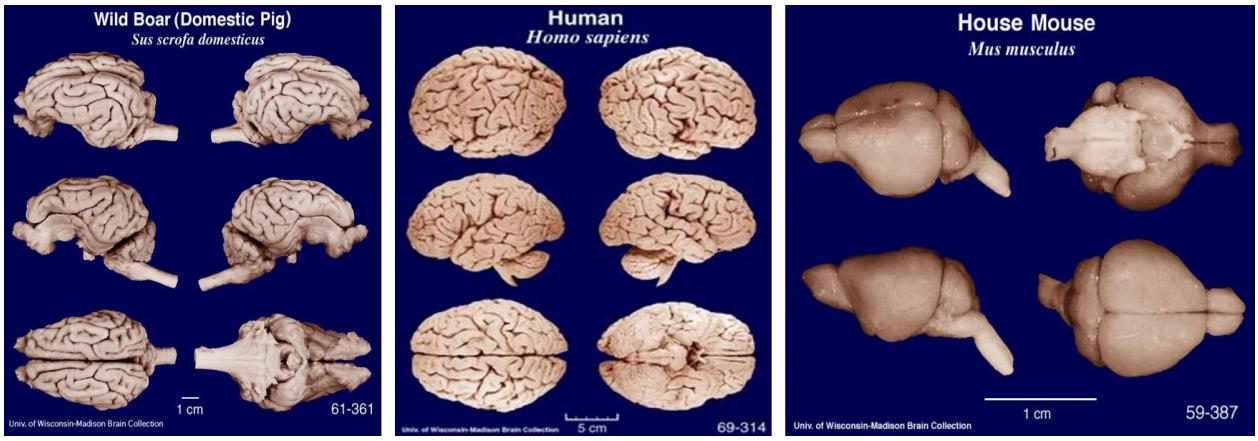

Fig.1.14 Comparative brain photos: from left to right, *Sus scrofa domesticus*, *Homo sapiens* and *Mus musculus*. Figure taken from University of Wisconsin-Madison brain collection (http://neurosciencelibrary.org/).

The production of transgenic or genetically modified pigs was boosted almost a decade ago, when a Chinese-Danish pig genome-sequencing consortium has published the sequence of large portions of genomic DNA from five pig breeds and a porcine brain cDNA library is also available. Then, the introduction of Somatic Cell Nuclear Transfer (SCNT) paved a way of unexpected success in the genetic manipulation of this species, which demonstrated to be particularly difficult with the most used techniques (pronuclear injection, retroviral infection, ES cells).

1.6 Critical step in the use of swine as animal model: porcine embryo *in vitro* production (IVP)

In the 1970s, for the first time, gametes of livestock species started to be used for embryo biology-connected research and for the development of advanced reproductive technologies. In particular, the porcine IVP techniques were not working to an acceptable level until the early 1990s, when the need of large numbers of embryos for research purposes drove the continuous improvement of the system. The porcine *in vitro* production is almost completely based on the use of ovaries collected at local slaughterhouses, a source of large numbers of immature oocytes (Fig.1.15). The first report of live piglets born after IVP from abattoir-sourced oocytes was in 1986 (Cheng *et al.*, 1986) and from that moment, a great effort from different laboratories in the world was taken to improve significantly the efficiency of the IVP procedure (Tab.1.1).

Unlike IVP procedure in other livestock species, the porcine IVP showed to have a very low efficiency right from the beginning, pointing the main problems as follows:

1. Male pronuclear formation: only a limited percentage of oocytes penetrated by the sperm were able to undergo sperm head decondensation and male pronuclear formation. It was clear that the maturation media was suboptimal and different studies demonstrated that the addition of cysteamine, a GSH precursor, could significantly increase the intra-oocyte GSH concentration and the relative percentage of oocytes able to undergo synchronous pronuclear formation (Grupen *et al.*, 1995). Now it is well known that for oocytes of all species, including humans, cysteamine supplementation in the maturation media is essential to boost pronuclear formation.
2. Polyspermic fertilization: polyspermy is always been the major problem in porcine IVP practice. Different studies demonstrated how the zona pellucida (ZP) of ovulated oocytes was significantly thicker than the one of IVM oocytes, suggesting a possible failure to block polyspermic fertilization. In addition, the rate of polyspermic fertilization could depend on the sexual maturity of the donor, as it was lower in oocytes from sows than in IVM oocytes from gilts. This phenomenon is observed not only in swine, but also in adult ewes compared to pre-pubertal ewes. Other factors that could possibly interfere with the block of polyspermy are the ratio sperm:oocyte during fertilization and the exposure of oocytes to oviductal fluid, which contains specific glycoproteins and glycosaminoglycans that bind to the ZP specific protein forming complexes which can be further stabilized with heparin exposure, therefore increasing ZP resistance to sperm penetration (Coy *et al.*, 2008). However, a big issue in porcine IVP is the ability of polyspermic embryos to develop up to the blastocyst stage, at the

same rate as those containing two normal pronuclei. This makes the blastocyst formation rate an inaccurate measure of viable embryo IVP efficiency. Nowadays, polyspermy in the porcine IVP procedure is still an unresolved issue.

3. Quality of oocytes selected for *in vitro* maturation: pigs are generally slaughtered at 6-7 months of age to meet the commercial demand for meat. Therefore, ovaries available at the slaughterhouse are often from pre-pubertal gilts. Studies showed that the quality of oocytes increases with the progression from first to third oestrous cycle of the donor gilt (Archibong *et al.*, 1992). In porcine pre-pubertal ovaries, the antral follicle distribution is such that there are fewer large follicles (5-8 mm) and many more small (~3 mm) compared to adult ovaries. Besides, porcine oocyte quality is also affected by season, being the developmental efficiency lower in summer (because of heat stress) than in winter.

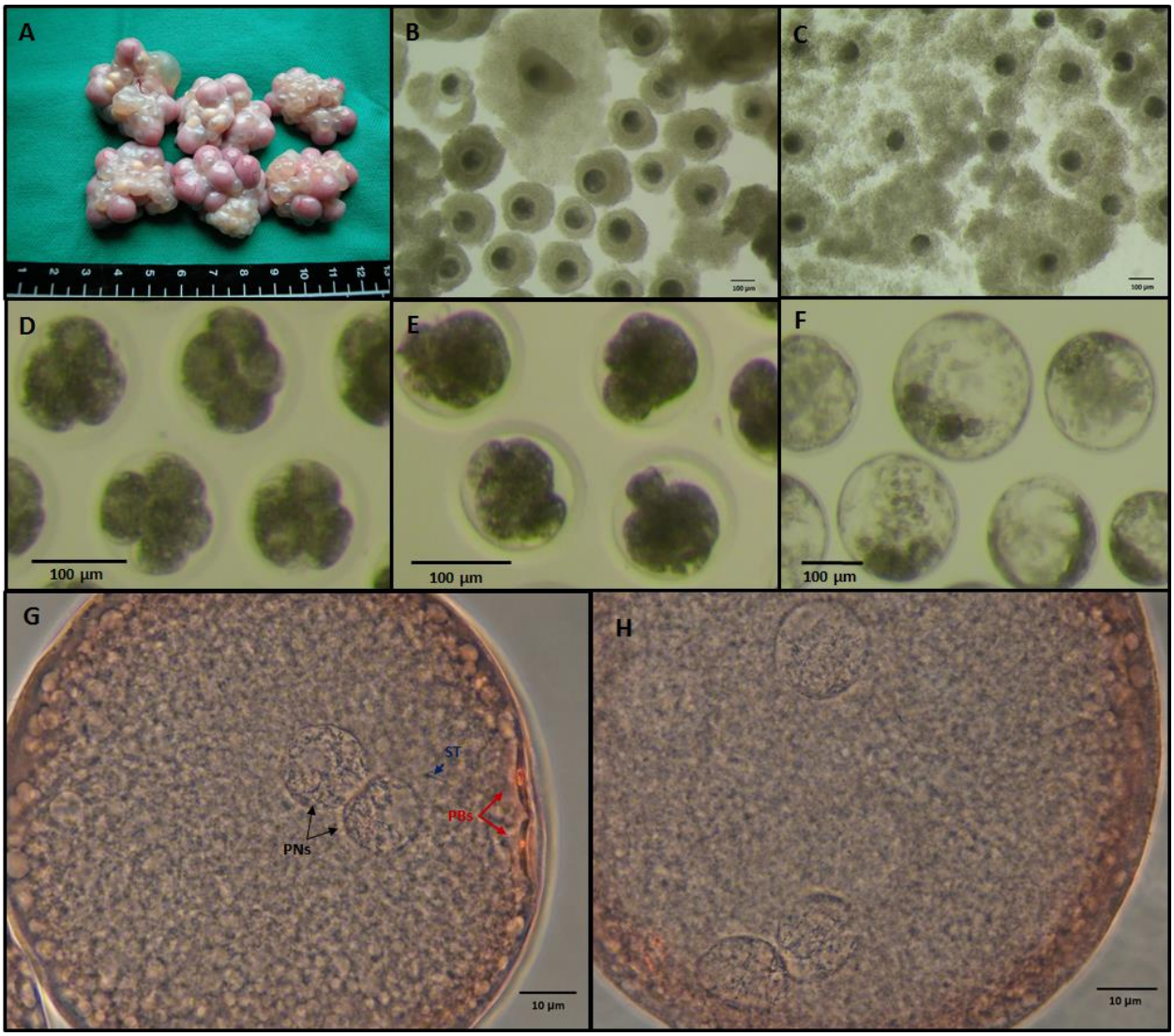

Fig.1.15 Swine in vitro embryo production (IVP). Representative images of IVP swine embryos produced through *in vitro* maturation (IVM), *in vitro* fertilization (IVF) and *in vitro* culture (IVC) in our laboratory at AVANTEA. A) Swine ovaries collected at a local slaughterhouse from pubertal gilts. B) Immature swine oocytes collected through aspiration. C) I*n vitro* matured swine oocytes. D) Swine embryos at day 2 post-IVF. E) Swine morulae at day 5 post-IVF. F) Swine blastocyst at day 7 post-IVF. G) High magnification of a correctly *in vitro* fertilized swine zygote presenting female and male pronuclei (PNs, black arrows), two extruded polar bodies (PBs, red arrows) and the residual sperm tail (ST, blue arrow). H) High magnification of polyspermic swine zygote (IVF) presenting three visible pronuclei. Scale bars: 100 µm in B), C), D), E), F); 10 µm in G), H).

These problems have guided the advancement of a porcine IVP system. The *in vitro* maturation process takes 40 hours, a much longer duration than usual (i.e. 22-24 hours), and different protocols are now available for single-step culture rather than step-wise IVM procedures to suit the changing requirements of the oocytes during this long process as it was done in the past (Grupen, 2014). A long-held belief was that the majority of immature oocytes selected for IVM were still in the germinal

vesicle stage (GV), but nuclear staining revealed that almost half of the oocytes were already well into the germinal vesicle break down stage (GVBD). This fact also contributes to the known difference in timing between oocytes, for which the time taken to reach the metaphase II stage varies substantially among oocytes and this could enhance cytoplasmic deficiency (Funahashi *et al.*, 1997; Grupen *et al.*, 1997). The treatment of oocytes with dibutyryl cAMP (dbcAMP) during the first 20 hours of IVM reversibly inhibits meiotic progression, promoting synchrony of oocyte nuclear and cytoplasmic maturation. Anyway, some studies showed problems related with the temporary inhibition of nuclear maturation, such as detrimental effects on blastocyst rate. Moreover, the efficiency of the treatment with dbcAMP was found to be restricted to oocytes from small follicles (∼ 3 mm). Recently, a chemically defined maturation medium was develop that enables porcine oocytes to acquire full developmental competence. The key features of this medium are the presence of polyvinyl alcohol and a total of 22 amino acids (Yoshioka *et al.*, 2008). At the end of the in vitro maturation process, oocytes are fertilized: many protocols are available, but none of them completely eliminate the problems. Once the fertilization has taken place, the zygote needs a suitable culture condition to reach successfully the blastocyst stage. In the pig female reproductive tract, embryos migrate from the oviduct to the uterine horns at the four-to-eight-cell stage about 2 days post-fertilization. A critical point for the embryo development was demonstrated to be the glucose concentration, as in the porcine oviductal fluid it was found to decrease markedly from the pre- to post-ovulatory period via unidentified systemic mechanism (Nichol *et al.*, 1992; Nichol *et al.*, 1998). Furthermore, the glucose utilization increases from one-cell to the blastocyst stage. For this reason, most commonly used protocols for porcine in vitro embryo culture are based on a two-step system in which media changes emulate the oviductal and uterine environment. Despite these advances, the porcine *in vitro* production is still considered suboptimal, as the *in vitro* blastocyst development rate is still poorer than the one obtained *in vivo*. (Lind *et al.*, 2007; Swindle *et al.*, 2012; Grupen, 2014; Holm *et al.*, 2016).

Year	Details of manipulation/*in vitro* production procedure in the swine species
1985	*In vivo* zygotes/transgene insertion by PN microinjection
1986	*In vivo* oocytes/IVF with fresh ejaculated sperm
1988	*In vivo* oocytes/IVF with FT epididymal sperm
1989	IVM oocytes/IVF with extended ejaculated sperm
	In vivo oocytes/NT using 4-cell stage blastomeres
	In vivo embryos/FT at the peri-hatching blastocyst stage
1993	IVM oocytes/IVF with fresh ejaculated sperm
1995	*In vivo* embryos/FT at the 4-cell stage[c]
1997	*In vivo* oocytes/IVF with sex-sorted sperm
1998	IVM oocytes/IVF with sex-sorted sperm
2000	*In vivo* oocytes/SCNT embryos
	IVM oocytes/SCNT embryos
	In vivo oocytes/NT using 4-cell stage blastomeres
2001	IVP embryos/IVC to the 2- to 4-cell and blastocyst stages
	SCNT embryos[a]/GM donor cells
2002	IVP embryos/IVC to the blastocyst stage[b]
	In vivo zygotes/IVC medium chemically defined[b]
	SCNT embryos[a]/targeted GM donor cells
2003	IVM oocytes/IVF and IVC media chemically defined[b]
2006	SCNT embryos[a]/IVC to the blastocyst stage[b]
	SCNT embryos[a]/FT at the blastocyst stage[bc]
2007	IVP embryos/FT at the 4- to 8-cell stage[c]
	SCNT embryos[a]/handmade cloning[b]
2009	IVP embryos/IVM, IVF and IVC media chemically defined[b]
	IVP zygotes/FT at the PN stage
	SCNT embryos[a]/handmade cloning/GM donor cells[b]
2011	SCNT embryos[a]/FT at the morula stage[bc]
	SCNT embryos[a]/handmade cloning/targeted GM donor cells[b]
2012	IVP embryos/non-surgical embryo transfer[b]
	IVP embryos/FT at the morula stage[b]

Tab.1.1 Milestones of porcine embryo manipulations and *in vitro* production procedures. Abbreviations: FT, frozen-thawed or vitrified-warmed; GM, genetically modified; IVC, *in vitro* culture; IVF, *in vitro* fertilized/fertilization; IVM, *in vitro* matured/maturation; IVP, *in vitro* produced/production (IVM, IVF and IVC); NT, nuclear transfer; PN, pronuclear. a IVM oocytes were used to generate the recipient cytoplasts. b Embryos were cultured *in vitro* for 5 or 6 days before transfer to recipient females. c Embryos were delipated, which involved the physical removal of cytoplasmic lipid droplets by centrifugation and/or micromanipulation. Table taken from (Grupen, 2014).

1.7 Somatic Cell Nuclear Transfer (SCNT)

The potential of animal cloning technique, exploiting selected cultured cells as nuclear donors, is the powerful opportunity to genetically modify, in a highly specific way, the genome of the donor cell and directly obtain a genetically modified animal. The first embryos of mammalian clones from embryonic-derived cells was obtained in rabbit, but it was not until the birth of the cloned sheep Dolly (Wilmut *et al.*, 1997) that an adult cell nucleus was efficiently used in the generation of viable offspring. Following this milestone experiment, numerous mammals, mostly animals of commercial importance but also endangered species, have been successfully used in the process later named somatic cell nuclear transfer (SCNT) (Tab.1.2).

YEAR	SPECIES (NUCLEI STATUS)	AUTHORS	EXP. ENDPOINT
1885	Sea urchin	H. A. E. Dreisch	offspring
1928	Salamander	H. Spemann	embryos
1952	Frog (early tadpole embryo)	R. Briggs and T. King	offspring
1958	Frog (differentiated nuclei)	J. Gurdon	offspring
1975	Rabbit (embryonic nuclei)	J. D. Bromhall	embryos
1984	Sheep (embryonic nuclei)	S. Willadsen	offspring
1987	Cow (embryonic nuclei)	N. First, R. Prather and W. Eyestone	offspring
1996	Sheep (differentiated nuclei)	I. Wilmut and K. Campbell	offspring
1997	Rhesus monkey (embryonic nuclei)	L. Meng, J. Ely, R. Stouffer and D. Wolf	offspring
1997	Sheep (genetically engineered differentiated nuclei)	A. Schnieke, K. Campbell and I. Wilmut	offspring
1998-1999	Mice, cows, goats (transgenic, embryonic and differentiated nuclei)	Multiple groups	offspring
2001	Gaur and Mouflon (differentiated nuclei)	Multiple groups	offspring
2003	Horse	(Galli, Lagutina, Crotti, *et al.*, 2003)	offspring
2007	Rhesus monkey (generation of embryonic stem cells)	S. Mitalipov and colleagues	offspring
2013	Human (generation of embryonic stem cells)	S. Mitalipov and colleagues	embryos

Tab.1.2 Cloning milestones in brief, modified from http://learn.genetics.utah.edu/content/cloning/clonezone/.

The basis of somatic cloning is nuclear transplantation from a donor somatic cell to an enucleated ooplast of the same species (or of a very close species, for endangered animals). The artificial activation of the reconstructed embryo initiate embryo development and the reprogramming acts of the somatic nucleus by the ooplasm cytoplasmic factors, in order to regain totipotency and give rise to a complete viable individual at term of pregnancy.

The main events of somatic cell cloning are nuclear remodelling and reprogramming. When the nucleus of the donor somatic cell is transferred to the cytoplasm of the oocyte and the reconstructed embryo is activated, the somatic nucleus is remodelled depending on the state of the oocyte itself. If the oocyte was arrested in metaphase II (even if the metaphase II plate has been removed), then the

donor nucleus will undergo nuclear envelope breakdown and chromosome condensation. This process is dependent on the activation of different nuclear proteins released and activated after the oocyte nuclear membrane breakdown. Once the reconstructed embryo, made up of the oocyte cytoplasm and the donor cell nucleus, is activated, a pseudo-pronucleus is assembled and the construct becomes a reconstructed-like zygote. This process is performed by oocyte proteins and RNAs. The pseudo-pronucleus is larger in size than the original donor cell nucleus and is characterized by a change in the 3-dimensional structure of its components (lamins, nucleoli, etc). As structure determines function, it is thought that the remodelling of the donor nucleus into the post-activation pseudo-pronucleus is functional to a reprogramming of a somatic nucleus into an embryonic one. The process by which the ooplasm is able to remodel the somatic cell nucleus has been identified as the same mechanism involved in the sperm nucleus remodelling after natural fertilization. An example of this extremely efficient and specific pathway is the substitution of somatic cell type histone H1 of the donor nucleus with oocyte-derived H1 within 60 minutes after SCNT in the mouse. The rapidity of this process witnesses an extremely organized process, which coordinates the ubiquitin-proteasome pathway (for the turnover of somatic H1) and translation of oocyte-derived H1. However, the degree of 3-dimensional remodelling of DNA architecture directly affects the gene expression pattern and the relative epigenetic modifications.

The reprogramming of the donor nucleus, on the other hand, is a non-natural process induced in the reconstructed zygote after activation. The result of an ideally complete reprogramming would be a 100% correct gene expression. Studies carried out in different animal species revealed that in most cases about 95-96% of genes are correctly expressed, whereas the remaining 4-5% of the coding genes have an aberrant expression. This can partly justify the lower developmental rates of SCNT embryos, that if compared to controls, show also higher rates of apoptosis and fragmentation.

Beyond nuclear remodelling and reprogramming, also cytoplasmic structures should undergo some changes to be compatible with the new cellular environment. In particular, naturally mitochondria are characterized by a unique embryo-type morphology and location: in porcine embryos, from the oocyte to the 8-cell stage the mitochondria are spherical or ovoid in shape and organized in small aggregates made up of only a few organelles with a complex structure; surprisingly, they only have a few cristae. At the morulae and blastocyst stage, the mitochondria are filamentous and possessed more cristae, of which many are tubular, resembling more the somatic typical organelles (both in normal and in parthenogenetic pig embryos) (Hyttel e Niemann, 1990; Jolliff e Prather, 1997). Notably, mitochondria are under a dual genetic control, as both mtDNA and nuclear DNA are needed to interact for the organelles functions. Therefore, in reconstructed zygotes the mtDNA from the

ooplasm need to immediately and strictly cooperate with the nuclear DNA from the somatic nucleus to correctly coordinate the embryonic-somatic switch of the mitochondria network. Moreover, donor cell mitochondria can be transferred along with the nucleus during SCNT procedure and, in some cases, can persist in the cloned offspring. However, in most cases, their abundance decreases as the development proceeds. The co-existence of two or more mitochondria haplotypes is known as heteroplasmy. It is well known that mitochondria are maternally inherited and paternal mitochondria, that are localized in the spermatozoa midpiece, are degraded and thus homoplasmy is maintained (Sutovsky *et al.*, 1999; Sutovsky *et al.*, 2004). In 2002, for the first time, paternal mtDNA was detected in muscle tissue of an heteroplasmic patient affected by mitochondrial myopathy (Schwartz e Vissing, 2002). The following year, the recombination of maternal and paternal mtDNA haplotypes in this patient was demonstrated (Kraytsberg *et al.*, 2004) and this case paved the way for several analogue studies which showed how mtDNA recombination is quite common in human skeletal muscle (Zsurka *et al.*, 2005; Sutovsky Peter, 2007). In SCNT-derived embryos and animals, heteroplasmy have been demonstrated to be present in moderate to high levels (Hiendleder *et al.*, 2003; Burgstaller *et al.*, 2007; Hua *et al.*, 2012). This phenomenon could be attributed to a gap in the foreign mtDNA recognition system, which is unable to detect mitochondrial genome from sources other than spermatozoa and therefore is unable to degrade it (Sutovsky Peter, 2007). Besides, SCNT-derived porcine embryos have been shown to be different from IVF-derived embryos in the ability to translocate mitochondria from oocyte cortex to the perinuclear area through microtubules. As mitochondria-pronuclei association was demonstrated to be a positive factor for subsequent embryonic development, the impaired capacity of SCNT-derived embryos to do so can be linked to low cloning efficiency (Katayama *et al.*, 2006). Heteroplasmy and nuclear-mitochondrial incompatibility have been suggested as possible limiting factors in cloning success. Different studies demonstrated clearly how nucleus-cytoplasmic incompatibility in cybrids of closely related primates (Kenyon e Moraes, 1997; Barrientos *et al.*, 2000) and murids (Dey *et al.*, 2000; Mckenzie e Trounce, 2000) does not affect mitochondrial protein synthesis, but impairs significantly the specific respiratory activity of complex I and complex IV. The steady-state levels of complexes subunits was negatively influenced, therefore complexes assembly was impaired, suggesting an altered compatibility between nuclear-encoded proteins and target mitochondria. Moreover, mitochondrial activation in interspecies SCNT-derived embryos around embryonic genome activation (EGA) period was studied, and only reconstructed embryos from taxonomically proximal species (e.g. bovine ooplasm with buffalo and sheep nuclei) were able to support activation of mitochondrial mass. On the other hand, mitochondria in porcine ooplasm were activated neither by ovine nor by horse or

rabbit nuclei, suggesting a complete nuclear-mitochondria incompatibility between these species (Lagutina *et al.*, 2013).

Sometimes, abnormal phenotypes are observed in nuclear transfer (NT)-derived animals, the first of which and most common in ruminants was large birth weight (Young *et al.*, 1998). Since then, the terms Large Offspring Syndrome (LOS) have been used to describe some of the abnormalities observed in pregnancies and newborn animals derived from NT- and, to a lesser extent, from *in vitro*-produced embryos. The aberrant phenotypes appear to be species-specific and, most interestingly, even when an animal with an abnormal phenotype is cloned, such abnormalities generally are not present in the offspring. In particular, an extensive work carried out by Kurome and colleagues lists possible factors influencing SCNT outcome in the swine, pointing out the most frequent LOS observed in cloned swine offspring (Kurome *et al.*, 2013). The most commonly LOS found among cloned piglets is macroglossia (enlarged tongue), and a possible correspondence between this LOS and human Beckwith-Wiedemann syndrome was observed. Characterization of Beckwith-Wiedemann patients resulted in the identification of a probable cause of the syndrome pathogenesis in the abnormal expression of imprinted genes, in particular IGF2 and/or KCNQ1OT1 genes, due to altered methylation patterns (Weksberg *et al.*, 2003). Besides, aberrant DNA methylation is presumably the cause of some LOS as methylation is a fundamental and highly controlled process regulating embryo development. At the zygote stage, active demethylation is performed on parental DNA, followed by passive (or dilution) demethylation during early cleavage stages and, finally, *de novo* methylation of the blastocyst inner cell mass (Beaujean *et al.*, 2004). In NT-derived embryos, it is possible that the initial pattern of complete demethylation and subsequent gene-specific methylation fail to be correctly established, and probably these aberrant phenotypes are not transmitted to the offspring because the correct DNA methylation pattern is re-established during gametogenesis.

SCNT technique consists of a profound manipulation of cells and their genomes and therefore it could get along with some undesirable side effects. However, since the widespread use of SCNT procedure amongst investigators all over the world, the number of cloning publications over time has bursted, highlighting the intrinsic potentiality of this technique and of its successful application to different research fields (Fig.1.16).

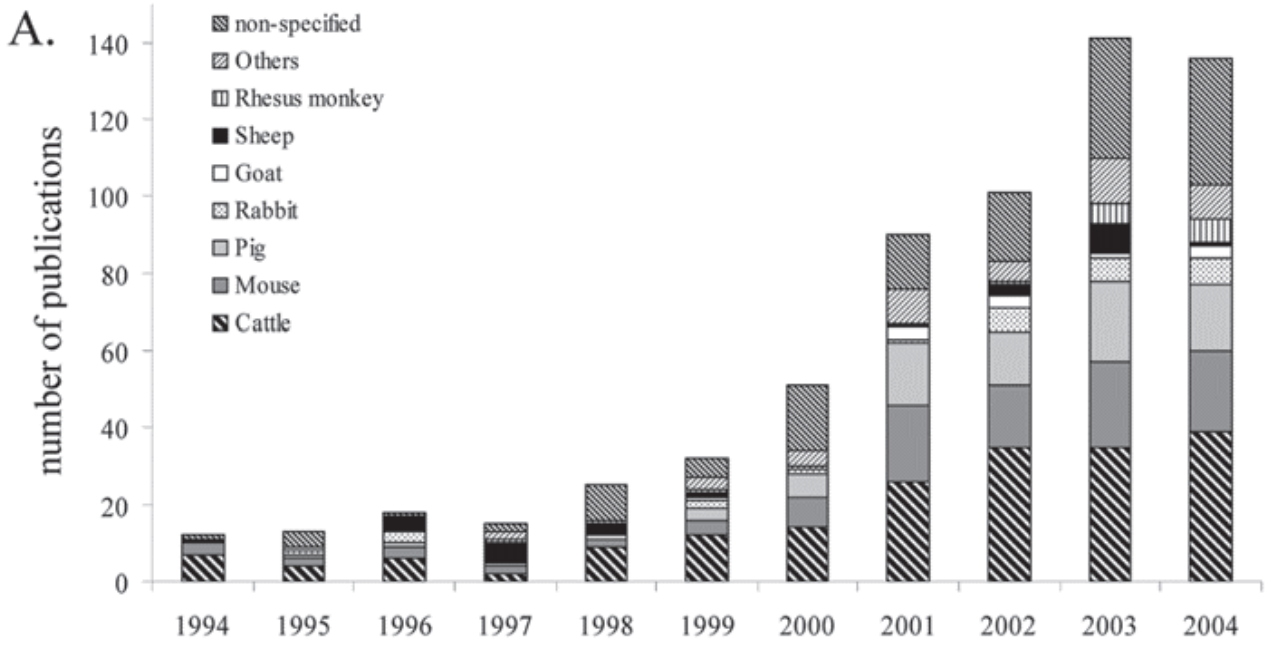

Fig.1.16 Survey on cloning publications over time. A) Number of cloning publications per species as a proportion of the total. Only peer-reviewed publications listed in PubMed were included. The category "nonspecified" includes papers that do not address one particular species (e.g. general reviews). Figure taken from (Sutovsky Peter, 2007).

Finally, SCNT is considered a unique tool both for research purposes and for animal reproduction, and efforts to improve the procedure are constantly been done (Galli, Lagutina e Lazzari, 2003). Recent small technical improvements in SCNT procedure have been made in order to obtain high-efficiency production of ESCs from SCNT-derived human embryos, making SCNT a promising therapeutic tool (Loi *et al.*, 2016). Moreover, recently the discussed issue of three-parents IVF babies has highlighted the potentiality and reliability of NT procedure (Amato *et al.*, 2014).

1.7.1 SCNT technique description

The methodological approach mostly used for SCNT consist in the removal of the nuclear material of the oocyte followed by the transfer of a somatic cell nucleus into the enucleated ooplast.

Oocytes can be harvested from naturally ovulated or superovulated animals, or can be collected from ovaries of slaughtered individuals. In most cases, oocytes are collected as immature ova from ovarian follicles and matured *in vitro* under appropriate conditions. Once arrested in metaphase II stage, the oocyte is enucleated: the metaphase II set of chromosomes, typically located underneath the first polar body, is aspirated through an enucleation pipette. The efficiency of this passage is controlled through the use of vital DNA fluorescent stains as Hoechst33342 and observed under UV light. In the swine, the contemporary fluorescent visualization of the metaphase plate during enucleation is crucial as the oocytes are characterized by a cytoplasm highly dense with lipid and it is otherwise impossible to visualize the metaphase II plate. On the other hand, the donor nucleus can be transferred into the ooplast or the entire donor cell can be fused to the ooplast. In any case, the ooplast deriving from a metaphase II oocyte contains high levels of Maturation-Promoting Factor (MPF), which drives the rapid disassembly of the donor nuclear envelope and the consequent chromosome condensation. The following crucial step is the induction of the reconstructed embryo to exit from meiosis and thus proceed through embryonic development. In mammals, the exit from meiosis requires the initiation of multiple rises of $[Ca^{2+}]_i$ oscillations. Different studies demonstrated that $[Ca^{2+}]_I$ elevations activate the type II Ca^{2+} /calmodulin-dependant protein kinase (CaMKII), which in turn is responsible for the initiation of a cascade that leads to the activation of the anaphase promoting complex/cyclosome (APC/C). The APC/C targets cell cycle proteins, such as cyclin B, for proteasomal degradation; as cyclin B is the regulatory subunit of MPF and the limiting factor for the maintenance of metaphase state, the consequence is the exit from M-phase and the resumption of meiosis. Moreover, it is a possibility that $[Ca^{2+}]_I$ activating stimulus enhances the recruitment of specific maternal mRNAs, the translation of which could be crucial for the activation of zygotic genome. In SCNT procedure, the generation of $[Ca^{2+}]_I$ oscillations can be performed in different ways. Generally, in large animals, and in the swine in particular, the administration of electrical DC pulses (electroporation) in presence of Ca^{2+} induces transient elevations of calcium concentration in the reconstructed embryo. The transient effect is due to the activation of Ca^{2+} pumps in the endoplasmic reticulum (ER, the cellular calcium store) and in the plasma membrane that bring the calcium concentration again to basal levels. Then, delivery of DC pulses allows subtle regulation of calcium concentration levels resulting in very high activation efficacy (Ozil e Huneau, 2001; Ozil *et al.*, 2005). Following activation, NT embryos are cultured in specific media (e.g. SOF, modified NCSU-37, NCSU-23, PZM) on the basis of different

available protocols, that require a step-wise culture with one or two changes of fresh culture media during the process. In pig NT-embryos, cleavage is assessed 48 hours post-activation, whereas morulae, compacted morulae and blastocyst rate are recorded on day 5, day 6 and day 7, respectively (considering day 0 the day of activation). Compacted morulae and blastocysts on day 5 or day 6 of development are then surgically transferred to the uterus of synchronized sows. Recipients are checked for pregnancy by trans-abdominal ultrasound examination 20 days after embryo transfer and pregnancy is confirmed around day 60 (Lagutina *et al.*, 2006; Sutovsky Peter, 2007).

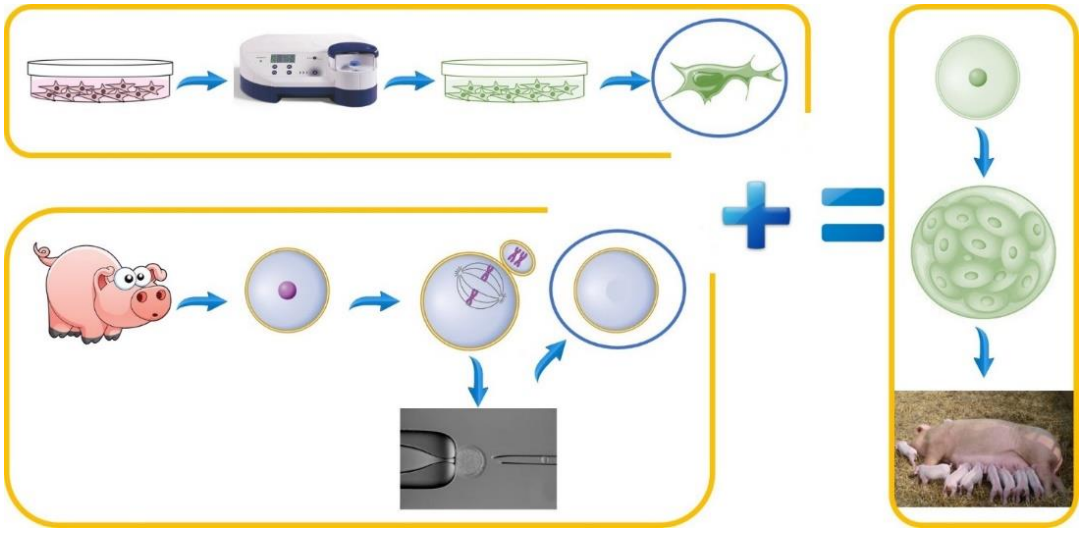

Fig.1.17 Somatic Cell Nuclear Transfer in pigs. The schematic image shows, at the top, the generation of a transgenic/genetically modified somatic cell clone of interest through nucleofection. At the bottom, the manipulation of immature oocytes through *in vitro* maturation and enucleation is shown. The selected nucleus donor cells and the enucleated oocytes are then electrofused and the reconstructed embryos are activated with electrical DC pulses in presence of Ca^{2+}. Blastocyst stage embryos are finally transferred in the uterus of synchronized recipient sows using surgical procedures that require mid-ventral laparotomy under general anaesthesia.

1.7.2 Recipient sows synchronization and transfer of reconstructed embryos

The sow has a bicornuate uterus and is polytocous, the pregnancy is established and maintained only if multiple embryos/foetuses attach and develop into the uterus (Fig.1.18).

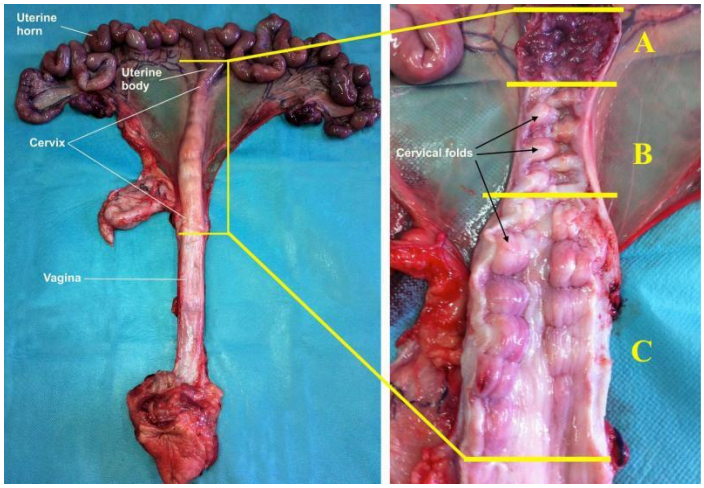

Fig.1.18 Reproductive tract of a sow during metaestrus (top panel). A) Internal wall of the uterine body. B) Uterine region and C) vaginal region of the cervix.

Figure taken from https://www.animalsciencepublications.org/publications/af/articles/3/4/40.

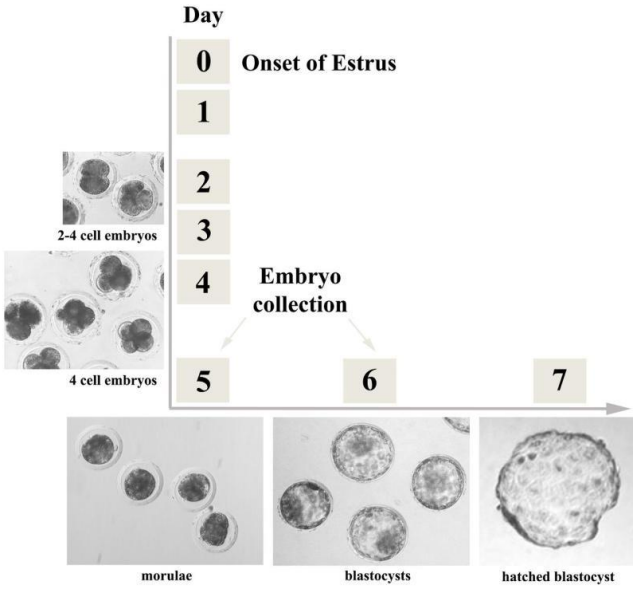

Chronology of porcine early embryonic development in relation to the day of the oestrous cycle (bottom panel). Figure taken from https://www.animalsciencepublications.org/publications/af/articles/3/4/40.

The gestation period is typically 114 days, with a range of 110 to 116 days. The average oestrous cycle is 21 days, with a range of 18 to 24 days, with oestrus being typically 2 days long and ovulation occurring 30 to 36 hours after the onset of oestrus (Swindle e Smith, 2015) (Fig.1.18).

1.8 Genetic engineering: emerging technologies and new frontier for precise genome editing

Since a long time ago, understanding the connection between genotype and phenotype have always been a great challenge. The understanding of candidate genes and relative genetic mutations at the basis of pathological mechanisms was traditionally investigated through the generation of animal models, most frequently mice. Historically, in order to generate adequate animal models, scientists used conventional gene targeting (Capecchi, 2005), which exploits spontaneous homologous recombination (HR) between homologous donor DNA containing a mutation or a gene of interest and target cells genome. This technique was recognized by the Nobel committee in 2007 ("The 2007 Nobel Prize in Physiology or Medicine - Press Release". Nobelprize.org. Nobel Media AB 2014. Web. 18 Jan 2017. http://www.nobelprize.org/nobel_prizes/medicine/laureates/2007/press.html). Unfortunately, the efficiency of HR in higher eukaryotic cells is an extremely rare event, ranging from 10^{-7} to 10^{-6} (Kim, 2016). As a consequence, it was unlikely to obtain gene-targeted mice of interest directly from fertilized eggs due to the limited availability of these cells. Therefore, the need for a large number of germline-competent cells drove scientists' attention to embryonic stem cells (ESCs),that in mouse are easily propagated and can extensively be used for conventional gene targeting. Nevertheless, generation of ESCs in species other than mouse have been proved to be particularly difficult, if not impossible (Hatada e Horii, 2016). To overcome these limitations, during the years different investigators worked on the understanding of homologous recombination mechanisms and possible ways of enhancing its efficacy. In 1988 it was demonstrated how HR efficacy could be boosted in yeast by introducing site-specific DNA double-strand breaks (DSBs) (Rudin e Haber, 1988) and the same results were obtained a few years after in mammalian cells (Rouet *et al.*, 1994).

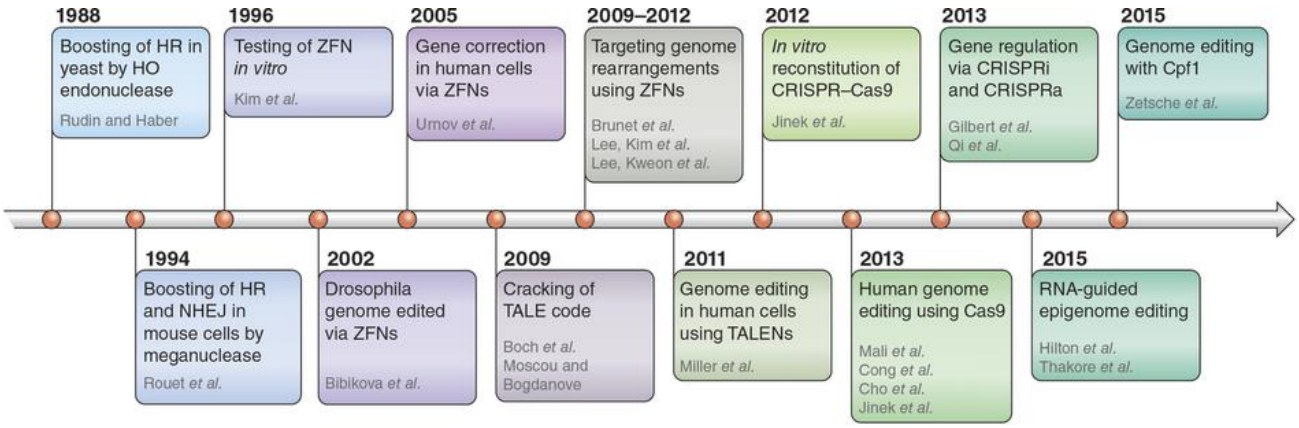

Fig.1.19 Timeline of genome editing methods. Figure taken from (Kim, 2016).

Traditionally, large animal genetic engineering was performed through pronuclear injection, which allowed random and inaccurate modifications leading to the generation of transgenic animals. However, this procedure was extremely inefficient and time-consuming. Moreover, the construct used for genome modification integrates randomly and usually in multiple copies, and considering the practical limitations of the construct, the expression levels and gene regulations are difficult, if not impossible, to control. These aspects made the genetic engineering of large animals a titanic effort and with low practical utility, above all because large animals have higher expenses and longer gestation times compared to laboratory animals, so that the tolerance level for error is necessarily lower. In the last two decades, new genome-editing technologies emerged, based on site-specific nucleases (SSNs), which allow precise and efficient editing of genomes. There are different types of nucleases, each recognizing the targeted region in a different way, but they all have in common the generation of a specific double-strand break (DSB). Consequently, the DNA repair mechanisms are triggered and in presence of homologous template (e.g. targeting vectors, oligos), the homologous-direct repair (HDR) mechanism will be activated, otherwise the non-homologous end joining (NHEJ) mechanism will be enhanced, resulting in site-specific mutagenesis (Fig.1.20).

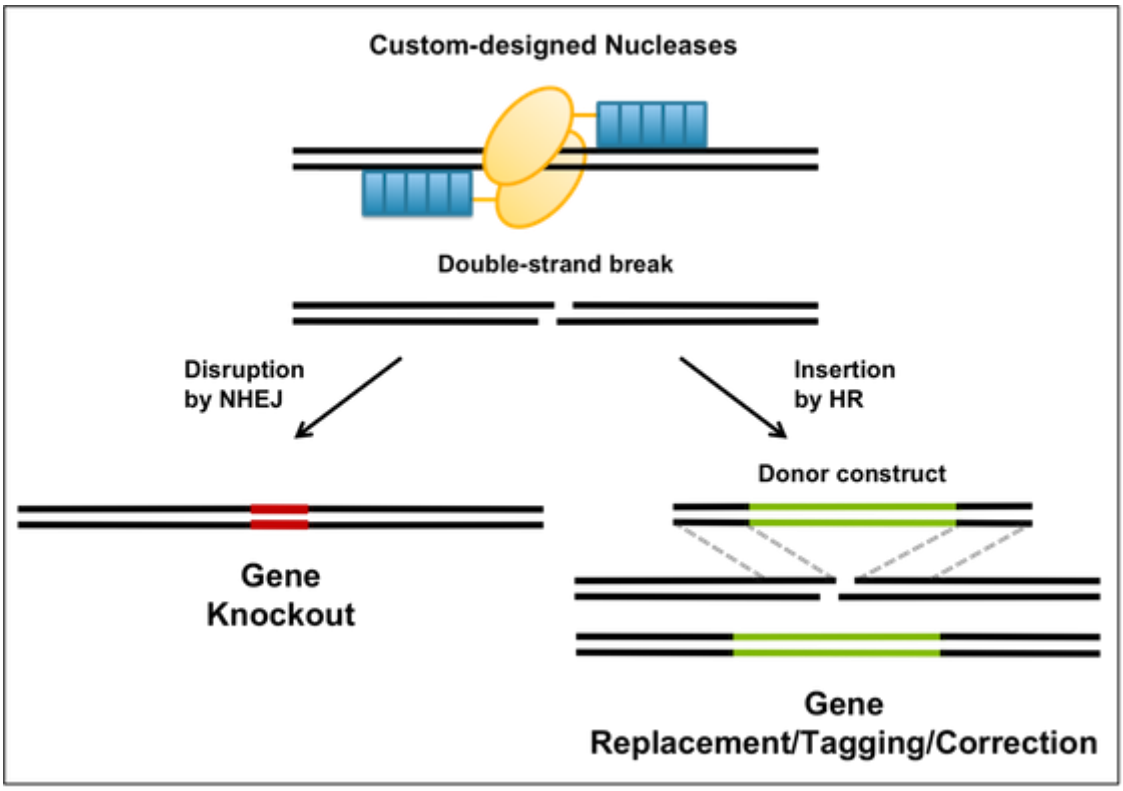

Fig.1.20 Genome Engineering using site-specific nucleases (SSN). SSN precisely introduce double-strand breaks (DSBs) at a target site. DSBs can be repaired either by non-homologous end-joining (NHEJ) or by homologous recombination (HR). NHEJ is error-prone and causes random insertions and/or deletions around the target site, whereas gene replacement, tagging, or correction can be achieved by HR-mediated targeted integration of a donor construct that is provided together with a nuclease pair. Figure taken from (http://www.ctm-basel.ch/genome-engineering-using-custom-designed-nucleases/).

The precise targeting of genome avoids problems related with random integrations and delivery of a limited-size vector, granting correct gene regulation and moderate to high efficiency (10% to 60%).

1.8.1 Eukaryotic DNA repair mechanisms

In eukaryotes, two mechanisms of DSBs repair have been described, HR and NHEJ, which differs for their requirements for DNA homology. DBSs are naturally occurring events and cells have developed a redundant collection of repair mechanisms, the main two being homologous recombination (HR) and non-homologous end-joining (NHEJ).

Homologous recombination repair (HR) is the primary mechanism of DSBs repair in yeast species (Takata *et al.*, 1998) and it works, to a lesser extent, in vertebrate cells. HR requires the presence of homologous DNA sequences in order to exchange nucleotide sequence between damaged and donor DNA molecules. HR repair mechanism is conserved across all three domains of life as well as viruses, highlighting its importance in DNA maintenance, and so are the fundamental steps of its functioning. In brief, after a DBS occurs, sections of DNA around the 5' ends of the break are cut away (resection). The following step is the strand invasion, consisting in an overhanging 3' end of the broken DNA molecule which invades a similar or identical intact DNA molecule. Then, the second 3' overhang, not involved in previous strand invasion, forms a Holliday junction with the homologous chromosome and the double Holliday junctions are further converted into recombination products by single-strand nicking endonucleases (Fig.1.21). The DSBR pathway usually ends in crossover. The eventual ending of DSBR in crossover depends on how the double Holliday junction is resolved, in fact chromosomal crossover will occur if one Holliday junction is cut on the crossing strand and the other Holliday junction is cut on the non-crossing strand. Alternatively, if the two Holliday junctions are cut on the crossing strands, then chromosomes without crossover will be produced (Boyle, 2008). Generally, HR occurring as DNA repair mechanism tends to result in non-crossover products, as the goal is to restore the damaged DNA molecule as it was before the DSB.

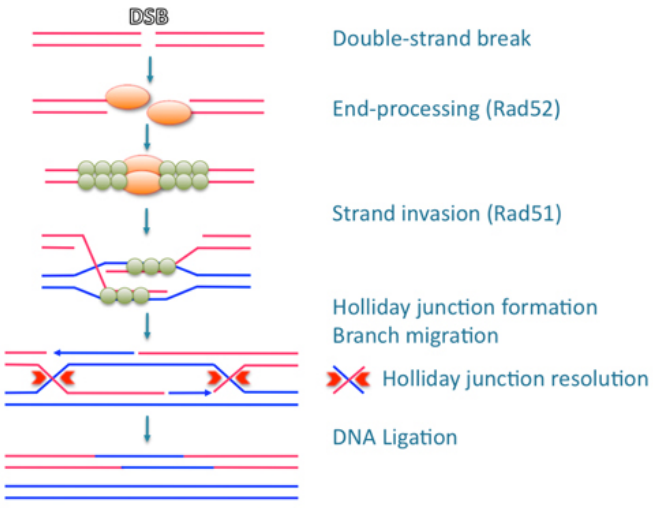

Fig.1.21 Schematic representation of DSB repair mechanism by HR and Holliday junction resolution. Figure taken from (https://www.biochem.mpg.de/en/rg/biertuempfel/research).

On the other hand, NHEJ does not require any donor homologous DNA. This mechanism is based on the direct ligation of the break ends and is therefore known as an error-prone mechanism where nucleotides can be lost or added, often leading to imprecise repair with the generation of insertions or deletions (InDels). Only if DSB is "clean" and broke ends are compatible, the repair through NHEJ is non-mutagenic. NHEJ mechanism of repair has been conserved during evolution and is the predominant repair pathway in mammalian cells (Guirouilh-Barbat *et al.*, 2004). The necessary elements for NHEJ mechanism functioning are DNA-dependent protein kinase (DNA-PK), XRCC4 protein and DNA ligase IV (Takata *et al.*, 1998). The DNA-binding subunit of DNA-PK is named Ku and is composed of two different subunits, Ku70 and Ku80, named on their molecular weight, which are recruited on the DSB site and assemble with the core subunit DNA-PKcs. Then, NHEJ factors are recruited for DSB processing and final ligation (Fig.1.22).

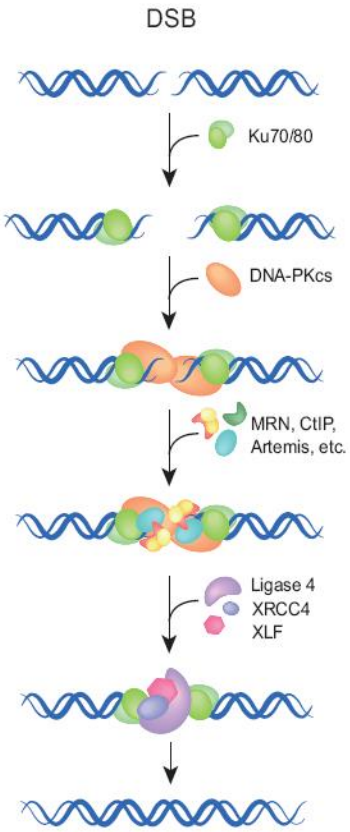

Fig.1.22 Schematic representation of non-homologous end joining (NHEJ) pathway. Figure taken from (http://tcr.amegroups.com/article/view/1152/html).

In the last decade, the most known and diffused genetic engineering tools are Zinc-finger nucleases (ZFNs), TAL effector-like nucleases (TALENs) and clustered regularly interspaced short palindromic repeats (CRISPRs). The main difference between these three technologies is that ZFNs and TALENs recognize target DNA sequence in a modular fashion, requiring the generation of a new

set of nucleases for each DNA target. On the other hand, CRISPRs are RNA-guided endonucleases, meaning that the effective domain is independent from the RNA guide, which can therefore be changed easily for each DNA target. The most discussed issue about these powerful technologies is the possibility of off-target effects. Though CRISPRs are more error-prone because of their RNA-recognition mechanism, there are different protocols and online-tools to predict off-target effects and in practice, there are substantial fidelity and specificity issues. As for ZFNs and TALENs, many studies have failed to find any evidence of off-target cleavage activity (West e Gill, 2016).

1.8.2 Most common site-specific nucleases (SSN) features and their applications

Zinc-finger nucleases (ZFNs) are made of a customizable site-specific DNA-binding domain associated with a nonspecific DNA cleavage domain derived from FokI restriction enzyme (Fig.1.23). The FokI cleavage domain needs to dimerize to be activated, so two different ZFN monomers, binding each to one DNA strand (forward and reverse), are needed to produce the DSB. The sequences recognized by the two ZFN monomers are flanking the target sequence of interest and are separated by a 5 to 7 spacer sequence. The DNA binding domain of each monomer can recognize a 3 bp sequence, so that several domains in tandem can bind a proportionally long target sequence. Usually, 3 to 6 ZFN domains are used to generate a single subunit able to bind a DNA sequence of 9 to 18 bp. The main disadvantage of ZFNs is the relatively low number of targets, due to their complex pattern of sequence recognition. Moreover, only a relatively low percentage of ZFNs are capable to generate efficiently a double strand break, and they are often in guanine-rich regions (e.g. 5'-GNN-3'), allowing the presence of targets likely to be cut only once every 100 bp (Kim *et al.*, 2009). This is not a problem in case of knockout experiment, but could be a great limitation in case of precise insertions, deletions or substitution needed at the target site. Finally, ZFNs have generally low cleavage efficiencies, can show a cytotoxic effect due to off-targets and are challenging to design. The main advantage of ZFNs is their mammalian origins, so that they have a low immunogenicity compared to bacterial-derived nucleases.

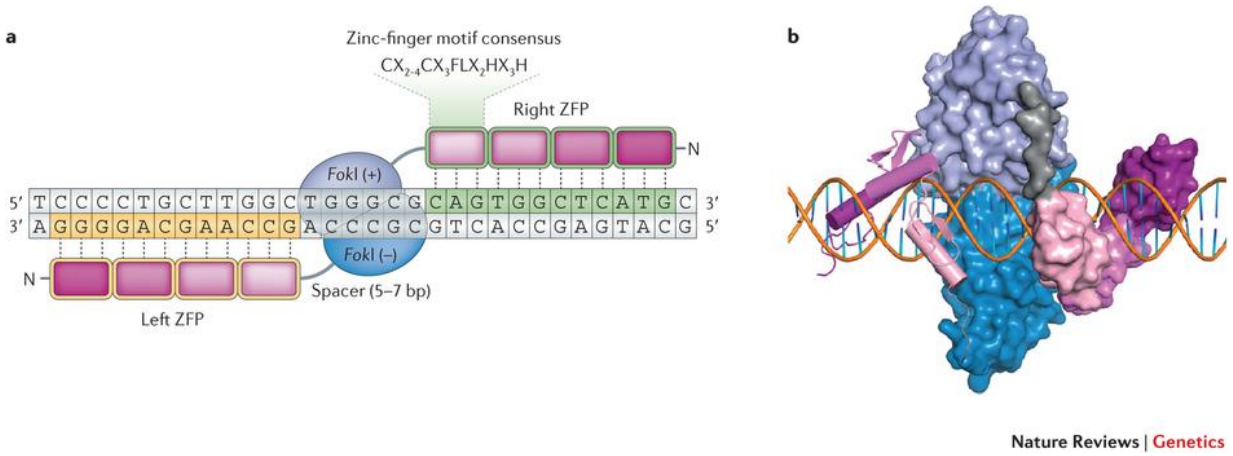

Fig.1.23 Zinc-finger nucleases. A) A schematic representation of a zinc-finger nuclease (ZFN) pair. Each ZFN is composed of a zinc-finger protein (ZFP) at the N and the FokI nuclease domain at the C terminus. In the zinc-finger motif consensus, X represents any amino acid. Generally, target sequences are 18–36 bp in length, excluding spacers. B) In silico model structure of a ZFN pair bound to DNA. Each zinc-finger is shown in shades of pink in ribbon (left) and space-filling (right) representations. The grey region represents the linker between the DNA-binding and catalytic domains. The FokI catalytic domains are shown in blue and purple at the centre using space-filling representations. Part b is modified, with permission, from Ref. 191 © (2011) Genetics Society of America. Figure taken from (http://www.nature.com/nrg/journal/v15/n5/fig_tab/nrg3686_F2.html).

Transcription activator-like effector nucleases (TALENs), like ZFNs, consist of a customizable site-specific DNA-binding domain associated with a nonspecific DNA cleavage domain derived from FokI restriction enzyme. The main difference compared to ZFNs is in the DNA-binding domain, which is known as transcription activator-like effector, derived from a species of plant pathogenic bacteria. The DNA-binding domain arrays recognize 1 to 1 the nucleotides of the DNA target sequence in the major groove, and is 33 to 35 bp long. The two amino acids in position 12 and 13 confer specificity and are known as repeat variable diresidues (RVD) (Fig.1.24). These characteristics allow the design of specific TALENs for ideally any given DNA sequence. TALENs are easier to design compared to ZFNs, but their large size can limit their delivery and expression, especially in mammalian cells where AAV-delivery is often used.

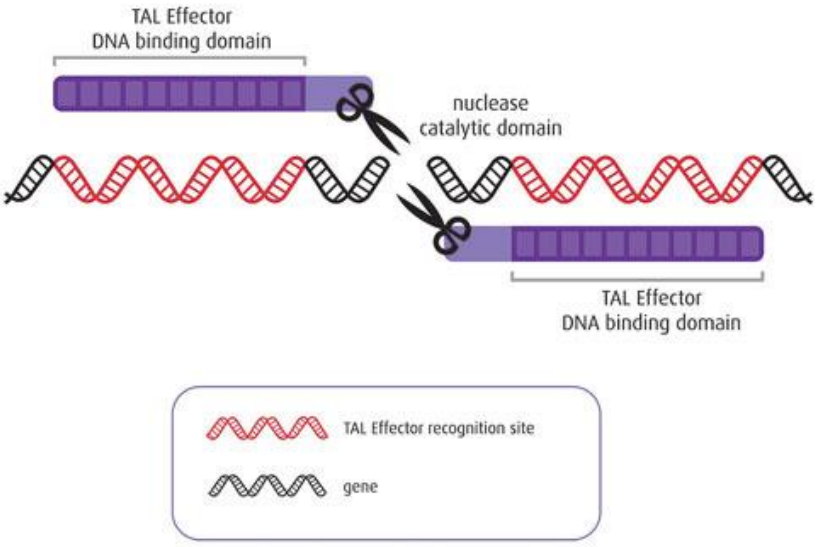

Fig.1.24 Schematic representation of TALENs nucleases structure. Figure taken from (http://www.cellectis.com/).

Clustered regularly interspaced short palindromic repeats (CRISPR)/Cas9 naturally exist as an adaptive immune system in bacteria and archaea and its functioning is based on the capture 20-nucleotides sequences of foreign DNA from invading phages or plasmids. These acquired sequences are termed protospacers and are transcribed to form the target-specific crRNA; trans-activating RNA (tracrRNA), which is not dependent on the target sequence, is also transcribed. These two RNA components and the CRISPR-associated protein 9 (Cas9) form the active form of the site-specific nuclease, able to cleave any DNA sequence that match the protospacer. The most used CRISPR/Cas9 system is the one from *Streptococcus pyogens*, which is characterized by a 23-nucleotide target sequence, where 20-nucleotide sequence is the protospacer and 3-nucleotide sequence is known as the protospacer-adjacent motif (PAM), recognized by the Cas9 itself (Fig.1.25). The synthesis of designable RNA guides, associated with Cas9 protein, can ideally cleave any DNA sequence with a downstream PAM. CRISPR/Cas9 are simple to design and produce and their specificity is based on small RNA molecules rather than on DNA-binding proteins as for ZFNs and TALENs. Moreover, Cas9 protein is independent from the target sequence. The major disadvantage of this system is the large size, and off-target effect are not yet well defined (Lee *et al.*, 2016).

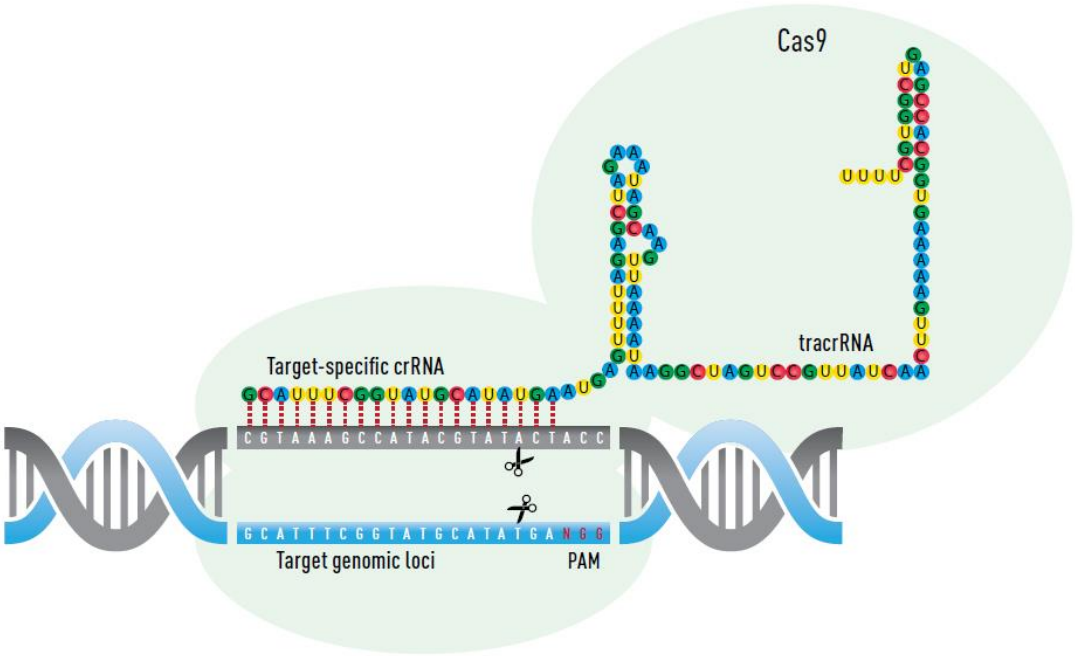

Fig.1.25 Schematic representation of CRISPR/Cas9 structure. Figure taken from (https://www.thermofisher.com/it/en/home/technical-resources/technical-reference-library/genome-editing-support-center/crispr-based-genome-editing-support/crispr-based-genome-editing-support-getting-started.html).

As for the efficacy, ZFNs usually have a low level of specific activity, whereas TALENs has been reported to range from 1% to 60% and CRISPRs from 3% to 79% in cultured mammalian cells. On the other hand, considering the safety of the three different site-specific nucleases, from a theoretical point a nuclease that recognize a 16 bp target sequence should eliminate the possibility to cleave at off-target sites, because the complexity of 16-bp sequences (4^{16} = 4.3 x 10^9) is greater than the size of the human haploid genome (3.2 x 10^9). Practically, each of the three types of nucleases, even with a targeting sequence of 16 bp or more, have shown some off-target effects (Lee *et al.*, 2016).

	ZFN	TALEN	RGEN (CRISPR/Cas9)
Recognition site	18-36 bp per ZFN pair	30-40 bp per TALEN pair	23 bp (20-bp guide sequence + 3-bp PAM)
Restriction in target site	G-rich	Start with T	End with NGG (NAG: lower activity) sequence
success rate	Low	High	High
off-target effects	High	Low	Variable
cytotoxicity	Variable to high	Low	Low
Size	~1 Kb x 2	~3 Kb x 2	4.2 Kb (Cas9) + 0.1 Kb (sgRNA)
ease of engineering	Difficult	Moderate	Easy
ease of multiplexing	Low	Low	High

Tab.1.3 Comparison of three classes of designed nucleases. ZFN, zinc-finger nuclease; TALEN, transcription activator-like effector nuclease; RGEN, RNA-guided engineered nuclease; CRISPR, clustered regularly interspaced short palindromic repeat; Cas9, CRISPR-associated protein 9; sg RNA, single-chain guide RNA. Figure taken from (Lee *et al.*, 2016).

In conclusion, site-specific nucleases have been developed as precious tools to enhance HR efficiency in mammalian cells, pushing cells towards the use of their own endogenous repair mechanisms to restore DSBs damages (Durai *et al.*, 2005). In particular, if a precise genome modification is needed, HR repair can be triggered giving a donor DNA with the mutation/gene of interest as template for DBS repair (i.e. targeting vectors, oligonucleotides). On the other hand, gene knockout can be rapidly achieved by activation of NHEJ, following site-specific DSBs. CRISPR/Cas9 is nowadays the most used technique thanks to its easy design and production, feasibility in applications and moderate to high efficiency. On the other hand, TALENs are still largely used thanks to their reliability and low off-target effects, due to the double recognition site needed in order to produce the DSB.

2. Aims of the study

- Since the swine Surf1 sequence annotated in public databases is incomplete and not confirmed, it is necessary to sequence the entire gene in order to set up our genetic engineering experiments accurately.

- Disruption of swine Surf1 gene in porcine primary fibroblast cell lines in order to obtain Surf1 KO and heterozygous colonies.

- Generation of Surf1 KO and heterozygous animals through somatic cell nuclear transfer (SCNT) using selected fibroblast colonies obtained in the previous point as nuclear donor cells.

- Characterization of clinical pathological phenotype in Surf1 KO and potentially in heterozygous animals.

- Biochemical and molecular characterization of mitochondrial status and functioning in Surf1 KO animals.

- Morphological and immunoistochemical characterization of Surf1 KO tissues, with particular focus on tissues known to be a specific target of Leigh Syndrome in patients.

3. Materials and methods

3.1 Animal experiments

All procedures involving the use of animals in this study were carried out in accordance with the Italian Law (D.Lgs 26/2014) regulating animal experimentation and after the approval of the local ethical Committee of AVANTEA (Comitato Etico del Laboratorio di Tecnologie della Riproduzione) and by the Ministry of Health (Aut. Min. n° 606/2016-PR).

3.2 Chemicals

All chemicals and reagents were from Sigma (Milan, Italy), unless otherwise stated.

3.3 Sequencing of swine Surf1 gene

Sequential reverse primers (S1R6, S1R5, S1R4, S1R3, S1R2, S1R1, S1R, S1Rlong) were used in association with two forward primers (S1F, S1Flong) in order to obtain the whole genomic sequence amplification of swine Surf1 gene using genomic DNA of cell line ID6639 as a template. The PCR amplification of the entire region of interest obtained (primers S1Flong + S1Rlong, 4582 bp) was cloned into TOPO-TA vector (Invitrogen, Thermo Scientific, Waltham, MA USA), transformed into competent DH5α strain of E. coli and Sanger-sequenced (GATC BIOTECH, Constance, Germany). Exons 1-9 sequences were further confirmed by RT-PCR (primers S1F+S1R) of cDNA of the same cell line (ID6639). To obtain the cDNA, *in vitro* cultured cells in active replication (80% confluence) were washed twice with PBS and harvested by direct application of solution D added with β-mercaptoehtanol in the culture dish. The RNA extraction was performed as previously described (Chomczynski e Sacchi, 1987). Retrotranscription of RNA was performed with RevertAid H Minus First Strand cDNA Synthesis Kit (Thermo Scientific, Waltham, MA USA) and RNA quality was assessed through the visualization of ribosomal RNA bands on a denaturing agarose gel, in addition to performing an RT-PCR on an house-keeping

gene (β actin). The specifications of primers used for the sequencing of swine Surf1 gene are listed in Tab.3.1 below.

ID	Strand (Fw/Rv)	Sequence (5' – 3')
S1F	Fw	atggcggcgcggtggctggg
S1Flong	Fw	atggcggcgcggtggctggggc
S1R6	Rv	cctttggcctggggacatgg
S1R5	Rv	cgccgaactggagtccagga
S1R4	Rv	ggggcactttgaccactcca
S1R3	Rv	cgcccacgttgtcactccct
S1R2	Rv	cgtggggatggtgaggctga
S1R1	Rv	ccccgttggaggacagacca
S1R	Rv	ggcggcctcctgcggtgtga
S1Rlong	Rv	tgaggcggcctcctgcggtgtga

Tab.3.1 Specifications of primers used along the swine Surf1 sequencing process.

The amplification conditions of the whole swine Surf1 gene by PCR are here specified. PCR reaction was performed with S1Flong and S1Rlong primers. Amplification was performed in 12.5 µL reaction volume (dNTPs 2.5 mM, primers 25 µM each, La Taq Takara 5U/µL, Buffer GCI 2X, Nuclease-free H2O to volume) and thermal cycler programme was a touchdown cycle characterized by 94°Cx2' as initial denaturation, 8 cycles: 94°Cx30", 72°Cx30"-1°C/cycle, 72°Cx5' and 32 cycles: 94°Cx30", 65°Cx30", 72°Cx5'+5"/cycle, followed by a final elongation at 72°Cx7'. The predicted specific PCR product is 4582 bp.

As for the RT-PCR, the reaction was performed with S1F and S1R primers. Amplification was performed in 12.5 µL reaction volume (dNTPs 2.5 mM, primers 25 µM each, La Taq Takara 5U/µL, Buffer GCI 2X, Nuclease-free H2O to volume) and thermal cycler programme was a touchdown cycle characterized by 94°Cx2' as initial denaturation, 3 cycles: 94°Cx30", 72°Cx30"-1°C/cycle, 72°Cx1' and 37 cycles: 94°Cx30", 70°Cx30", 72°Cx1', followed by a final elongation at 72°Cx7'. The specific PCR product is 921 bp.

3.4 Swine Surf1 gene disruption

3.4.1 Cell isolation and culture

Cell culture medium was DMEM/TCM199 (1:1) with 10% Fetal Bovine Serum (FBS) and bFGF (5 ng/ml). Culture conditions were 38.5°C under controlled atmosphere with 5% CO_2 and 5% O_2. Primary porcine fibroblast cultures were derived from adult Large White female (ID: 167) and male (ID6639) ear biopsies (Pig Adult Fibroblasts, PAFs) and 40-day-old male foetuses biopsies (Pig Foetal Fibroblasts, PFFs originating from a clone of ID6639, see below) by cutting the biopsies in small pieces with a scalpel blade. Tissue pieces were plated in triplicate in 60-mm culture dishes with 2 ml of DMEM/TCM199 (1:1) supplemented with 20% Fetal Bovine Serum (FBS). Cells were allowed to grow until 50% of confluence with complete medium changes every 3 days, then tissue fragments were removed and cells sub-cultured in 4 ml of DMEM/TCM199 (1:1) supplemented with 10% FBS and bFGF (5 ng/ml) until 80% of confluence. Cells were then cryopreserved at early passages in DMEM/TCM199 (1:1) with 20% FBS and 10% DMSO and stored in liquid nitrogen. These batches were used throughout the experiments. The same procedure was followed for the setting up of Surf1genome-edited animals' cell lines bank.

3.4.2 Site-specific nucleases design and validation

TALEN vectors design and production was outsourced to Genecopoeia (www.genecopoeia.com) in order to target exon 3 and exon 4 of the swine Surf1 gene (GenBank: AK391958.1). The detail of swine Surf1 exon 3 and exon 4 sequences targeted by TALENs is illustrated in Fig.3.1. Three different pairs of TALENs were obtained: GT-EN-12532-01L+R (Tal01), GT-EN-12532-02L+R (Tal02), GT-EN-12532-03L+R (Tal03). TALENs repeated variable dinucleotides (RVDs) sequences details are listed in Tab.3.2.

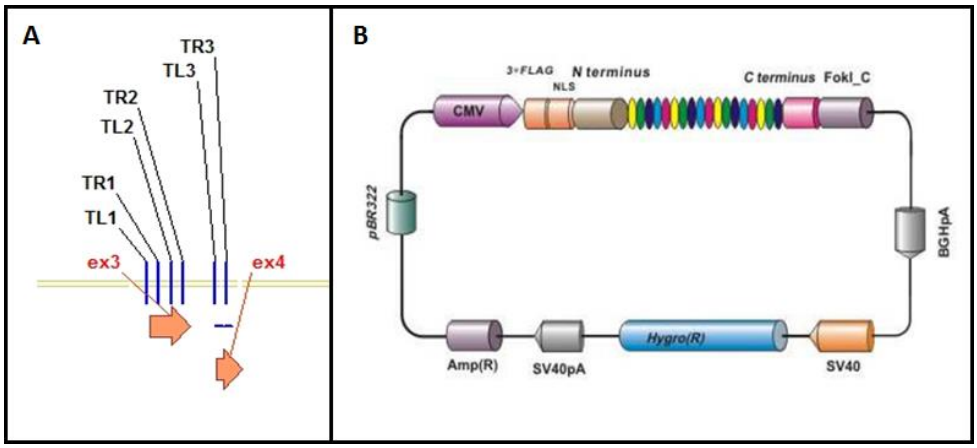

Fig.3.1 TALENs nucleases details. Schematic representation of A) TALENs target positions on swine Surf1 exons 3 and 4 and B) TALENs vector map purchased from Genecopoeia (www.genecopoeia.com).

ID	Arm (L/R)	Sequence
GT-EN-12532-01L (Tal01L)	L	HD NG HD HD NG NI NN NN NN HD NN NN NN HD HD NG NN
GT-EN-12532-01R (Tal01R)	R	NG HD NI NN HD NG NN NI NI NN NI NN HD NG NN HD HD
GT-EN-12532-02L (Tal02L)	L	NG NG HD NG HD HD NI NN NG NN NN NG NG NG HD NG NI
GT-EN-12532-02R (Tal02R)	R	HD HD HD HD NI NN NN HD HD NI NI NI NN NN HD NI NN
GT-EN-12532-03L (Tal03L)	L	NI NN NN NG HD HD NI NN HD NN NG HD NN NN NI NI NN
GT-EN-12532-03R (Tal03R)	R	NN NN NI HD NG HD HD NI NN NG NG HD NN NN HD NN NI

Tab.3.2 TALENs repeated variable dinucleotides (RVDs) sequence details.

For the validation of the three pairs of TALENs, cell line ID6639 was transfected (Nucleofector TM, LONZA, Basel, Switzerland). For each transfection, $1*10^6$ fibroblasts were used and 2µg for each TALEN arm was used. A separate transfection was performed for each TALEN pair (Tal01, Tal02, Tal03). Nucleofector program was V024. Seventy two hours post-transfection, the pool of cells obtained for each experiment was washed twice with PBS and lysed through direct application of cell lysis solution (100 mM Tris HCl pH 8.3, 5 mM EDTA pH 8.1, 0.2% SDS, 200 mM NaCl) supplemented with 100 µg of Proteinase K/ml (Macherey-Nagel, Germany). Each pool

was then processed for genomic DNA extraction (Sambrook *et al.*, 1989), re-suspended in 50 µL of TE buffer and quantified using the Qubit fluorometric assay (Invitrogen, S. Giuliano Milanese, Italy). A specific PCR targeting the genomic sequence of interest was made using S1T Forward primer (5'gagcctccacttctttgtcc3') and S1T Reverse primer (5' ccgcagagtgagtgtatgtgg3'). The PCR product of 375 bp was used as template for the Surveyor® Assay (IDT Surveyor® Mutation Detection Kit, Iowa, USA) in order to evaluate TALENs efficiency.

Two different CRISPR/Cas9 single-guides RNA (sgRNA) were designed to target swine Surf1 exon 3 according to the software CRISPR Design Tool (www.crsipr.mit.edu). Details of CRISPRs guide sequences are listed in Tab.3.3. Complementary oligonucleotides were annealed to generate duplex and cloned in the CAG-hspCas9-H1-gRNA linearized Smart Nuclease vector according with the user manual (CAS920A-1 System Biosciences, Fig.3.2). As the two different RNA guides were designed through a software that predicted their cutting efficacy as "high", the two corresponding vectors were directly used for transfection experiments.

ID	Strand (Fw/Rv)	sgRNA Sequence (5'-3')
♯Guide1	Fw	tgtatgagaccacacgatgatgcctttctccag
♯Guide1	Rv	aaacctggagaaaggcatcatcgtggtctca
♯Guide2	Fw	tgtatgagaccacggcatcatcgtgcgcttttg
♯Guide2	Rv	aaaccaaaagcgcacgatgatgccgtggtctca

Tab.3.3 Details of CRISPRs guides sequences targeting exon 3 of swine Surf1 gene.

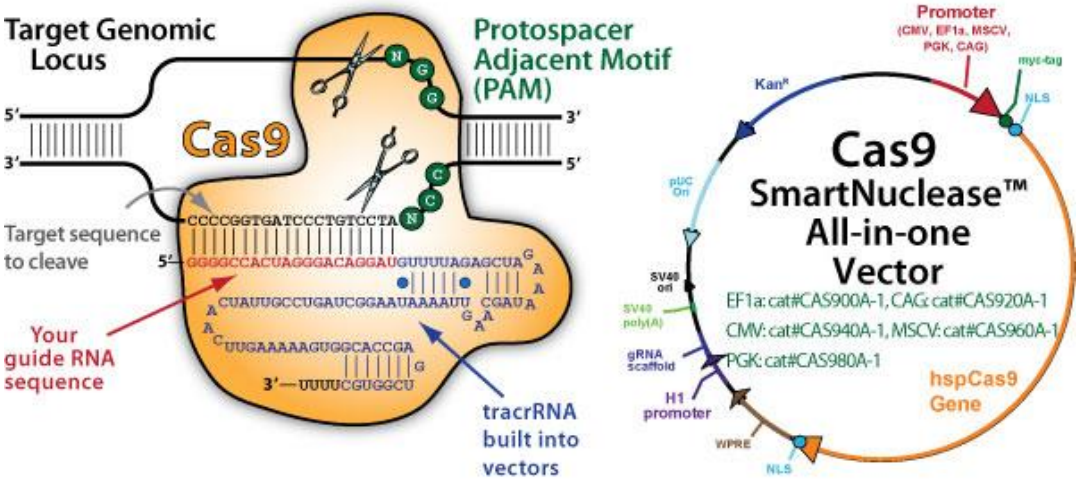

Fig.3.2 Cas9 Smart Nuclease all-in-one vector scheme from producer. Figure taken from (https://www.systembio.com/)

3.4.3 Homologous recombination (HR) vector construction

Genomic DNA was extracted from pig fibroblasts (ID6639) and a PCR product covering the Surf1 region between exon 2 and exon 5 was cloned into the pSMART-GC-HK vector (Sigma-Aldrich). An inside-out PCR was performed, using primers with adapted ends (NotI restriction enzyme cutting site included) flanking exon 3 in order to delete 106 bp of exon 3. The resulting linear construct was re-ligated by Gibson assembly (New England Biolabs, Ipswich, MA). Finally, a loxable puromycin resistance cassette was cloned into the vector thanks to the newly created NotI site. This vector targets swine Surf1 exon 3 by exploiting homology regions upstream (exon 2) and downstream (exon 4 and exon 5) in order to exchange wild type exon 3 with the 106 bp-deleted version of exon 3 present in this vector and thus making a null allele at the insertion site (Fig.3.3). This HR vector is used to enhance homologous recombination repair after DSBs induced by site-specific nucleases have occurred and to have a selectable marker to enrich for genome-edited cells.

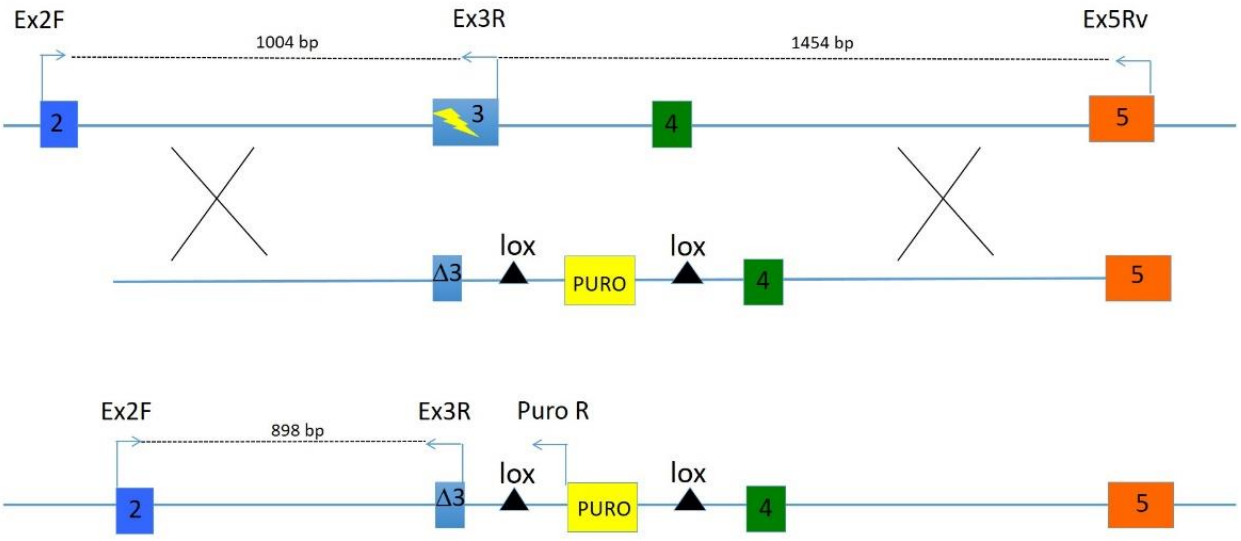

Fig.3.3 Production of an HR vector carrying a deleted version of Ex 3 and a loxable PuroR cassette.

3.4.4 Transfection of pig fibroblasts and screening

PAFs were thawed two days before the transfection experiment in order to have $1*10^6$ cells/transfection. For TALENs transfection experiments, on the day of the experiment, cells were trypsinized, counted and re-suspended in the suggested amount of Nucleofector TM solution (Basic Nucleofector TM Kit, Primary Fibroblasts, LONZA, Basel, Switzerland) supplemented with 2 μg of each TALEN plasmid (L+R) and 1 μg of HR vector. For CRISPRs transfection experiments, cells were prepared as above and Nucleofector TM solution was supplemented with 3 μg of the CAG-hspCas9-H1-gRNA vector alone (to enhance NHEJ) or with the addition of 2 μg HR vector (to enhance HR) in co-transfection experiments. In all transfection and co-transfection experiments, Nucleofector program used was V-024 (Brunetti *et al.*, 2008). For clonal isolation and selection, approximately 150 transfected cells were plated in each 150-mm culture dish with fresh culture medium (day 0) and after 24 hours puromycin (was 1 μg/ml) was added for antibiotic selection (day 1). A 60-mm culture dish with non-transfected cells of the same line was used as control for antibiotic selection, in order to detect on which day of selection all non-transfected cell were dead. On day 8 after transfection, puromycin-resistant colonies were picked up and transferred into 24-well dishes with fresh culture medium. For each colony, an aliquot was cryopreserved at - 80°C for eventual SCNT and the remaining cells were PCR-analysed and sequenced, respectively for the integration of the targeting vector and for the presence of InDels.

Due to nucleases (CRISPRs and TALENs) different efficiency and taking into account the various goals of our study, the experimental design was split in one single-step experiment involving TALENs, and one two-step experiment using CRISPRs (Fig.3.4). TALENs transfection experiments, except for the initial transient transfections necessary to validate the nucleases, were performed co-transfecting both the nuclease plasmid and the HR vector as described above, in order to obtain both one-step biallelic Surf1 KO colonies and heterozygous colonies to be directly used in SCNT. This was possible thanks to the high cleavage efficiency of our TALENs, Tal01 in particular. Colonies were PCR-analysed for NHEJ-derived mutations (primers S1T F + S1T R, see Tab.3.4) and for the integration of HR vector (primers Ex2F + PuroF2, see Tab.3.4). The presence of small to moderate insertions or deletions (InDels) due to NHEJ in the non-targeted allele was confirmed by Sanger sequencing. As for CRISPRs experiments, a two-step protocol was needed to obtain biallelic Surf1 KO colonies. The first step of transfection with CAG-hspCas9-H1-gRNA vector alone (no HR vector) lead to the generation of colonies with possible NHEJ-derived InDels. Colonies where partially lysed for genomic DNA extraction, PCR-amplification (primers S1T F + S1T R, see Table 3.4) and Sanger sequence. Confirmed NHEJ-mutated colonies were used for first

step-SCNT for the production of foetuses. Rejuvenated fibroblasts derived from these foetuses were genotyped and used for a second round of co-transfection (HR vector + CAG-hspCas9-H1-gRNA 1:1). Puromycin resistant colonies were PCR-screened for the detection of HR vector integration as previously described (primers Ex2F + PuroF2, see Table 3.4). NHEJ-mutated colonies were also used in SCNT experiments for the generation of heterozygous piglets. Sequencing analysis were carried out at GATC Biotech (Constance, Germany). See Tab.3.4 for relevant PCR analysis specifications.

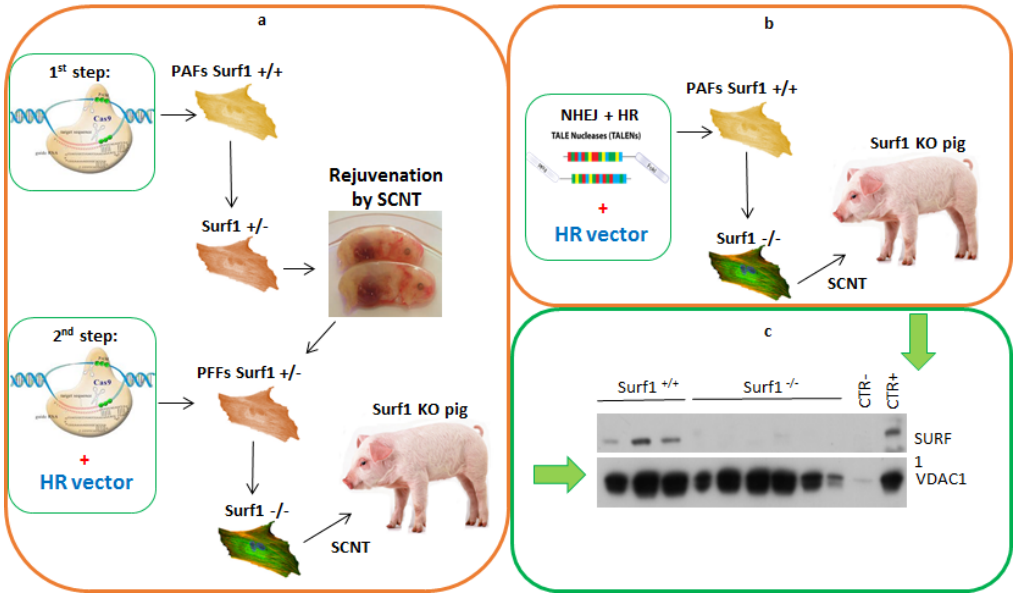

Fig.3.4 Schematic representation of experimental designs for the generation of Surf1 KO pigs through A) 2-step transfection with CRISPR/Cas9 technology and HR vector. B) Single-step transfection with TALENs technology and HR vector, in association with SCNT. C) Example of Western Blot analysis confirming the absence of Surf1 protein in Surf1 KO pigs, compared to wild type controls.

Primers (sequence)	Aim	Amplification cycle	PCR product
Ex2F Forward (5'cgtcgggaggagcgtccttg3') + PuroF2 Reverse (5'tcatgagtgggaggaatgagctgg3')	Detection of HR vector insertion	Touchdown cycle 94°Cx2' 8 cycles: 94°Cx30", 68°Cx30"-1°C/cycle, 72°Cx1'45" 30 cycles: 94°Cx30", 60°Cx30", 72°Cx1'45" 72°Cx7'	1237bp
S1T Forward (5'gagcctccacttctttgtcc3') + S1T Reverse (5'ccgcagagtgagtgtatgtgg3')	Colony screening and sequencing	Standard cycle 94°Cx2' 35 cycles: 94°Cx30", 60°Cx30", 72°Cx30" 72°Cx7'	375bp

Tab.3.4 Most relevant PCR analysis details. Amplification for all PCR reactions was performed in 12.5 µL reaction volume composed as follows: dNTPs 2.5 mM, primers 25 µM each, La Taq Takara 5U/µL, Buffer GCI 2X, Nuclease-free H_2O to volume.

3.5 Somatic Cell Nuclear Transfer (SCNT)

Oocyte recovery and *in vitro* maturation, preparation of nuclear donor cells and SCNT were performed as previously described (Lagutina *et al.*, 2006) with minor modifications. Briefly, ovaries of pubertal gilts were collected at a local abattoir and transported to the laboratory at 31°C-33°C. Follicles larger than 3 mm were aspirated, cumulus-oocyte complexes with an adequate morphology were selected and *in vitro* matured at 38.5 °C in 5% CO_2 in humidified atmosphere for 42 hours in TCM199 (Life technologies) supplemented with 10% FCS, 147 μg/ml alanyl glutamine, 75 μg/ml kanamycin, 2.1 mg/ml sodium bicarbonate, 1 μl/ml ITS media supplement (insulin, transferrin, and sodium selenite; Corning), 5 ng/ml bFGF, 110 μg/ml sodium pyruvate, 75 μg/ml ascorbic acid, 100 μg/ml glutamine, 5 μg/ml myoinositol, 25 μg/ml PVA, 0.4 mM cysteine (Sigma), 0.6 mM cysteamine (Sigma), 0.05 IU/ml FSH + 0.05 IU/ml LH (Meropur, Ferring spa), 100 μg/ml human Long R3 IGF-I (Sigma) and 50 μg/ml human Long R3 EGF (Sigma). The day before SCNT, selected nuclear donor genome-edited fibroblasts were induced into quiescence by serum starvation (0.5% FCS). The day of SCNT, cells were trypsinized, washed and resuspended in SOF (Tervit *et al.*, 1972) supplemented with 25mM Hepes and amino acids (SOF-Hepes). At the end of maturation process, only matured oocytes were selected (presence of an extruded polar body). NT-embryos were reconstructed following a modification of the zona-free method (Vajta *et al.*, 2010), where the *zona pellucida* was digested with 0.5% pronase in PBS. All manipulations were performed in SOF-Hepes with 10% FCS. Enucleation was performed following a 5 minutes exposure to cytochalasin B (7.5 μg/ml) and Hoechst (5 μg/ml), and enucleated cytoplasts were then rinsed in phytohemagglutinin P in PBS and quickly dropped over a single nuclear donor cell. Donor cell-cytoplast couples were washed in 0.3 M mannitol solution and fused by double DC-pulse of 1,2 KVolts/ cm and returned into maturation medium. After two hours, at about 48 hours from the beginning of maturation, NT embryos were activated by double DC-pulses (Lagutina *et al.*, 2006), followed by two hours culture in maturation medium supplemented with cycloheximide (10 μg/mL) and cytochalasin B (5 μg/mL) to avoid polar body extrusion. At the end of the activation, reconstructed embryos were cultured in mSOF supplemented with essential and non-essential amino acids and with 4 mg/mL BSA, in a modification of the Well Of the Well system (Vajta *et al.*, 2000) and the culture was continued as described in (Lagutina *et al.*, 2006) until D+6 when they reached the late morula or blastocyst stage suitable for transfer to synchronised surrogate recipients. Nuclear donor cells utilized were from selected colonies and from characterized Surf1 KO piglet (ID487) for re-cloning experiments.

3.5.1 Recipient sows synchronization, surgical Embryo Transfer (ET), post-implantation development and farrowing

Recipient sows of approximately 140 kg of weight were used. The estrus was synchronized by feeding 12 mg of altrenogest (Regumate, Intervet, Peschiera Borromeo, Italy) per sow for 15 days, followed by an injection of 0.15 mg of PgF2α (Dalmazin, Fatro, Ozzano Emilia, Italy) at the 13th day of altrenogest treatment and one of 1000 IU of hCG (Chorulon, Intervet, Peschiera Borromeo, Italy) 96 hours after the last altrenogest administration. SCNT embryos were surgically transferred to the uterus of synchronized sows under general anesthesia, on day 6 of development (compacted morula and blastocyst stages) through a mid-ventral laparotomy procedure (Swindle e Smith, 2015), seven days after hCG injection. Recipients were checked for pregnancy by trans-abdominal ultrasound examination 20 days after ET and pregnancy were confirmed around day 60 post-ET. Similar protocols are described by (Stevenson e Davis, 1982; Davis *et al.*, 1985; Wood *et al.*, 1992; Kaeoket, 2008). Farrowing was induced by a PgF2α (Dalmazin, Fatro, Ozzano Emilia, Italy) injection on day 119 and 120 of gestation to optimise assistance of personnel and maximise the survival of the piglets. Piglets were weighted at birth and proper weight gain was monitored every 3 hours for the first week, then once a day until weaning (28 days). Immediately after birth, piglets were taken care of and assisted in colostrum assumption. Cobactan® (2 mL/25 Kg of live weight, Intervet Italia srl) intramuscular injections were given daily as preventive antibiotic treatment for the first week, whereas vitamin supplement injection (0.5 mL/animal, Selevit®, Fatro) and iron supplement injection (2 mL/animal, Endofer®, Fatro) were a given only once on second and third day after birth, respectively. Self-sufficient animals were allowed to remain with the mother, whereas weak and/or exceptionally small piglets were artificially fed. The humane endpoint was defined as lack of appetite, weight loss, dyspnea, persistent diarrhoea and lethargy. Animals who reached the humane endpoint were anesthetized (Zoletil®, Virbac, Carros, France) and euthanized with an intra-cardiac injection of Tanax® (0.3 ml/Kg of live weight, Intervet Italia srl), and tissue samples were collected within 30 minutes.

3.5.2 Univocal identification and genotyping of Surf1 piglets and specimens biobanking

Soon after birth, univocal ear tags were applied to all born animals and ear or tail biopsies were taken (from stillborn or alive piglets, respectively). A small piece of tissue was incubated at 55°C overnight with cell lysis solution (100 mM Tris HCl pH 8.3, 5 mM EDTA pH 8.1, 0.2% SDS, 200 mM NaCl) supplemented with 100 μg of Proteinase K/ml (Macherey-Nagel, Germany). Samples were then processed for genomic DNA extraction (Sambrook *et al.*, 1989), re-suspended in 500 μL of TE buffer and quantified using the Qubit fluorometric assay (Invitrogen, S. Giuliano Milanese, Italy). The same PCRs used for colony screening (see Tab. 3.4) were used for piglets' genotyping, and piglet/colony correspondence was established. The screening for HR vector integration was performed with primer Ex2F and PuroF2. PCR reaction for sequencing was performed with S1T F and S1T R primers (see Tab.3.4).

Ear or tail biopsies from Surf1 KO and heterozygous animals were also used to establish a cell bank of primary fibroblast cell lines as described in "3.4.1 Cell isolation and culture".

Tissue samples of Surf1 KO and heterozygous animals and age-matched controls were collected immediately after death and cryopreserved and/or fixed for further analysis. Numbers and specifications of sampled animals are listed in Tab.3.5. Cryopreservation was performed through isopentane-liquid nitrogen or liquid nitrogen alone snap freezing. Fixation was performed by immersion of specimens in 10% neutral buffered formalin and/or 4% paraformaldehyde. Tissue samples were also conserved in RNAlater® solution (Tab.3.6).

Genotype	M/F	Age (days)	N° sampled animals
Surf1 KO	M	Newborn	**26**
Surf1 KO	M	4-9	9
Surf1 KO	M	>9	2
Wild type CTR	M	Newborn	**13**
Wild type CTR	M	4-9	1
Wild type CTR	M	>9	12
Surf1 heterozygous	F	Newborn	2
Surf1 heterozygous	F	4-9	-
Surf1 heterozygous	F	>9	1

Tab.3.5 Surf1 KO and heterozygous animals and wild type controls sampled in this study. We considered "newborn" animals died in the perinatal period and at 1 day of age.

Tissue	Precooled isopentane	Liquid nitrogen	10% buffered formalin	4% paraformaldehyde	RNAlater
Brain	✓	✓	✓	✓	✓
Quadriceps	✓	✓	x	x	✓
Liver	✓	✓	x	x	x
Jejunum	✓	✓	x	x	x

Tab.3.6 Summary of Surf1 and control animals' specimens sampling.

3.6 Clinical phenotype assessment

Starting from the third day of post-natal life, piglets were daily tested for hind limb retraction and cranial-tibial reflexes. Any other phenotypical examinations were avoided because of the delicate nature of newborn piglets. Standard hematochemical blood test analysis, blood cell count and blood lactate measurements were performed on Surf1 KO, heterozygous and age-matched control animals' blood samples. TSH, FT3 and FT4 levels were also investigated. In newborn piglets, conspicuous blood samples (~10 ml) necessary for blood test analysis and blood cell count were collected immediately before Tanax® administration, after anesthesia, because of the small dimensions of animals. Blood lactate measurement were taken immediately after birth and then every 24 hours with Lactate Scout Analyzer (LSA) (Rocha *et al.*, 2015) in neweborn Surf1 KO and heterozygous animals and in age-matched controls. We chose to use this device in order to minimize the necessary amount of blood (LSA only requires 0.2 μL of capillary blood), and the stress related to this procedure. As no literature is available to date on newborn piglets blood lactate range, we considered our control animals as reference group for our analysis. Blood lactate levels in one longer-lived Surf1 KO animal (pig ID498 at 58 days of age) and two age-matched controls were assessed through Lactate reagent kit (Sigma) from ear vein blood sample in order to avoid complications related to pad puncture of heavier animals.

3.7 Mitochondrial state and functioning

3.7.1 Spectrophotometric biochemical analysis on MRC enzymes activity

Biochemical assays of individual respiratory complex activities were carried out on tissue homogenates and on cell lysates (Tiranti *et al.*, 1995). Briefly, approximately 50 mg of frozen tissues were cut into small pieces and homogenized in 10 volumes of cold homogenization medium (0.075 M sucrose, 0.225 M mannitol, 1 mM ethylene glycol tetra-acetic acid (EGTA), 0.01% bovine serum albumin (BSA), pH 7.4) through Dounce-type glass homogenizer with a manually driven glass pestle. Samples were then centrifuged at 800xg for 5 minutes, supernatant was transferred in clean tubes and three cycles of freeze-and-thaw were performed immediately before mitochondrial respiratory complexes activity measurements. As for cell lysates, cells were harvested by trypsinization, washed twice with PB and resuspended in 2 ml MOPS-sucrose buffer. Digitonin (200 µg) was added and samples were incubated on ice for 5 minutes. After centrifugation at 5000xg for 3 minutes, the pellet was resuspended in 1.5 ml of 1 mM EDTA, MOPS-sucrose buffer. After a second 5 minutes incubation on ice, cells were centrifuged at 10000xg for 3 minutes and pellet was resuspended in 0.5 ml of 10 mM K-phosphate buffer, pH 7.4 and frozen-thawed three times, immediately before starting the spectrophotometric assays.

The activity of complex I, II, III and IV were individually evaluated. Specific activities of each complex were normalized to that of citrate synthase (CS), representative of the number of mitochondria.

3.7.2 Mitochondria isolation

Standard methods were used for the preparation of mitochondrial and post-mitochondrial fractions from pig tissue (brain, muscle and liver) (Fernandez-Vizarra *et al.*, 2002). The mitochondria extraction and following washings were performed using cold homogenization medium AT (0.075 M sucrose, 0.225 M mannitol, 1 mM ethylene glycol tetra-acetic acid (EGTA), 0.01% bovine serum albumin (BSA), pH 7.4). The liquid nitrogen-frozen tissue samples were weighted, cut into small pieces and washed to remove blood and connective tissue. The tissue pieces were then homogenized with 10–15 strokes using a Dounce-type glass homogenizer with a manually driven glass pestle, adding 5 ml of homogenization medium AT per gram of starting material. The sample was centrifuged at low speed (1000 xg for 5 min at 48°C) and the resulting

supernatant was transferred to a clean tube and spun at high speed (9000 xg for 10 min at 48°C). The resulting supernatant containing the cell cytosolic fractions was discarded. To further clean the mitochondrial pellet obtained, it was re-suspended with 5 ml of homogenization medium AT, transferred to 1.5 ml Eppendorf tubes and washed to obtain a single pellet. The pellet containing free mitochondria and synaptosomes was re-suspended in the appropriate volume of MAITE medium (25 mM sucrose, 75 mM sorbitol, 100 mM KCl, 0.05 mM EDTA, 5 mM MgCl2, 10 mM Tris–HCl, 10 mM H3PO4, pH 7.4).

3.7.3 Western blot, Blue Native PAGE and In-Gel Activity

Western blot analysis, performed on electroblotted denaturing sodium-dodecyl sulphate polyacrylamide gel electrophoresis (SDS–PAGE), and two-dimension blue native electrophoresis (2D-BNE) analysis were performed as previously described (Tiranti *et al.*, 1999; Nijtmans *et al.*, 2002). Approximately 100 mg of non-collagenous protein from tissue homogenates (quadriceps, liver, brain) were used for each sample in SDS-PAGE and 20 mg of isolated mitochondria from quadriceps samples were used in Blue Native PAGE (BN-PAGE). Chemiluminescence-based immunostaining (ECL kit, Amersham) was performed for protein-specific signal detection in both SDS-PAGE and BN-PAGE using the following antibodies: polyclonal Surf1 (abcam ab110256); monoclonal antibodies against subunits COX1 (Molecular Probes, Eugene, OR, USA), COX5a and COX4 (Mitosciences LLC, Eugene, OR, USA). Each antibody was previously tested for swine specific protein detection in wild type tissue preparations.

In-Gel Activity analysis were performed as previously described (Calvaruso *et al.*, 2008).

3.7.4 Mitochondrial morphology evaluation

Mitochondrial morphology was assessed following primary fibroblast cells staining with 10 nM Mitotracker CMX-Red (Invitrogen) for 30 min at 37°C. Fluorescence was visualized with a digital imaging system using an inverted epifluorescence microscope with Å~63/1.4 oil objective (Nikon, Japan). Images were captured with a back-illuminated Photometrics Cascade CCD camera system (Crisel).

3.8 Morphological analysis of pig brain, muscle and jejunum specimens

3.8.1 Histochemical and immune-histochemical analysis of quadriceps and jejunum specimens

Analyses were performed on formalin-fixed and paraffin-embedded brain tissues. Five-µm-thick serial sections were stained with haematoxylin–eosin and viewed by light microscopy. Tissues were frozen in liquid-nitrogen precooled isopentane and serial 8-µm-thick sections were stained for COX, SDH and NADH as previously described (Sciacco e Bonilla, 1996).

3.8.2 Histopathological and immune-histochemical analyses of brain specimens

Isolated brains were fixed by immersion in 10% buffered formalin, embedded in paraffin and 5-µm sectioned. For histological analyses, sections were stained with hematoxylin–eosin or Luxol Fast Blue/Hematoxylin and visualized under a light microscope (Leica Microsystem). For immunohistochemistry, sections were quenched for 30 minutes in methanol and 0.3% hydrogen peroxide. Antigen retrieval was performed by incubating the slides in 10 mM citrate buffer (pH 6.0) for 15 minutes. For immunofluorescence analyses, brains were fixed in 4% paraformaldehyde, cryoprotected in 30% sucrose and embedded in O.C.T. compound frozen in liquid nitrogen-cooled isopentane. Twenty-µm thick sections were cut with cryostat, permeabilized in 0.5% Triton X-100 in PBS for 20 minutes and blocked in 5% normal donkey serum in PBS for 1 hour. The following primary antibodies were incubated overnight at 4°C: anti-GFAP (1: 1000; Millipore), anti-Iba 1 (1: 600, Biocare), anti-Cleaved Caspase 3A (1: 300, Cell Signalling), anti-MBP (1: 400, Millipore), anti-DCX (1: 1000, Abcam). After several washes, slides were incubated with the biotinylated secondary antibody followed by ABC complex reagents (Vector Labs) and DAB staining. For immunofluorescence, the following secondary antibodies were used: donkey Alexa Fluor 488 or 555 conjugated (Thermo Fisher Scientific). Slides were then washed in PBS, counterstained with DAPI and mounted with Fluoromount G (SouthernBiotech). All fluorescence images were captured on a confocal laser-scanning microscope (Leica TCS SP8, Leica Microsystem). To label endothelial cells, biotinylated Griffonia Simplicifolia Lectin I (Isolectin B4 1: 400, Vector Labs) was used.

The thickness of the cerebral cortex grey matter was quantified using the software NIS Elements (Nikon). Object identification was performed using a protocol adapted from Lin *et al.*, 2005 and

Chen *et al.*, 2007. A constant sized image segment was converted to 8 bits per pixel gray scale. The images were then binarized using a fixed interval intensity threshold series, followed by erosion/dilation filtering to detect boundaries of object. Fluorescent signal areas were binarized and quantified to be expressed as a percentage of the total area. Image analysis were performed using ImageJ.

3.9 Statistical analysis

Two-tailed, unpaired, unequal variance Student's t-test and ANOVA with post-hoc Tukey HSD test were used for statistical analysis ($p<0.05$). Survival probability was calculated using the Kaplan–Meier and log-rank tests ($p<0.05$).

4. Results

4.1 Swine Surf1 gene complete sequence

The cloning of the correct PCR product of the swine Surf1 gene (4582bp) in TOPO-TA vector and its isolation revealed to be time-consuming and difficult to achieve, therefore to date we managed to obtain multiple sequences of a single DH5α clone from wild type cell line ID6639 (AVANTEA srl). We decided to further confirm the exons sequences (Exon 1 to 9) of swine Surf1 gene through Sanger sequencing of different clones of DH5α transformed with TOPO-TA vector-cloned specific RT-PCR product (primers S1F + S1R, 921bp), using ID6639 cell line cDNA as template. The sequences obtained were aligned with predicted exons sequences (NCBI AK391958). For the complete genomic sequence of *Sus scrofa* Surf1 gene, we considered as consensus sequence of each exon the most frequent form present among our clones (for the exons alignments, see BOX 1). The complete swine Surf1 sequence we obtained from male porcine cell line ID6639 is listed in BOX 2.

4.2 Swine Surf1 gene disruption

The efficiency of the three TALEN pairs (Tal01L+R, Tal02L+R, Tal03L+R) was evaluated through Surveyor Assay and results indicated that each pair cut with a moderate (Tal03L+R) to high efficiency (Tal01L+R and Tal02L+R) in the targeted region. Surveyor® Assay result is illustrated in Fig.4.1.

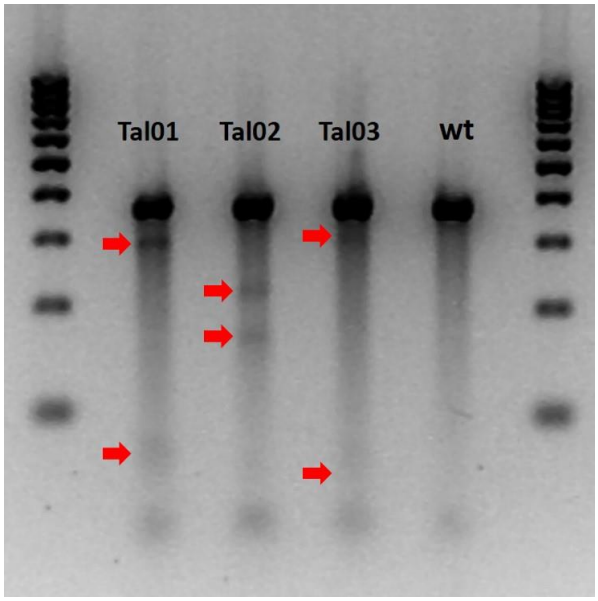

Fig.4.1 Surveyor Assay on specific PCR product obtained from fibroblast pools 72 hours after transfection with TALENs (Tal01, Tal02, Tal03) and wt genomic DNA as control. The expected bands were 295bp+80bp (Tal01), 225bp+150bp (Tal02), 300bp+75bp (Tal03). Marker is 100 bp DNA ladder (Thermo Fisher Scientific).

Transfection experiments on the male fibroblast cell line (ID6639) were carried out with Tal01 and Tal02, each one used in association with the HR vector, in order to select Surf1 KO (homozygous or compound heterozygous) colonies for SCNT. Selected colonies were PCR-screened for the integration of the HR vector, then colonies with the vector insertion where PCR-analysed and sequenced for the assessment of the status of the second Surf1 allele (Fig.4.2).

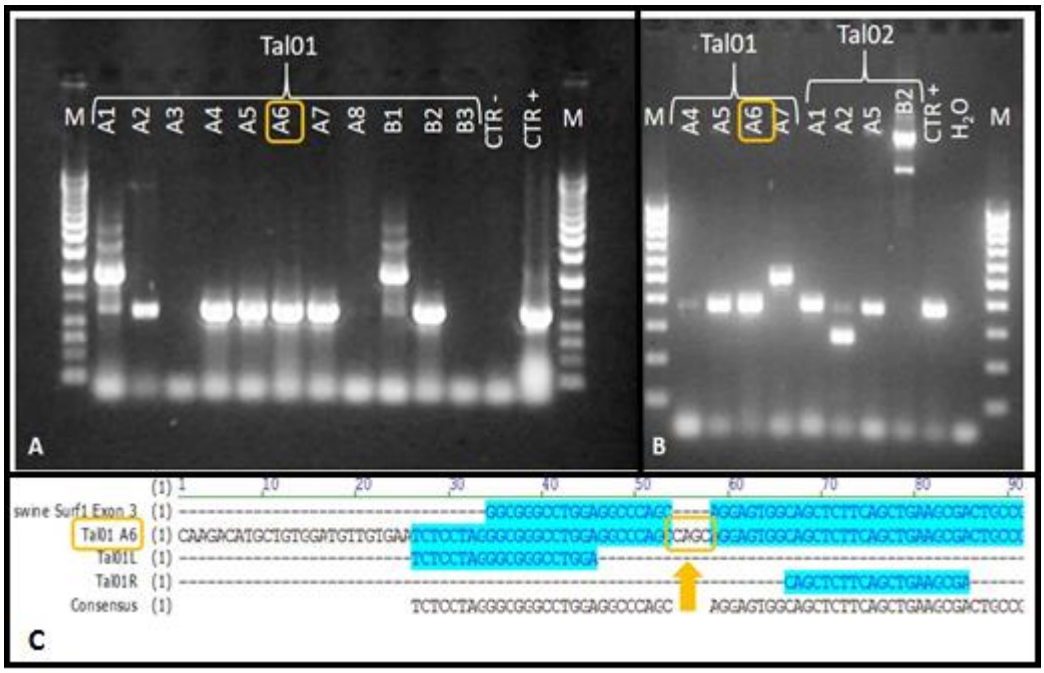

Fig.4.2 Representative sample of PCR-screening results on Tal01- and Tal02-derived colonies. A) Targeting vector integration screening, PCR product: 1237bp (1 kb DNA ladder). B) Assessment of the status of the second allele, PCR product: 375bp (100bp DNA ladder). Colonies with a PCR product correspondent to 375bp, therefore without visible alteration of the molecular weight, were sequenced for detection of small InDels (e.g. colony A6); on the other hand, colonies with a PCR product of molecular weight visibly higher or lower than expected were also sequenced and used in separate SCNT experiments (e.g. colonies A7, higher, and B2, lower). C) Alignment of Sanger-sequenced PCR product presenting small InDels on non-targeted allele with the reference sequence of swine Surf1 exon 3 and TALEN arms used for transfection of this set of colonies (Tal01L+R). InDels in the genomic region between the two TALEN arms are generated by the specific cutting activity of the nuclease.

Since for the male line (ID6639) the aim was to generate Surf1 KO colonies, colonies with InDel mutations in the non-targeted allele were considered suitable for SCNT (being compound heterozygous for Surf1 gene mutations), though we preferred to use only colonies with InDels causing frameshift mutation to assure the complete loss of function of the gene. On the other hand, for the female line (ID167) the aim was to generate heterozygous colonies, so that colonies with one allele with the integration of the HR vector and one wild-type allele were considered suitable for SCNT.

The experiments carried out with CRISPR/Cas9 system where done using the guide identified as Guide#2, which resulted to be more efficient than others in the generation of mutated colonies. A two-step experiment was scheduled, where a first round of transfection was meant to generate NHEJ-mutated colonies characterized by the presence of small InDel mutations. The suitability of

these colonies to be used in further experiments was analysed through genotyping and Sanger sequencing. Confirmed Surf1 heterozygous colonies with small InDel mutations were used both as nuclear donor cells in SCNT experiments to obtain rejuvenated foetal fibroblasts from D40 foetuses, and as nuclear donor cells in SCNT to generate male heterozygous piglets without HR vector insertion. One SCNT experiment using 2 CRISPR/Cas9-generated heterozygous colonies was made and 8 foetuses were collected at day 40 of gestation. Each foetus was genotyped and clone-5 was selected to be used in further experiments. Clone-5 foetal fibroblast cell line was generated as rejuvenated cell line to be further transfected. A second transfection round was made on rejuvenated foetal fibroblasts obtained as above, using the same CRISPR/Cas9 sgRNA associated with HR vector in order to obtain Surf KO colonies to be used in SCNT.

We selected Surf1 KO colonies (one allele with the insertion of the HR vector and one allele with a not-in-frame InDel) to be used as nuclear donor cells in SCNT experiments for the generation of Surf1 KO animals. Transfection experiments results are summarized in Tab.4.1.

Transfection mix	Fibroblast cell line ID (M/F)	N° colonies	N° targeted colonies (%)	N° sequenced colonies (%)	N° colonies suitable for SCNT (%)
Tal01L+R + HR vector	6639 (M)	48	32 (67%)	14 (29%)	10 (21%) KO
Tal02L+R + HR vector	6639 (M)	42	23 (55%)	8 (19%)	3 (7%) KO
Tal01L+R + HR vector	167 (F)	38	25 (66%)	5 (13 %)	5 (13%) HET
CRISPR sgRNA #2	6639 (M)	118	16 (14%)*****	79 (67%)	10 (8%) HET
CRISPS sgRNA #2 + HR vector	clone-5	100	14 (14%)	40 (40%)	10 (10%) KO

Tab.4.1 Transfection experiments results. Percentages are calculated on the total number of colonies picked up for each experiment. Colonies are defined "targeted" when HR vector integration on one Surf1 allele was PCR-detected. A second PRC was used to investigate the status of the other Surf1 allele, and only colonies with one targeted allele and one allele with putative small InDel mutations were Sanger sequenced ("sequenced colonies"). *****: in this experiment, HR vector was not used so the number of colonies indicated in "targeted colonies" indicate the number of colonies with InDels in the expected genomic position, necessarily without the insertion of the HR vector. KO knockout; HET heterozygous.

4.3 Somatic Cell Nuclear Transfer

Colonies carrying the mutation/s of interest were used as nuclear donors in SCNT experiments. A total of 23 SCNT experiments were carried out using six different combination of donor cell types (exp. 1-6), and 10 positively ended in farrows. Data of embryo production and development, embryo transferred and pregnancy outcomes are presented in Tab.4.2 according to the genetic background of the nuclear donor cell line used. A detailed summary of farrows in presented in Tab.4.3. Each SCNT experiment was made using a combination of 4 colonies with similar mutations on the non-targeted allele (InDels < 10bp, InDels>10bp) and only nuclear donor colonies with small InDels (<10bp) resulted in positive pregnancy diagnosis. Only experiments with a positive pregnancy diagnosis are considered from now on.

exp.	Nuclear donor cell line	Genome-editing nuclease	Genotype (M♂/F♀)	N° SCNT constructs	N° TE	Outcome (% of TE)
1	ID6639 colonies	CRISPRs	KO (M♂)	134	82	○: 1 (1%) (ID498, KO) †: 0
2	ID6639 colonies	TALENs	KO (M♂)	797	247	○: 4 (2%) KO (ID487*****) †: 1 (0.4%)
3	ID487 re-cloning	TALENs	KO (M♂)	1137	371	○: 13 (4%) KO †: 5 (1%)
4	IDclone-5 + ID487***** re-cloning	CRISPRs + TALENs	KO and HET (M♂)	793	355	○: 12 (3%) (1 KO; 11 HET) †: 6 (2%) (2 KO; 4 HET)
5	ID167 colonies + ID487***** re-cloning	TALENs	HET (F♀) and KO (M♂)	389	188	○: 8 (4%) (6 ♀ HET; 2 ♂ KO) †: 7 (4%) (1 ♀ HET; 6 ♂ KO)
6	ID167 colonies	TALENs	HET (F♀)	134	82	○: 8 HET (10%) †: 3 HET (4%)

Tab.4.2 Summary of SCNT experiments and outcome. EXP.: experiment type; each "type" defines one or a combination of cell lines used as nuclear donor cells in one single SCNT session. Numbers are cumulative of experiments of the same type. N° SCNT CONSTRUCTS: construct is the term used to describe the ooplasm fused with nuclear donor somatic cell immediately after SCNT procedure.TE: transferred embryos. †: stillborn; ○: born alive. KO knockout; HET heterozygous. ID487*: this piglet was characterized and chosen for subsequent re-cloning experiments.

Recipient sow ID	N° born alive piglets (ID)	N° stillborn	Genotype (M/F)
189	4 (485-488)	1	Surf1 KO (M)
194	1 (498)	0	Surf1 KO (M)
202	4 (525-528)	2	Surf1 KO (M)
208	7 (539-547)	0	Surf1 KO (M)
463	2 (583, 584)	2	Surf1 HET (F)
233	6 (630-635)	3	Surf1 HET (F) n°4 Surf1 KO (M) n°2
235	6 (667-676)	4	Surf1 HET (M) n°3 Surf1 KO (M) n°3
237	6 (677-682)	2	Surf1 HET (M)
246	2 (697, 701)	3	Surf1 HET (F)
244	6 (702-707)	0	Surf1 HET (F)
TOT	**44**	**17**	

Tab.4.3 Summary of Surf1 animals at term. KO, knockout; HET, heterozygous.

All Surf1 piglets born (males/females, KO/heterozygous) were PCR-genotyped. The different types of Surf1 animals obtained are listed below:

- TALENs-edited Surf1 KO nuclear donor male line: the first SCNT experiment was made using Surf1 KO colonies obtained through the transfection of the swine male line ID6639 with Tal01 pair and HR vector. The outcome of this first experiment was a 5-piglet litter, four of which were born alive. Considering the general conditions of the piglets, in particular the possible presence of potential Large Offspring Syndromes (LOSs) due to SCNT procedure (e.g. macroglossia, etc; (Kurome *et al.*, 2013)) we decided to select the most suitable piglet among this litter, which resulted to be ID487, to be used for subsequent re-cloning experiments. To this aim, we proceeded with the derivation of a primary fibroblast cell line from ID487 to be used as nuclear donor cells. The genotypic characterization of pig ID487 showed that the animal presented one Surf1 allele with the 106 bp deletion consequent to the HR vector insertion, and the other Surf1 allele carrying a 5 bp-deletion (nucleotide positions 12 to 16 of exon 3). This genetic condition matched with the one of colony C2Tal01, used as nuclear donor in this first SCNT experiment. Further experiments were done to obtain Surf1 KO animals using ID487-derived fibroblasts as nuclear donor cells for SCNT (re-cloning). Given the necessary genetic homogeneity of piglets generated through re-cloning, all animals obtained were PCR-genotyped, and a representative sample of each litter was confirmed by Sanger sequencing (Fig.4.3).

- TALENs-edited Surf1 heterozygous nuclear donor female line: all animals were characterized by the insertion of HR vector on one Surf1 allele (therefore presenting the expected 106 bp deletion in exon 3) and one wild type allele. The piglets were all genotyped, except for three born-dead animals due to the high level of tissue decay, which prevented the extraction of genomic DNA of suitable quality for molecular analysis.
- CRISPR/Cas9-edited Surf1 KO and heterozygous nuclear donor male lines: the first round of transfection using CRISPRs/Cas9 plasmid generated a monoallelic single base pair insertion (+A) in nucleotide position 60 of Surf1 exon 3; the second round of transfection, using a combination of CRISPRs/Cas9 plasmid and HR vector, resulted in the integration of HR vector in the homology positions of Surf1 exon 3, introducing the expected 106 bp deletion. Only one live piglet was obtained from Surf1 KO CRISPR-modified cell line (pig ID498) and its genotype matched with the one of colony 171C2. The male Surf1 heterozygous animals obtained were generated after the first round of transfection, (donor cell line identified as IDclone-5) and were characterized by the single base insertion (+A) on one allele and one wild type allele.

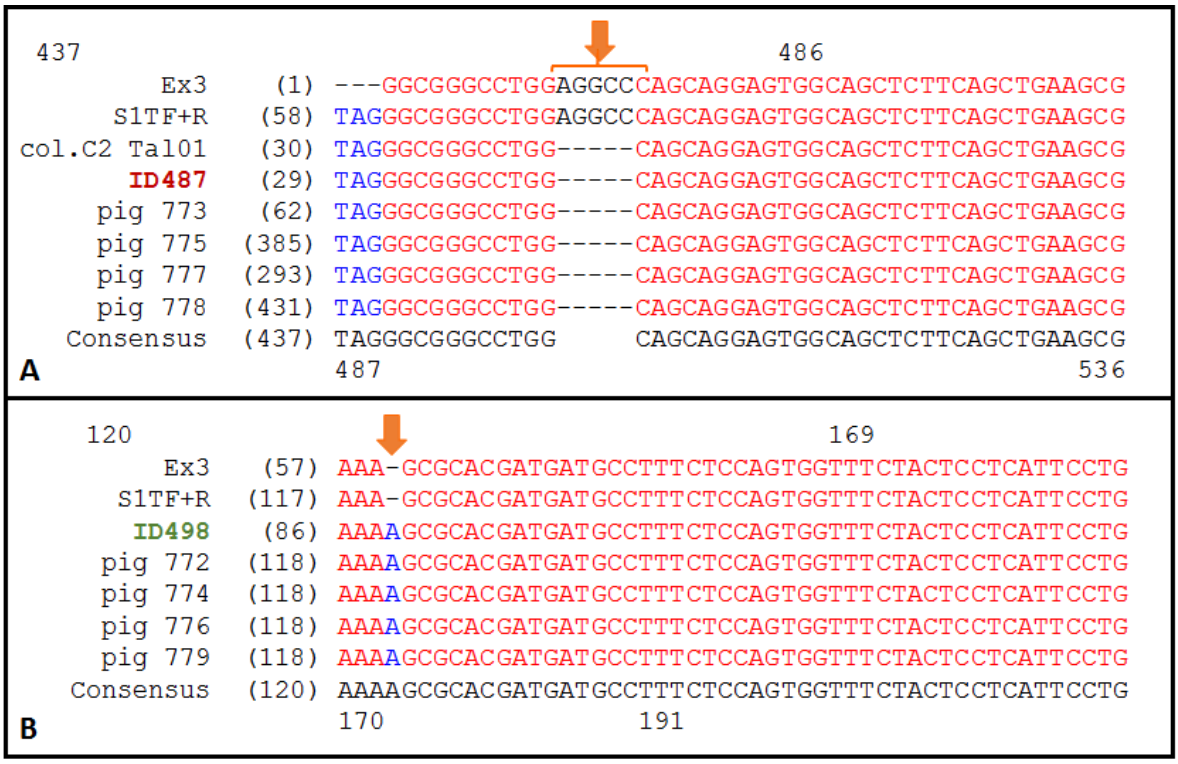

Fig.4.3 Representative sample of Sanger sequences alignments of Surf1 KO piglets. A) TALEN-derived Surf1 KO male line, in particular col. C2Tal01 is the colony used as nuclear donor line for the generation of ID487; pigs 773, 775, 777 and 778 are ID487 re-clonings. The sequences show the presence of a 5bp deletion on the non-targeted Surf1 allele which is maintained throughout the cloning and re-cloning experiments. B) CRISPR/Cas9-derived Surf1 KO and heterozygous male lines, in particular ID498 is the longer-lived Surf1 KO obtained after a second round of transfection on rejuvenated clone-5 fibroblasts; pigs 772, 774, 776, 779 are Surf1 heterozygous obtained using rejuvenated clone-5 fibroblast directly as nuclear donor cells in SCNT experiments. Sequences show the presence of a monoallelic single base pair insertion (+A) in Surf1 exon 3 which is maintained throughout the experimental procedure.

Genotyping results are summarized in Tab.4.4.

Somatic cell nuclear donor ID	M/F	HET or KO (nuclease + vector)	Offspring (% alive)	Genotype confirmed by Sanger sequencing
6639	M	KO (TALENs + HR)	5 (80%) (pig ID487)	4
487	M	KO (re-cloning)	26 (62%)	11
6639	M	KO (CRISPRs + HR)	1 (100%)	1
6639	M	HET (CRISPRs - NHEJ)	14 (71%)	14
167	F	HET (TALENs + HR)	20 (70%)	17

Tab.4.4 Summary of cloned Surf1 piglets obtained following SCNT experiments. All Surf1 animals born were PCR-genotyped and the heterozygous or KO condition was confirmed by Sanger sequencing. Considering the necessary genetic equivalence of piglets deriving from re-cloning experiments of ID487, only a representative sample of each litter was confirmed by Sanger sequencing analysis. Conversely, all Surf1 heterozygous piglets were genotyped, except for three born-dead female heterozygous piglets because the high level of tissue decay avoided processing the samples for molecular analysis. KO knockout; HET heterozygous.

4.4 Surf1 KO piglets clinical phenotype

A total of 33 Surf1 KO male piglets were generated, 12/33 (36%) were stillborn. Seven out of 21 born alive died or were culled the same day of birth due to severe clinical phenotype (tremors and absent or weak suckling and rooting reflexes). Six male Surf1 KO piglets lived until 6-9 days and neurological examination revealed a deficit in the hind limb retraction and in cranial tibial reflex starting from day 3; these reflexes were normal in age-matched wild type controls. Since the first day, all piglets showed difficulties in swallowing and weak suckling and rooting reflexes, incapacity in recognizing food, inconsistent weigh gain and altered perception of the space with a tendency to hurt themselves. These clinical signs worsened in the following days, and piglets developed a severe failure to thrive with lack of appetite, weight loss and persistent diarrhoea. Some animals were culled for the reaching of the humane endpoint of the study, whereas others died of general infections. Two Surf1 KO piglets (one TALENs-derived and one CRISPR/Cas9-derived) lived for more than three weeks (80 days and 29 days, respectively) thanks to immediate transfer of the animals in intensive care rooms and artificial milk administration. Both longer-lived Surf1 piglets showed facial dimorphism (Fig.4.4) characterized by shorter nose, relaxed facial muscle, in addition to pronounced body tremors with muscle weakness, respiratory problems and markedly reduced growth.

Fig.4.4 Example of facial dimorphism in Surf1 KO piglet compared to Surf1 heterozygous littermate. Heterozygous animals were totally comparable to wild type controls.

The mean growth curves of longer-lived Surf1 KO compared with heterozygous piglets and adequate age-matched controls is showed in Fig.4.5. Interestingly, birth weights of Surf1 KO piglets was in the same range as Surf1 heterozygous and wild type controls, suggesting an impairment in post-natal, but not intrauterine, growth.

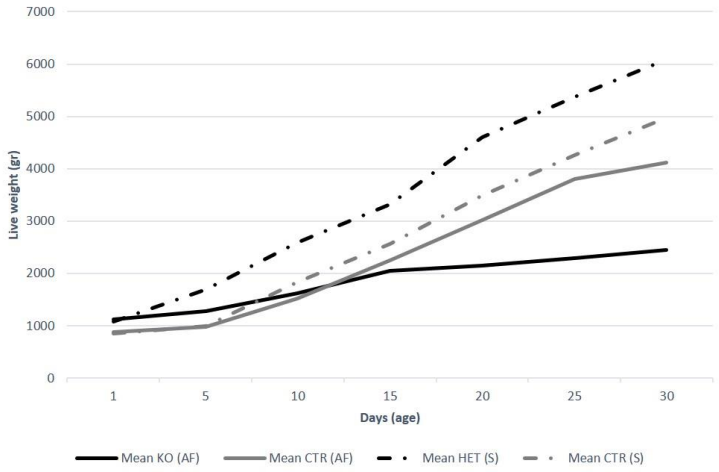

Fig.4.5 Mean growth curves of longer-lived Surf1 KO piglets compared with Surf1 heterozygous and age- and feed-matched controls. Longer-lived Surf1 KO piglets were fed with an automatic feeder (AF) due to their incapacity to feed naturally (continuous black line), compared with control age-matched animals fed in the same way (continuous grey line). The mean growth curve of Surf1 heterozygous (HET) piglets naturally fed (dotted black line), compared

with age-matched controls fed in the same way (dotted grey line), is also shown. The graph is relative to the first 29 days after birth.

The two longer-lived Surf1 KO piglets were necessary fed with an automatic feeder (AF) because of their incapacity to suck properly the milk from the recipient mother sow, therefore in Fig.4.3 their weights are compared with respective measurements of control animals fed under the same conditions. The growth rate of Surf1 KO piglets resulted to be approximately 2-fold lower than controls at 29 days of age. On the other hand, the mean growth curves of Surf1 heterozygous animals and relative controls, both fed naturally by the recipient mother (S), result in a slightly higher weight gain in heterozygous animals, probably because of different milk quality and quantity from the recipient mother. In any case, no negative effects on growth were attributable to Surf1 heterozygote genetic condition.

Lastly, both longer-lived Surf1 KO piglets died of septicemia, favoured by the overall critical state of the animals in the last weeks before death. The infections of which the two piglets died were only detected in these two animals, but not in any other piglets housed in the same facility, suggesting an impaired immune response.

A total of 15 Surf1 heterozygous male piglets were generated through CRISPR/Cas9 system, with the same genetic background as Surf1 KO animals (ID6639) to serve as controls. Heterozygous male piglets appeared phenotypically normal and did not show any clinical signs observed in the Surf1 KO clones. The same normal phenotype was evident in female heterozygous piglets generated through TALENs (ID167, 18 animals). Surf1 heterozygous males are characterized by a monoallelic single-base insertion (+A) in exon 3, whereas heterozygous females by the monoallelic insertion of the HR vector in the same position.

Kaplan-Meier analysis performed to compare survival rate in Surf1 KO, heterozygous and age-matched control piglets are shown in Fig.4.6. All animals considered in the analysis were raised by the recipient mother sow until weaning (28 days of age) or until the humane endpoint for animal welfare was reached. The endpoint of the analysis was the survival until 28 days of age, as the weaning is a particularly critical point in pig breeding (Dividich *et al.*, 2003) and we wanted to exclude eventual external factors interfering with our specific pathological phenotype. The Kaplan-Meier analysis revealed a marked significant difference between Surf1 KO piglets compared to Surf1 heterozygous piglets and controls. In particular, KO animals' survival rate is significantly lower compared to heterozygous and controls. No differences resulted from the comparison between Surf1 heterozygous piglets and controls.

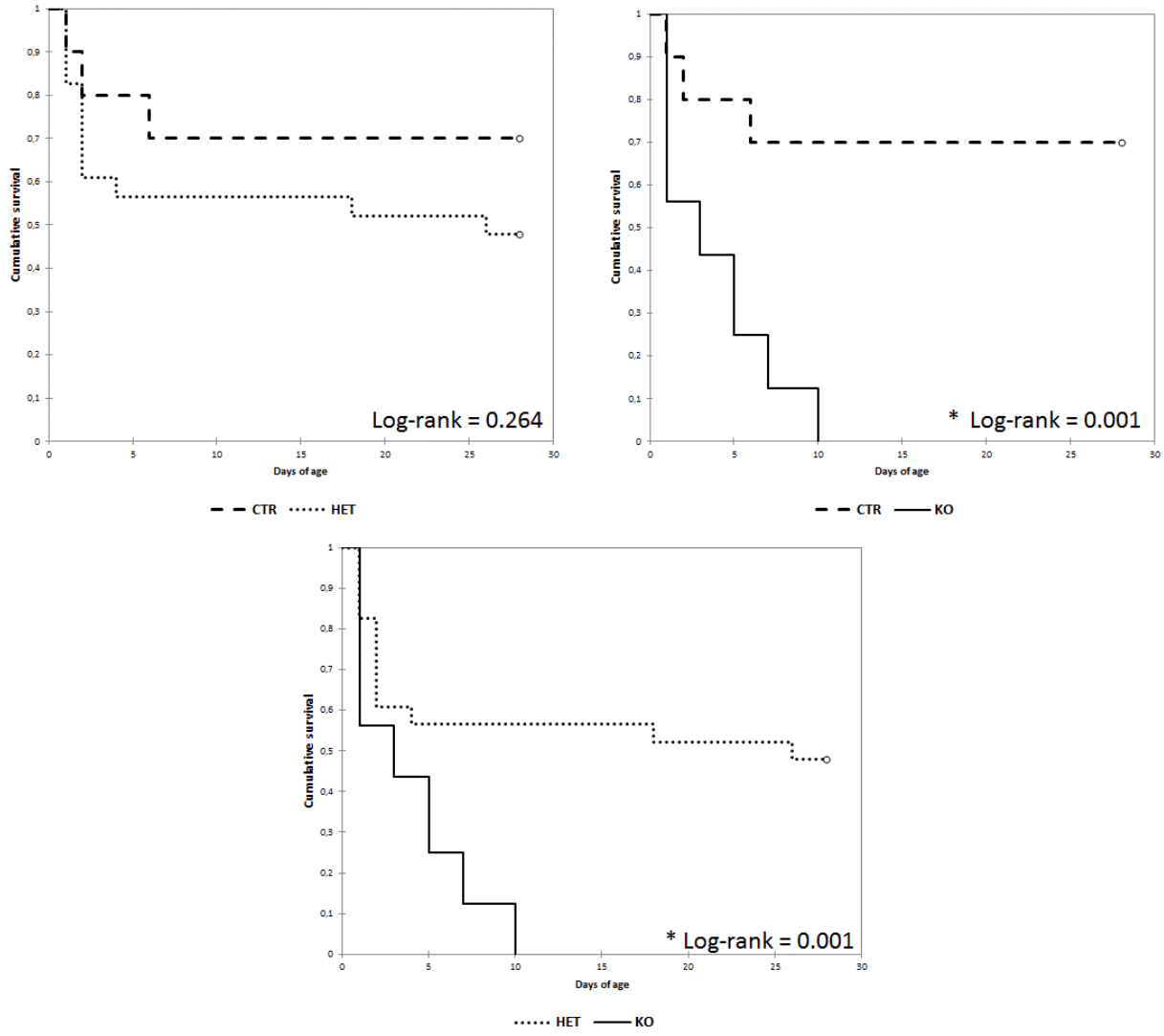

Fig.4.6 Kaplan-Meier survival curves of Suf1 KO and heterozygous piglets compared to control animals. Piglets were raised by the recipient mother sow until 28 days of age or until the humane endpoint for animal welfare was reached. The endpoint of the analysis was the survival until weaning (28 days of age), as this is a particularly critical point in pig breeding and different factors could interfere with the detection of specific phenotypical traits. Statistical analysis with Log-rank were performed (*$p<0.05$).

Blood test analysis showed no significant differences between Surf1 KO animals and controls in any analysed value (data not shown).

In LS patients, a block in aerobic energy metabolism is usually associated with an increase of blood lactate, sometimes leading to severe metabolic acidosis (Zeviani *et al.*, 1996). Since all piglets were fed by the recipient mother sow (a part from the two longer-lived, which are analysed separately) and differences in birth weight can influence their capacity to feed properly in competition with littermates (English e Wilkinson, 1982), we divided animals in weight groups and compare, for each group, Surf1 KO and heterozygous animals, and age- and weight-matched

controls. The analysis revealed a significant increase of blood lactate in 0.5-1 Kg Surf1 KO piglets compared to controls (6.1±0.9 and 4.0±0.2 mmol/L, respectively; p=0.01, ANOVA with post-hoc Tukey HSD test), and an increase slightly under significance in Surf1 heterozygous piglets of the same weight group compared to controls (6.2±1.0 mmol/L and 4.0±0.2 mmol/L, respectively; p=0.06). Only a small increase was detected in 1-1.5 Kg Surf1 KO animals vs. controls (3.6±0.7 mmol/L and 3.0±0.1 mmol/L, respectively; p=0.67). No significant difference was detected in blood lactate levels of Surf1 KO pig ID498 and age-matched controls.
Results are shown in Fig.4.7.

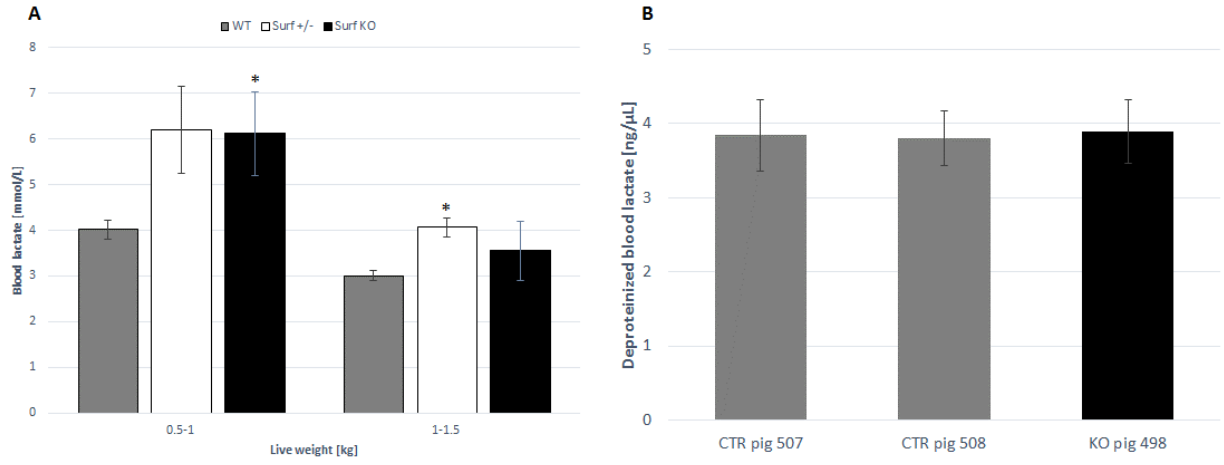

Fig.4.7 Surf1 piglets and control animals blood lactate measurements. A) Blood lactate measurements (mmol/L ± SEM) with Lactate Scout Analyzer (LSA) on newborn Surf1 KO and heterozygous piglets compared with age- and weight-matched controls. B) Blood lactate measurements (ng/µL ± SEM) with Lactate reagent kit (Sigma) on KO pig 498 at 80 days of age, compared with two age-matched controls (pig 507 and pig 508). Statistical analysis was performed with ANOVA with post-hoc Tukey HSD (*p<0.05).

4.5 Mitochondrial state and functioning

The spectrophotometric measurement of MRC enzymes activity on tissue homogenates from post-mortem tissue samples (quadriceps, brain and liver) of Surf1 KO newborn animals highlighted the presence of high individual variability, with a relevant number of animals showing reduced activity of complex IV (CIV) and concomitant decrease in citrate synthase (CS), an index of mitochondrial mass. However, when CIV specific activities were normalized to CS, no significant changes were observed between Surf1 KO and age-matched controls. No significant differences were detected in other MRC complexes (CI, SDH, CII and CIII). The analysis was performed also on quadriceps homogenates from the two longer-lived Surf1 KO animals (pig ID498 and pig ID525, 80 and 29 days of age, respectively), compared to age-matched controls, and no significant differences were detected. MRC enzyme activity assays on cell lysate from primary fibroblast cell lines derived from newborn Surf1 KO animals and age-matched controls (P15) confirmed the absence of isolated COX deficiency. Results are shown in Fig.4.8.

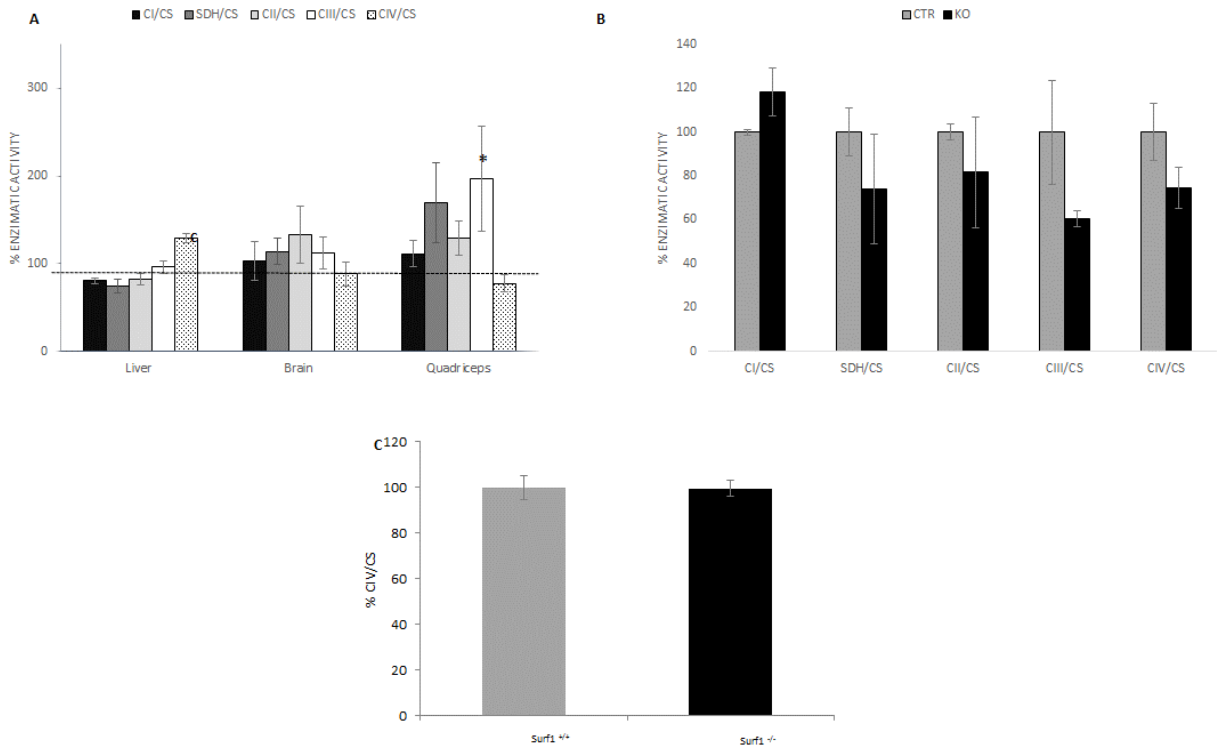

Fig.4.8 Results of spectrophotometric biochemical analysis on MRC enzymes activity of Surf1 KO animals' specimens and Surf1 KO-derived primary fibroblast cell lines. A) Mitochondrial Respiratory Chain (MRC) enzymatic activity (control = 100%), normalized on CS activity, in liver, brain and quadriceps of newborn Surf1 KO piglets (± SEM). B) MRC enzimatic activity (control = 100%), normalized on CS activity, in quadriceps of the two longer-lived animals (29 days and 80 days) (± SEM) compared to age-matched controls (100%). C) COX enzymatic activity, normalized on CS activity, in high-passage (P15) primary fibroblast cell lines derived from Surf1 KO piglets and controls (wild type animals). Two-tailed, unpaired, unequal variance Student's t-test was used for statistical analysis (*$p<0.05$).

The absence of an isolated deficit of COX activity in Surf1 KO piglets quadriceps tissue was confirmed through In-Gel activity (IGA) analysis (Fig.4.9), which showed no differences between Surf1 KO and control animals COX reaction.

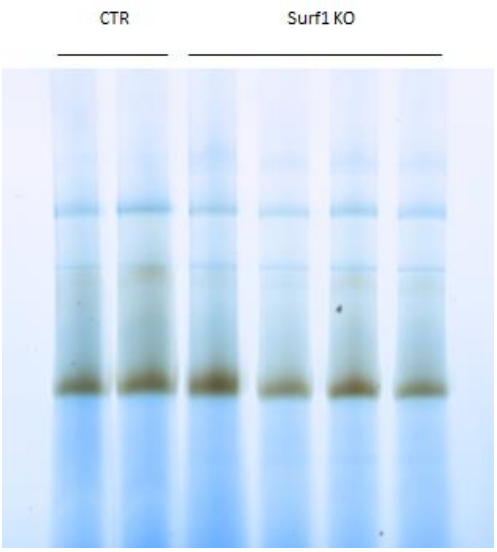

Fig.4.9 In-Gel Activity (IGA) on isolated mitochondria from quadriceps samples of Surf1 KO animals compared to age-matched wild type controls (CTR).

One-dimensional denaturing SDS–PAGE (Western blot) was performed on total lysate (tissue homogenates) from quadriceps samples of all Surf1 animals to confirm the complete loss of Surf1 protein (representative sample shown in Fig.4.10).

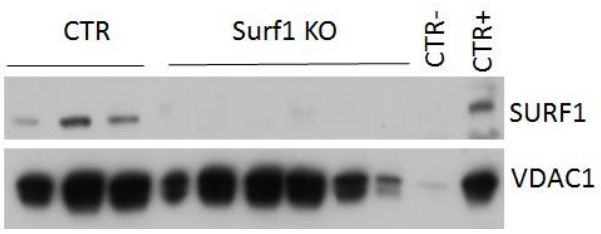

Fig.4.10 Example of WB analysis on quadriceps homogenates of Surf1 KO piglets and age-matched control using anti-Surf1 antibody. The complete absence of Surf1 protein in Surf1 KO animals is clear, compared to the presence of bands in age-matched wild type controls (CTR).

WB analysis on quadriceps homogenates using a specific antibody against subunit COX5a revealed a significant reduction of this subunit quantity in Surf1 KO compared to age-matched controls. However, normal amounts of COX4 and COX1 subunits were detected (Fig.4.9A).

To evaluate the effects of Surf1 protein ablation on the assembly of COX, experiments based on two-dimensional-gel blue-native electrophoresis (2D-BNE) were performed in quadriceps mitochondrial enriched fraction obtained from Surf1 KO pigs and relative controls. The COX1 monoclonal antibody was used to immunostain COX specific subcomplexes. The spot of the assembly intermediate (AI) is usually prominent in LS patients (Kovarova *et al.*, 2016), whereas in our Surf1 KO pigs the AI distribution is comparable with the one of controls. However, a mild reduction in the intensity and size of the spots corresponding to fully assembled COX1 (monomer, M) and supercomplexes (I-III-IV and III-IV) was present in Surf1 KO tissue, compared to control. These results indicate that the amount of fully assembled, functional COX is only partially decreased in newborn Surf1 KO piglets, supporting the results of the almost normal COX

enzymatic activity found in biochemical analysis performed on animals' tissue samples. Results are shown in Fig.4.11.

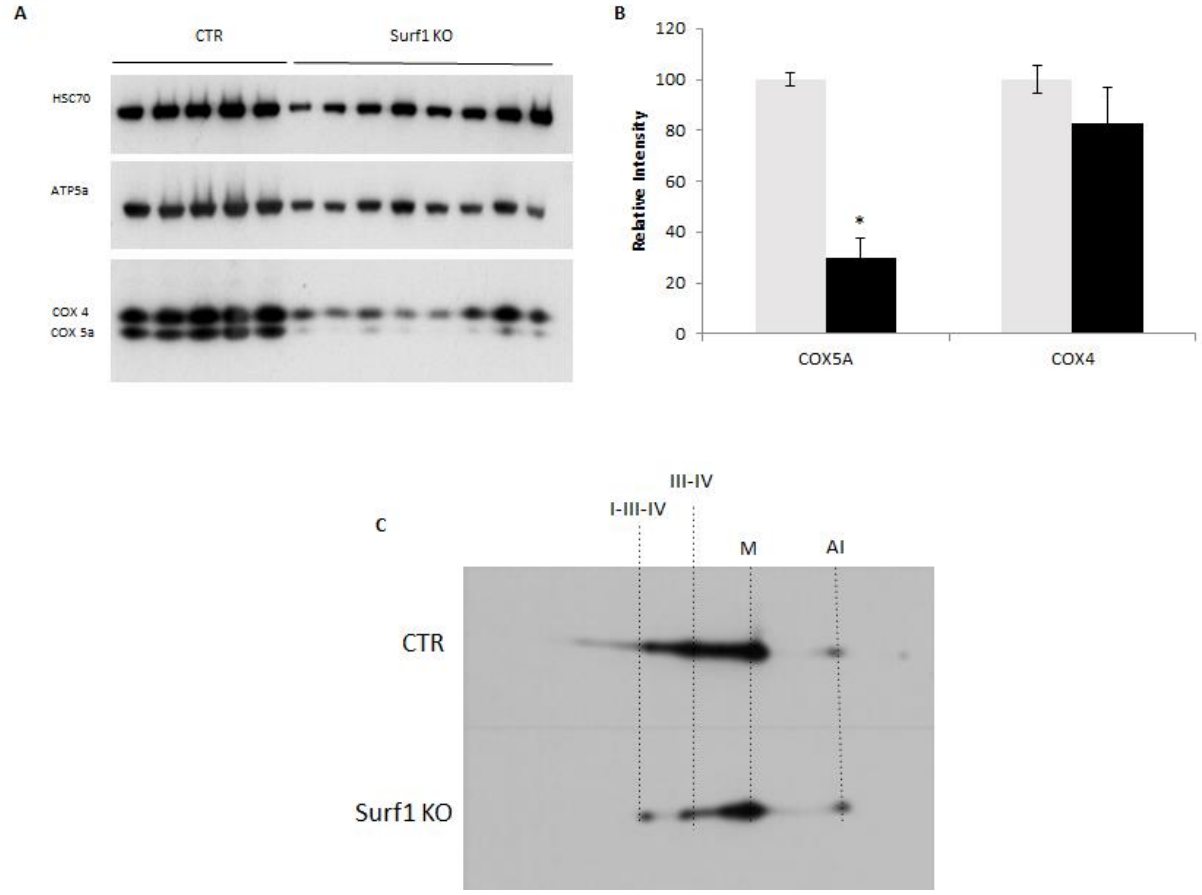

Fig.4.11 Protein expression and assembly analysis on Surf1 KO newborn piglets and age-matched controls. A) Western Blot analysis on quadriceps homogenates of newborn Surf1 KO piglets and age-matched controls (CTR) and B) relative densitometry analysis. Two-tailed, unpaired, unequal variance Student's t-test was used for statistical analysis (*$p<0.05$). C) Example of Blue Native PAGE analysis (2D-BNE) on quadriceps isolated mitochondria from newborn Surf1 KO piglets and age-matched controls (CTR).

In view of the fact that the great majority of our Surf1 KO piglets died in the first week after birth and that, at that point, the expected isolated COX deficiency was not detected, we hypothesized that the impairment in COX activity could be related to tissue age, then not detectable in newborn and young animals. Therefore, we cultured *in vitro* different fibroblast cell lines derived from our animals (Surf1 KO and controls) until late passages (P15) in order to exacerbate possible COX impairment. No abnormalities were detected in COX activity measurements on an enriched mitochondrial fraction of high-passage (P15) primary fibroblast derived from Surf1 KO pigs, compared to controls-derived cell lines (Fig.4.6C). Furthermore, COX and SDH cells staining did

not reveal differences between controls- and Surf1 KO-derived fibroblasts, in line with biochemical analysis results (Fig.4.10). We also investigated through MitoTracker Red vital staining of cells whether Surf1 deficiency can alter the organization of the mitochondrial network, but no significant differences between Surf1 KO-derived cells and control-derived cells were detected (Fig.4.12).

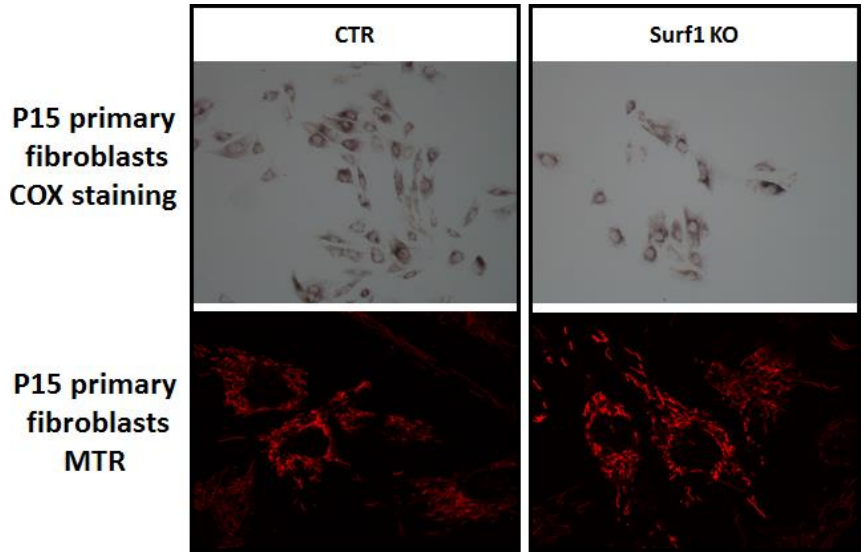

Fig.4.12 Histochemical COX reaction (upper panels) and MitoTracker Red (MTR, lower panels) staining in swine primary fibroblast cell lines derived from Surf1 KO animals and controls (CTR).

4.6 Histological and histochemical findings in Surf1 KO tissues

Histological and histochemical analysis were performed on skeletal muscle (quadriceps) and jejunum samples of Surf1 KO animals and relative controls. For these analysis, samples frozen in isopentane were cryosectioned and stained. A representative sample of morphological analysis based on hematoxilin-eosin staining on skeletal muscle (quadriceps) of newborn Surf1 KO piglets and relative controls is shown in Fig4.13. Different fibres number and diameter are detected in animals of the same genotype (Surf1 KO and CTR), highlighting a strong individual variability between samples.

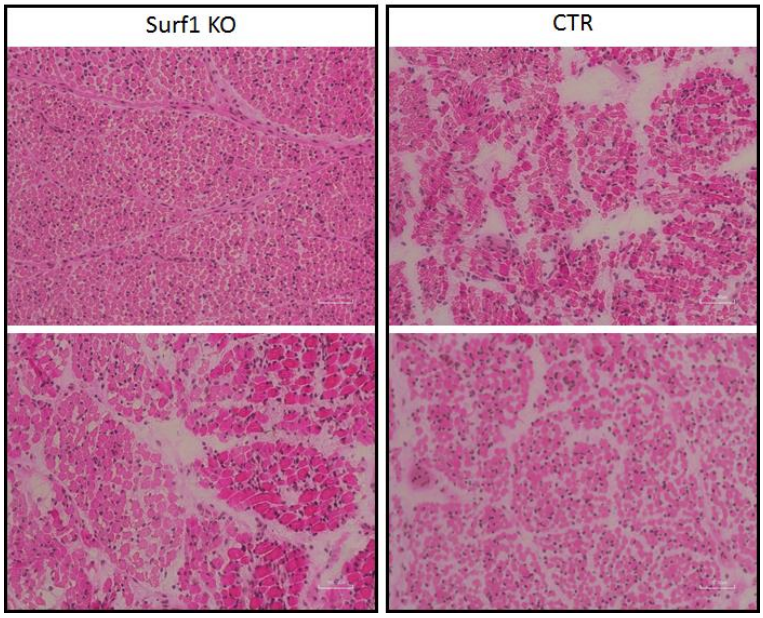

Fig.4.13 Morphological analysis (hematoxilin-eosin) of newborn Surf1 KO quadriceps samples, compared to age-matched controls (CTR).

Histochemical analysis were performed on quadriceps and jejunum samples of newborn Surf1 KO and control animals, as these tissues are considered the most affected in LS disease because of their high ATP consumption rate, to evaluate COX and SDH reactions. Analysis performed on muscle specimen (Fig.4.14A) show that COX activity is not as severely impaired as expected in Surf1 KO skeletal muscles compared to controls, considering LS patients muscle biopsy reactivity (Fig.4.14B). In our animals, only isolated cases of slight COX reactivity reduction are detectable in skeletal muscle, and could be attributable to individual variability rather than to actual COX impairment. Conversely, the succinate dehydrogenase (SDH) reaction was comparable to controls in all the Surf1 KO quadriceps analysed.

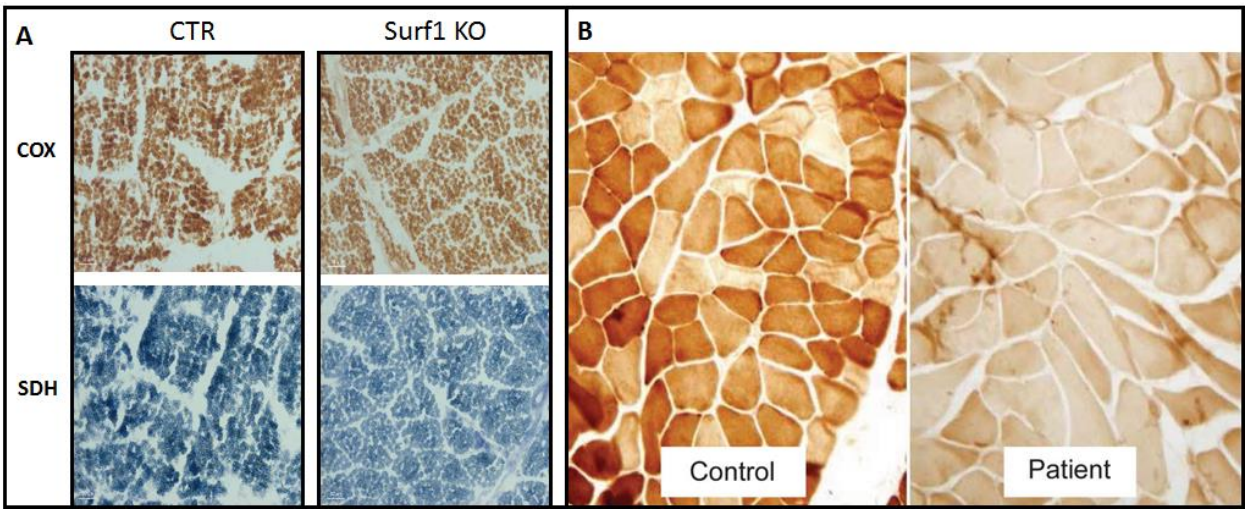

Fig.4.14 Histochemical COX reaction in skeletal muscle specimen. A) Example of COX (top, brown) and SDH (bottom, blue) stainings on Surf1 KO and age-matched controls (CTR) quadriceps samples compared to B) COX staining of LS patient skeletal muscle compared to control. The B) section of this image has been taken from Echaniz-Laguna *et al.*, 2013.

On the other hand, analysis of COX and SDH reaction in jejunum samples (Fig.4.15) showed a clear reduction in COX activity in newborn Surf1 KO intestinal villi compared to controls, suggesting a possible impairment in food nutrients and colostrum absorption.

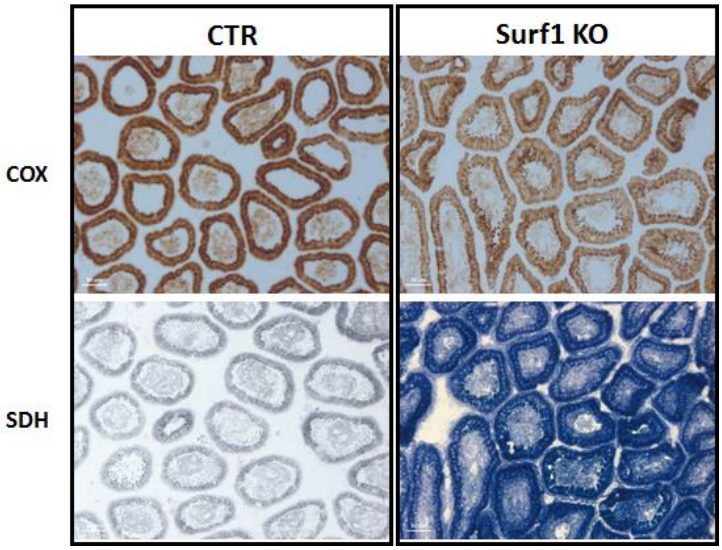

Fig.4.15 histochemical COX and SDH reaction on jejunum specimen of newborn Surf1 KO and control (CTR) animals.

To further investigate energy metabolism in our Surf1 KO model, Oil Red O (ORO) and Sudan Black B (SBB) staining were carried out in quadriceps specimens of newborn Surf1 KO piglets and age-matched controls to assess intramuscular fat (IMF) distribution (Fig.4.16). Both these stainings are based on the use of fat-soluble dyes to stain neutral triglycerides and lipids of frozen tissues. Surprisingly, intracellular lipids in quadriceps samples of Surf1 KO piglets were severely reduced compared to controls, suggesting an impairment of energy storage in this tissue and, in particular, the consumption of intracellular lipid as an energy source. This result is in line with the marked reduced growth rate observed in Surf1 KO animals and could be related to the reduced COX activity in jejunum villi observed above.

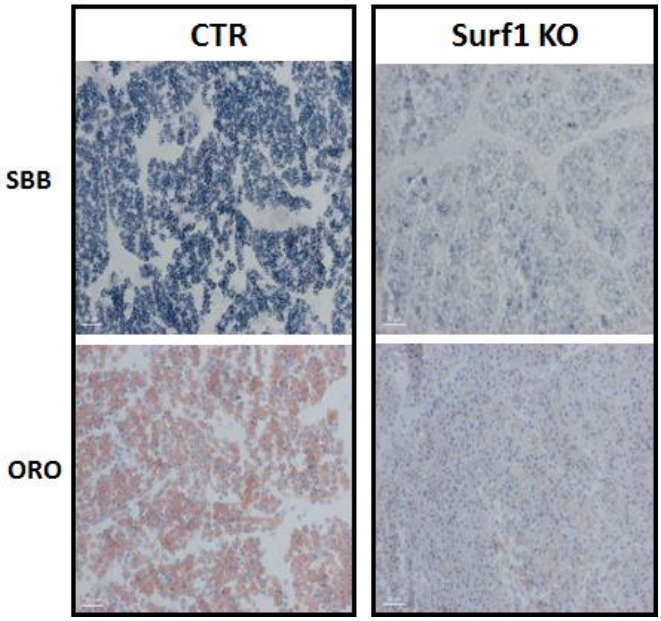

Fig.4.16 Histochemical evaluation of intramuscular fat in quadriceps sections of newborn Surf1 KO and age-matched control (CTR). Sudan Black B (SBB); Oil Red O (ORO).

To evaluate the presence of abnormalities in the nervous system, we examined four Surf1 KO piglets culled at perinatal stage (newborn) and the two longer-lived Surf1KO piglets (29 and 80 days of age). No overt neurodegeneration was detected in haematoxylin-eosin stained sections through the entire extension of the central nervous system; only some cleaved caspase 3 positive neurons were detected in hypoglossal nerve nuclei in the brainstem of 29-days old Surf1 KO piglet (data not shown).

The most consistent finding in Surf1 KO newborn piglets was a significant reduction in grey matter cortical thickness at early postnatal ages as compared with wild type controls (newborn Surf1 KO: 738 ± 16 µm vs CTR: 1057 ± 23 µm; unpaired t test $p \leq 0.0001$; Surf1 KO 1 day old: 921 ± 31 µm

vs 1150 ± 31 µm, unpaired t test p ≤ 0.0001). This data was not statistically significant in the 29-days old Surf 1 KO piglet (Surf1 KO: 1108 ± 43 µm vs 1186 ± 41 µm, unpaired t test p= n. s;). Moreover, cortical layering differences were observed in newborn Surf1 KO piglets as compared to controls. In particular, Surf1 KO animals showed a higher cellular density and a still disorganized cortical structure (Fig.4.17A)with several immature neurons as also revealed by DCX immunostaining (Fig.4.17B). Architecture of basal ganglia, hippocampus, thalamic region and cerebellum were similar to age matched control.

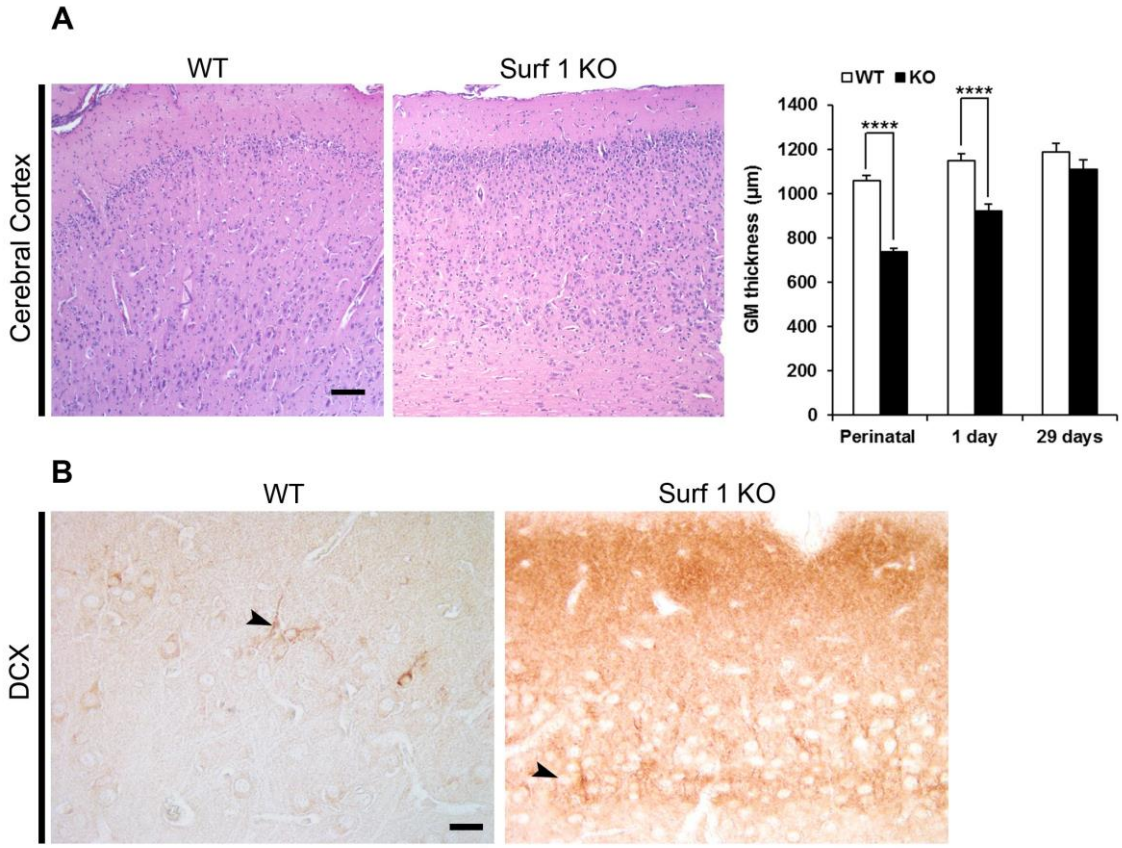

Fig.4.17 Perinatal Surf 1 KO piglet exhibit alteration of cerebral cortex cytoarchitecture. A) H&E of WT (wild type controls) and Surf1 KO piglets showing unidentifiable layer formation, high cellular density and a significant reduction of cerebral cortex gray matter thickness in newborn Surf 1 KO piglets, as confirmed by quantification. Data are means ± SEM, unpaired t test, **** p< 0,0001. Scale bar, 100 µm. B) DCX staining of some immature neurons in the superficial region of cerebral cortex in newborn Surf 1 KO piglets as compared to age-matched WT animals. Scale bar, 25 µm.

GFAP staining revealed a different distribution pattern between Surf1 KO and wild type CTR piglets at all analysed ages. In wild type CTR animals GFAP was expressed mainly in the white matter (WM) areas whereas Surf1 KO animals showed numerous GFAP positive astrocytes in the grey matter (GM) of cerebral and cerebellar cortex and especially around vessels. Quantification

of the signal in the cerebellum confirmed this trend in the longer-lived Surf1 KO (Fig.4.18A, upper panel). Iba1 staining pattern was similar in Surf1 KO and wild type CTR piglets and revealed a more uniform distribution between WM and GM areas in newborn animals and at 29 days of age. Quantification of Iba 1 signal in the cerebellum revealed an increase in 80 days longer-lived Surf1 KO piglet (Fig.4.18A, lower panel). The same piglet showed a diffuse microgliosis more prominent in the cerebral cortex grey matter GM (Fig.4.18B) with activated microglial cells showing hypertrophic rounded soma with thickened, short and few ramified processes as confirmed by quantification (Fig.4.18B, lower panel).

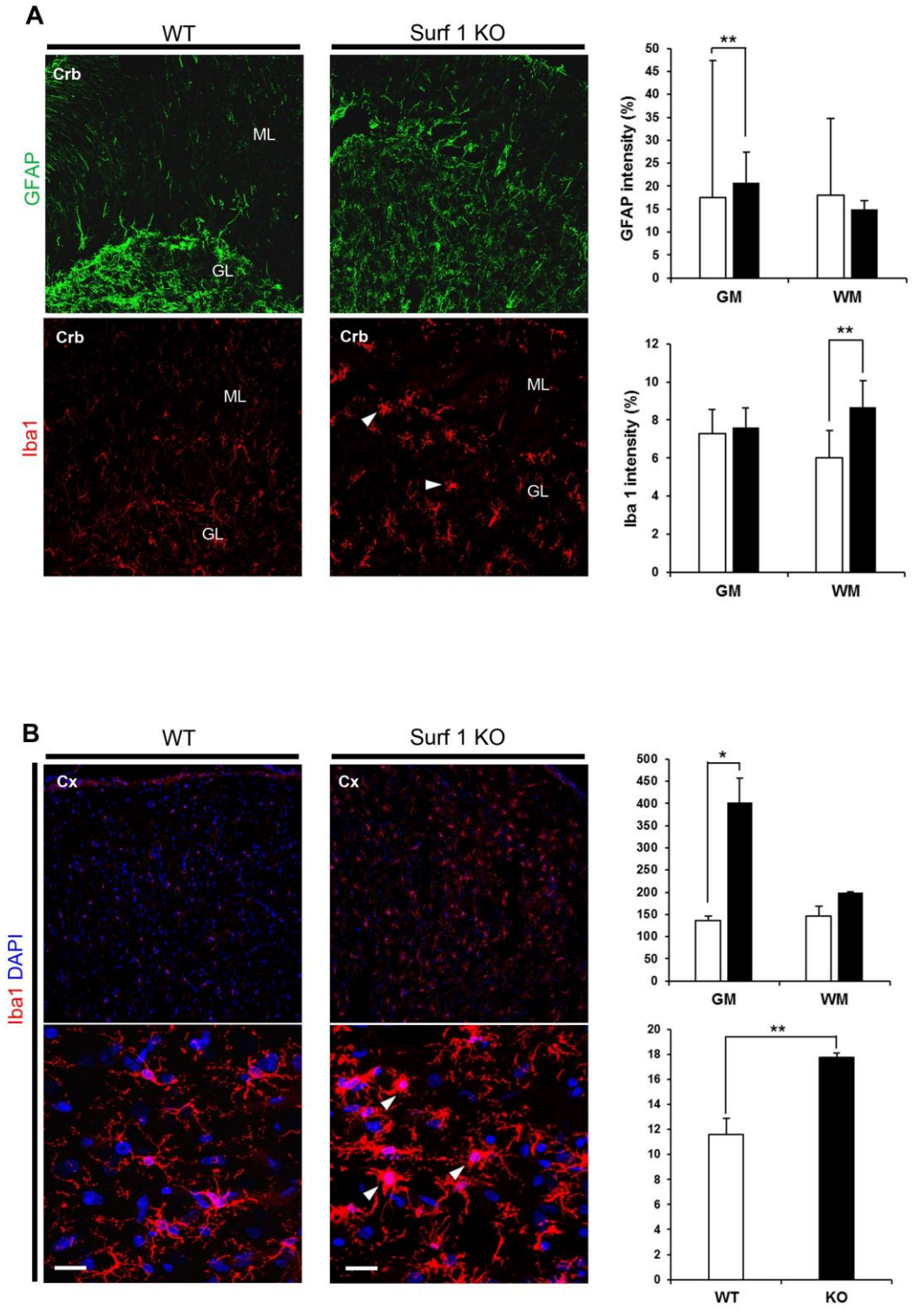

Fig.4.18 Longer-lived Surf 1 KO piglet show gliosis with prominent microgliosis in cerebral cortex. A) Representative images of GFAP (top) and Iba 1 staining (down) in WT and Surf 1 KO piglets' cerebellar cortex. Graphs showing quantification of the two signals (% of the total area) in gray and white matter areas. Data are means ± DS. Scale bar, 50 µm. B) Iba 1 staining of the cerebral cortex from WT and Surf 1 KO animals. Graph showing the number of Iba1 positive cells (top). Control animal shows resting microglia with a small soma and ramified

morphology. In the Surf1 KO litter, activated microglia appeared swollen with shorter less ramified and thick processes. Graph showing microglia mean size (down). Data are presented as means ± DS. Scale bar, 20 µm.

The analysis of Luxol Fast Blue histological staining and MBP immunohistochemical staining in cortex, basal ganglia, mesencephalon and cerebellum of the older KO Surf1 piglet revealed normal myelinating process (Fig.4.19).

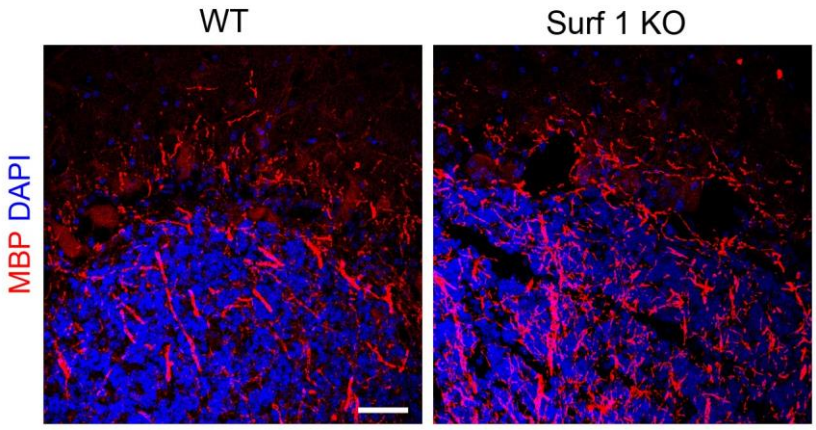

Fig.4.19 Longer-lived Surf 1 KO piglet develop normal myelination. Representative images of immunofluorescence staining with MBP in WT and Surf 1 KO cerebellar cortex showing comparable myelinating process at 80 days of age. Scale bar, 50 µm.

No signs of vascular proliferation were also detected at all ages analyzed by means of Isolectin B4 (Fig.4.20).

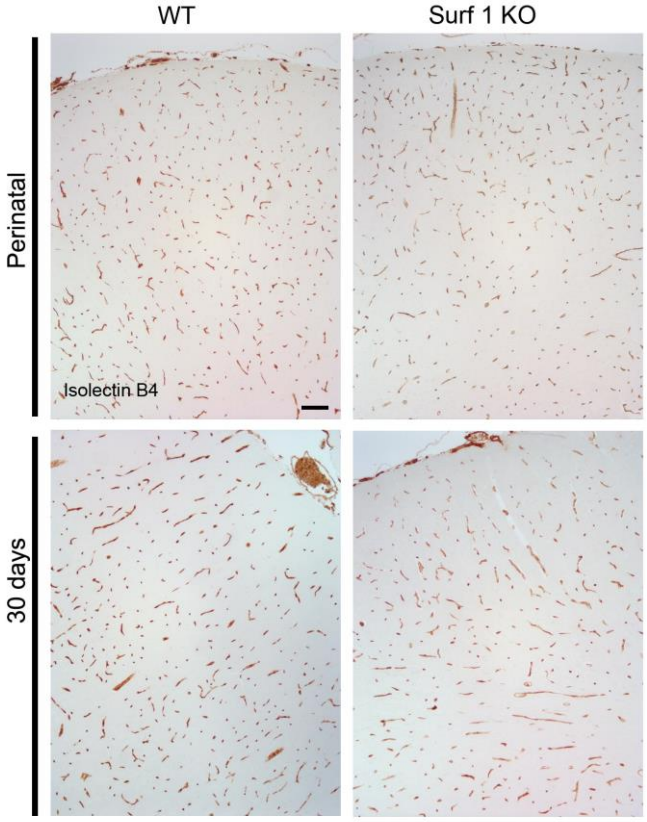

Fig.4.20 Surf 1 KO piglets did not show vascular proliferation. (A) Representative images of Isolectin B4 staining of endothelial cells. No differences in vasculature in WT and Surf 1 KO piglets were detected at all ages analyzed. Scale bar, 100 µm.

BOX 1. Swine Surf1 gene exons 1-9 alignments

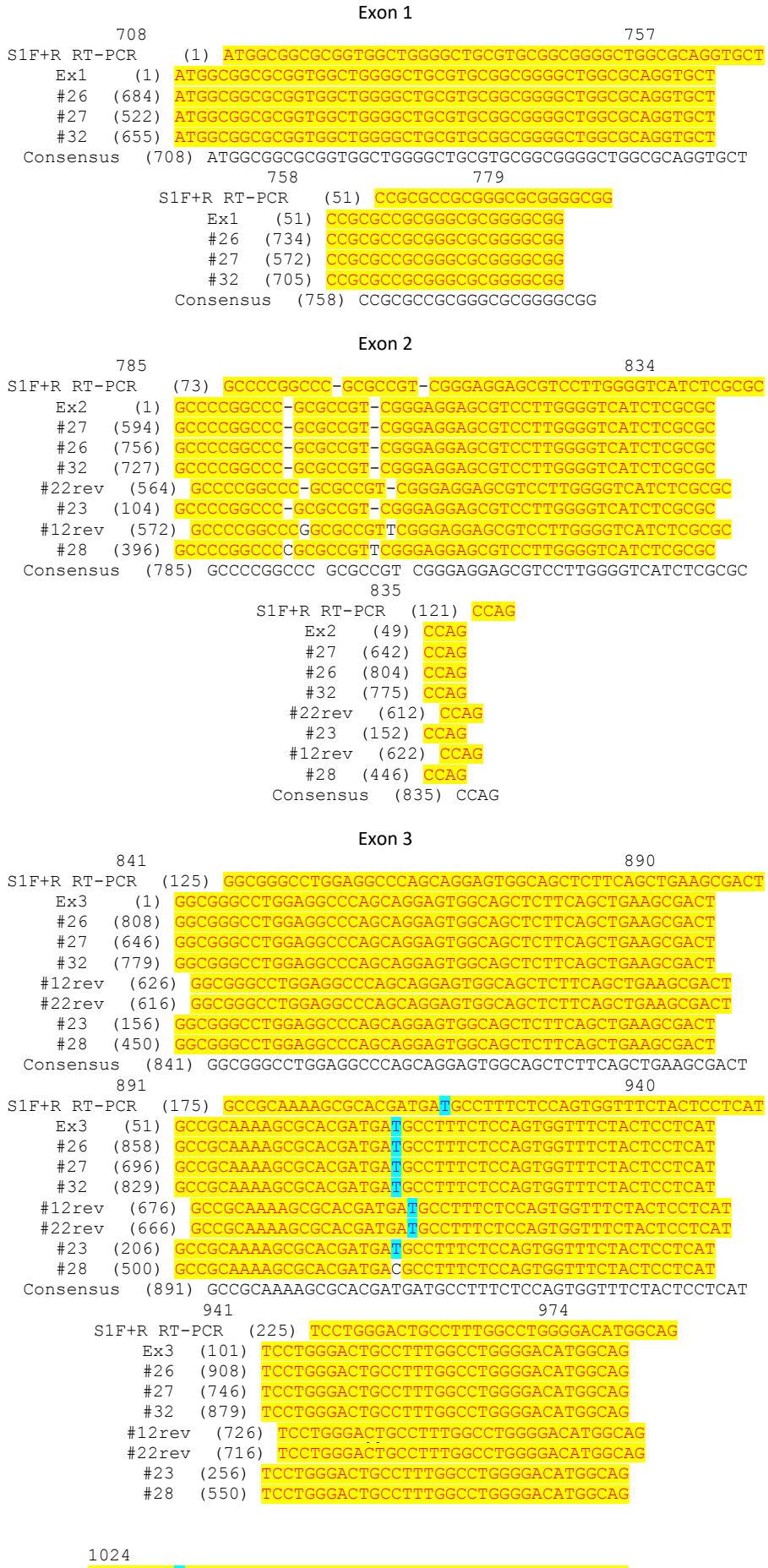

BOX 1. Swine Surf1 gene exons 1-9 alignments

Exon 4

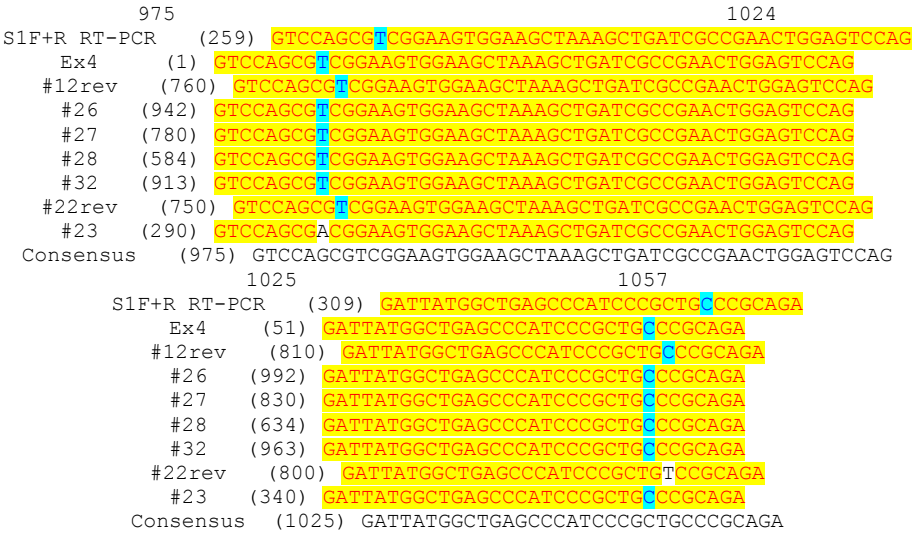

Exon 5

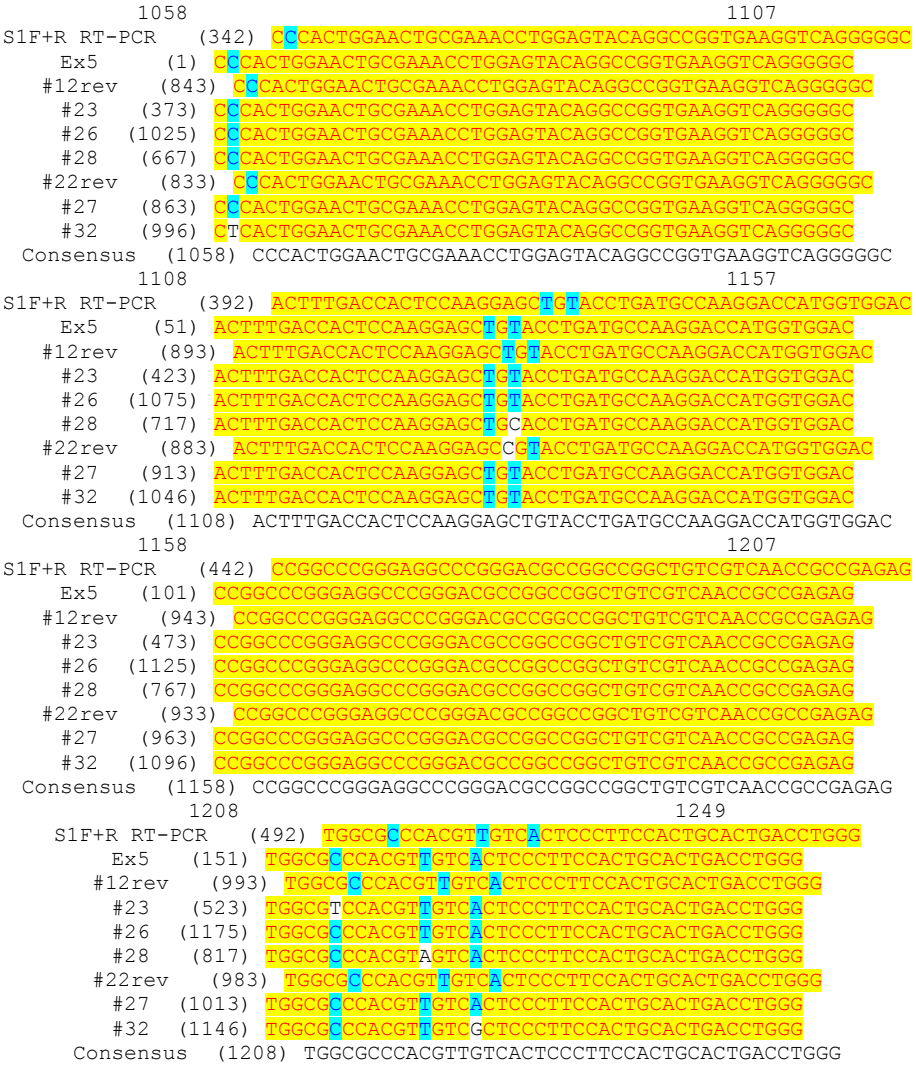

BOX 1. Swine Surf1 gene exons 1-9 alignments

Exon 6

```
          1251                                                1300
S1F+R RT-PCR   (534) AATCACCATCCTGGTAAATAGAGGGTTTGTGCCCAGGAAGAAAGTGAATC
     Ex6       (1) AATCACCATCCTGGTAAATAGAGGGTTTGTGCCCAGGAAGAAAGTGAATC
   #12rev   (1035) AATCACCATCCTGGTAAATAGAGGGTTTGTGCCCAGGAAGAAAGTGAATC
     #23    (565) AATCACCATCCTGGTAAATAGAGGGTTTGTGCCCAGGAAGAAAGTGAATC
     #26   (1217) AATCACCATCCTGGTAAATAGAGGGTTTGTGCCCAGGAAGAAAGTGAATC
     #27   (1055) AATCACCATCCTGGTAAATAGAGGGTTTGTGCCCAGGAAGAAAGTGAATC
     #28    (859) AATCACCATCCTGGTAAATAGAGGGTTTGTGCCCAGGAAGAAAGTGAATC
     #32   (1188) AATCACCATCCTGGTAAATAGAGGGTTTGTGCCCAGGAAGAAAGTGAATC
   #22rev   (1025) AAACACCATCCTGGTAAATAGAGGGTTTGTGCCCAGGAAGAAAGTGAATC
  Consensus  (1251) AATCACCATCCTGGTAAATAGAGGGTTTGTGCCCAGGAAGAAAGTGAATC
                    1301          1323
            S1F+R RT-PCR   (584) CTGAGACGCGTCTTAAAGGCCAG
                 Ex6       (51) CTGAGACGCGTCTTAAAGGCCAG
               #12rev    (1085) CTGAGACGCGTCTTAAAGGCCAG
                 #23     (615) CTGAGACGCGTCTTAAAGGCCAG
                 #26    (1267) CTGAGACGCGTCTTAAAGGCCAG
                 #27    (1105) CTGAGACGCGTCTTAAAGGCCAG
                 #28     (909) CTGAGACGCGTCTTAAAGGCCAG
                 #32    (1238) CTGAGACGCGTCTTAAAGGCCAG
               #22rev    (1075) CTGAGACGCGTCTTAAAGGCCAG
              Consensus  (1301) CTGAGACGCGTCTTAAAGGCCAG
```

Exon 7

```
          1323                                                1372
S1F+R RT-PCR   (607) ATTGAGGGAGAGGTGGACCTCGTGGGGATGGTGAGGCTGACAGAGACCCG
     Ex7       (1) ATTGAGGGAGAGGTGGACCTCGTGGGGATGGTGAGGCTGACAGAGACCCG
   #12rev   (1108) ATTGAGGGAGAGGTGGACCTCGTGGGGATGGTGAGGCTGACAGAGACCCG
   #22rev   (1098) ATTGAGGGAGAGGTGGACCTCGTGGGGATGGTGAGGCTGACAGAGACCCG
     #23    (638) ATTGAGGGAGAGGTGGACCTCGTGGGGATGGTGAGGCTGACAGAGACCCG
     #26   (1290) ATTGAGGGAGAGGTGGACCTCGTGGGGATGGTGAGGCTGACAGAGACCCG
     #27   (1128) ATTGAGGGAGAGGTGGACCTCGTGGGGATGGTGAGGCTGACAGAGACCCG
     #28    (932) ATTGAGGGAGAGGTGGACCTCGTGGGGATGGTGAGGCTGACAGAGACCCG
     #32   (1261) ATTGAGGGAGAGGTGGACCTCGTGGGGATGGTGAGGCTGACAGAGACCCG
  Consensus  (1323) ATTGAGGGAGAGGTGGACCTCGTGGGGATGGTGAGGCTGACAGAGACCCG
          1373                                                1422
S1F+R RT-PCR   (657) GAAGCCTTTGTCCCGGAGAATAATCCAGAGAGGAATCACTGGCATTATC
     Ex7       (51) GAAGCCTTTGTCCCGGAGAATAATCCAGAGAGGAATCACTGGCATTATC
   #12rev   (1158) GAAGCCTTTGTCCCGGAGAATAATCCAGAGAGGAATCACTGGCATTATC
   #22rev   (1148) GAAGCCTTTGTCCCGGAGAATAATCCAGAGAGGAATCACTGGCATTATC
     #23    (688) GAAGCTCTTTGTCCCGGAGAATAATCCAGAGAGGAATCACTGGCATTATC
     #26   (1340) GGAGCCCTTTGTCCCGGAGAATAATCCAGAGAGGAATCACTGGCATTATC
     #27   (1178) GAAGCCCTTTGTCTCGGAGAATAATCCAGAGAGGAATCACTGGCATTATC
     #28    (982) GAAGCCCTTTGTCCCGGAGAATAATCCAGAGAGGAATCACTGGCATTATC
     #32   (1311) GAAGCCCTTTGTCCCGGAGAATAATCCAGAGAGGAATCACTGGCATTATC
  Consensus  (1373) GAAGCCCTTTGTCCCGGAGAATAATCCAGAGAGGAATCACTGGCATTATC
          1423                                                1472
S1F+R RT-PCR   (707) GGGACCTGGAGGCCATGGCCAGGCTCACGGGGGCAGAGCCCATTTTCATA
     Ex7   (101) GGGACCTGGAGGCCATGGCCAGGCTCACGGGGGCAGAGCCCATTTTCATA
   #12rev   (1208) GGGACCTGGAGGCCATGGCCAGGCTCACGGGGGCAGAGCCCATTTTCATA
   #22rev   (1198) GGGACCTGGAGGCCATGGCCAGGCTCACGGGGGCAGAGCCCATTTTCATA
     #23    (738) GGGACCTGGAGGCCATGGCCAGGCTCACGGGGGCAGAGCCCATTTTCATA
     #26   (1390) GGGACCTGGAGGCCATGGCCAGGCTCACGGGGGCAGAGCCCATTTTCATA
     #27   (1228) GGGACCTGGAGGCCATGGCCAGGCTCACGGGGGCAGAGCCCATTTTCATA
     #28   (1032) GGGACCTGGAGGCCATGGCCAGGCTCACGGGGGCAGAGCCCATTTTCATA
     #32   (1361) GGGACCTGGAGGCCATGGCCAGGCTCACGGGGGCAGAGCCCATTTTCATA
  Consensus  (1423) GGGACCTGGAGGCCATGGCCAGGCTCACGGGGGCAGAGCCCATTTTCATA
                    1473     1485
            S1F+R RT-PCR   (757) GATGCCGACTTCA
                 Ex7       (151) GATGCCGACTTCA
               #12rev    (1258) GATGCCGACTTCA
               #22rev    (1248) GATGCCGACTTCA
                 #23     (788) GATGCCGACTTCA
                 #26    (1440) GATGCCGACTTCA
                 #27    (1278) GATGCCGACTTCA
                 #28    (1082) GATGCCGACTTCA
                 #32    (1411) GATGCCGACTTCA
              Consensus  (1473) GATGCCGACTTCA
```

BOX 1. Swine Surf1 gene exons 1-9 alignments

Exon 8

```
          1529                                                1578
S1F+R RT-PCR   (770) AGAGCACGGTCCCTGGAGGCCCCGTTGGAGGACAGACCAGAGTCACTCTG
    Ex8     (1) AGAGCACGGTCCCTGGAGGCCCCGTTGGAGGACAGACCAGAGTCACTCTG
  #12rev  (1271) AGAGCACGGTCCCTGGAGGCCCCGTTGGAGGACAGACCAGAGTCACTCTG
  #22rev  (1261) AGAGCACGGTCCCTGGAGGCCCCGTTGGAGGACAGACCAGAGTCACTCTG
    #23   (843) AGAGCACGGTCCCTGGAGGCCCCGTTGGAGGACAGACCAGAGTCACTCTG
    #26  (1453) AGAGCACGGTCCCTGGAGGCCCCGTTGGAGGACAGACCAGAGTCACTCTG
    #27  (1291) AGAGCACGGTCCCTGGAGGCCCCGTTGGAGGACAGACCAGAGTCACTCTG
    #28  (1095) AGAGCACGGTCCCTGGAGGCCCCGTTGGAGGACAGACCAGAGTCACTCTG
    #32  (1424) AGAGCACGGTCCCTGGAGGCCCCGTTGGAGGACAGACCAGAGTCACTCTG
 Consensus  (1529) AGAGCACGGTCCCTGGAGGCCCCGTTGGAGGACAGACCAGAGTCACTCTG
                  1579                          1610
       S1F+R RT-PCR   (820) AGGAACGAGCACCTGCAGTACATCATTACCTG
           Ex8    (51) AGGAACGAGCACCTGCAGTACATCATTACCTG
         #12rev  (1321) AGGAACGAGCACCTGCAGTACATCATTACCTG
         #22rev  (1311) AGGAACGAGCACCTGCAGTACATCATTACCTG
           #23   (893) AGGAACGAGCACCTGCAGTACATCATTACCTG
           #26  (1503) AGGAACGAGCACCTGCAGTACATCATTACCTG
           #27  (1341) AGGAACGAGCACCTGCAGTACATCATTACCTG
           #28  (1145) AGGAACGAGCACCTGCAGTACATCATTACCTG
           #32  (1474) AGGAACGAGCACCTGCAGTACATCATTACCTG
         Consensus  (1579) AGGAACGAGCACCTGCAGTACATCATTACCTG
```

Exon 9

```
          1611                                                1660
    Ex9     (1) GTATGGACTGTGCGCAGCCACGTCGTATCTGTGGTGTAAGAAATTCCTGA
S1F+R RT-PCR   (852) GTATGGACTGTGCGCAGCCACGTCGTATCTGTGGTGTAAGAAATTCCTGA
  #12rev  (1353) GTATGGACTGTGCGCAGCCACGTCGTATCTGTGGTGTAAGAAATTCCTGA
  #22rev  (1343) GTATGGACTGTGCGCAGCCACGTCGTATCTGTGGTGTAAGAAATTCCTGA
    #23   (925) GTATGGACTGTGCGCAGCCACGTCGTATCTGTGGTGTAAGAAATTCCTGA
    #26  (1535) GTATGGACTGTGCGCAGCCACGTCGTATCTGTGGTGTAAGAAATTCCTGA
    #27  (1373) GTATGGACTGTGCGCAGCCACGTCGTATCTGTGGTGTAAGAAATTCCTGA
    #28  (1177) GTATGGACTGTGCGCAGCCACGTCGTATCTGTGGTGTAAGAAATTCCTGA
    #32  (1506) GTATGGACTGTGCGCAGCCACGTCGTATCTGTGGTGTAAGAAATTCCTGA
 Consensus  (1611) GTATGGACTGTGCGCAGCCACGTCGTATCTGTGGTGTAAGAAATTCCTGA
                       1661          1680
           Ex9    (51) GGCGGCCTCCTGCGGTGTGA
      S1F+R RT-PCR   (902) GGCGGCCTCCTGCGGTGTGA
         #12rev  (1403) GGCGGCCTCCTGCGGTGTGA
         #22rev  (1393) GGCGGCCTCCTGCGGTGTGA
           #23   (975) GGCGGCCTCCTGCGGTGTGA
           #26  (1585) GGCGGCCTCCTGCGGTGTGA
           #27  (1423) GGCGGCCTCCTGCGGTGTGA
           #28  (1227) GGCGGCCTCCTGCGGTGTGA
           #32  (1556) GGCGGCCTCCTGCGGTGTGA
         Consensus  (1661) GGCGGCCTCCTGCGGTGTGA
```

BOX 2. Swine Surf1 gene complete sequence

5’atggcggcgcggtggctggggctgcgtgcggcggggcaggcgcaggtgctccgcgccgcgggcgcggggcgggtgagcggggcggggagcccgggcgg
ggggcggcccggctgggggctcgcccggactggacgagctcagccggcccctcgcgtctccgcaggccccggcccgcgccgtcgggaggagcgtccttggg
gtcatctcgcgcccagggtgaggagtcgtttggcacctgggaaagctgccctgcactttgccaggggccatggggtcacgatgaaccctggaactgcctcctgcgcc
tcggggacaggccctggccacgcgccggcccgtcccttgcggcagtccgacgccctcggcggaagacgtgcggtagttgcccagacacctcctcgggctaatgc
ggggccagcccaaggctgaaaccgtccgggatcctgaagaaaagcataaccagtcgcgacggtttgcacgttgcctcccgggtacagcgaagggcaatcgtgtg
tgtgtgtgtggagtgcggtgcacatttaaaggtcgcaagcctgctccaggccagcttgtttagcggccccaagacccatgttgctttccgttgacggcactcgcccgct
gagtgtctaaaggcactttctgtgtacctttttcgaggtttaaatgctgagagctctgtaaaccactgtcctgagtgtttcacgctctcttcagagcactgtggctggtggacct
gtgtggtcggcgtataggatgcatcttagcgggttcttgtgcgaaaggcacaggttggttacgtgaatcggtcagggtcatggttggtggcagagccaggactgaatg
ctagatctcctcgtcagtgaacgtccgctgagtgggggtcaaggcccgggtactgggtaggggcagggctgggctgctggttggctcctgactgcacacggtggcct
gtgccctcctcccggcccatgttccctttggcaatagtggcagttttgagaactcggagcctccacttctttgtcccaggcctctagccccatgcccgtgttgtgacatctcct
aggcgggcctggaggcccagcaggagtggcagctcttcagctgaagcgactgccgcaaaagcgcacgatgatgcctttctccagtggtttctactcctcattcctggg
actgcctttggcctggggacatggcaggtaaagcctgacctctggctctcctggccctgagcccttgaccctgctgccacccgctcgagctaatgctctgtgtctgtgtag
gtccagcgtcggaagtggaagctaaagctgatcgccgaactggagtccaggattatggctgagcccatcccgctgcccgcagagtgagtgtatgtggctgcccacc
agggctgcgctggccggaggtcacatgccttcctgaccctgatgggagctctcacatcagtgggcctgctaggcttcctgttgtcactcgactgcccttgtgacactgcct
gacatacacaggaaaatttttgaacctgggattcacctttttttccatgccctgtgcagccaagggtccctcgaggatggcccccatagcagtcattcttagccggcgcta
gggtacacgtatctcttgacaggagaagtactttgaaaaagtgcccagtgagtctacagccctgtcccctcattttaatttttttaatttttattttttgtctttctgccatttctagg
gccactcccgcggcacatggagggttcccaggctagggatctaagcggatctgtagctgctggcctacaccagagcctcagcaacacgggatctgagccgcgtct
gcaagcaacaccacagctcacggcaatgccagatccttaacccactgagcaaggccagggatcaaacccacaaccccatggttcttagattcgttaaccactgag
ccacaacaggaactcccctgtcccctcatttaaaagcaccatccagagttcctgttgtgccgcagcagcgagtcccactagtaaccatgaggatgtgggttccatccct
ggccttgctcggtgggttaaggatccggcattgccgcgaggtgtgatttaggtcacaggagaggcttggatcccacgtggctgtggctctgatatgacccctagcctgg
gaacttatatgtgccacgggtgcggccctaaaaaacaaaaaataaaagccccatcctagaggaacagctgtaatcagaatgctttccgctcaagacagcaaacga
gtgggtcccacttggcttgcggatgtggctttggctcatgtgttttatcccgttcatgcgggagtccatctctaagcttttcctgaacacttgctccgttgggcagcccagacc
cacattcccatgtggcatcaaaggccccggcttcctccttcagagggcacctcagtcaccgtgggcttcatggcagatccaagagggttcgtcttcctgccaaaccttg
cgcggccccagctccgtttctcctctcccctgcagcccactggaactgcgaaacctggagtacaggccggtgaaggtcaggggcactttgaccactccaaggagc
tgtacctgatgccaaggaccatggtggacccggcccgggaggcccgggacgccggccggctgtcgtcaaccgccgagagtggcgcccacgttgtcactcccttcc
actgcactggcctggggtgagtggggctcaggggccgactggcctgtgaggcgttcatttccttggctttgcttctcagcccccaaccccagggcacccaggatactc
agacaagttcagttgctttttgagtttgaaatgtgtaattttagcattaaagccattaatttactgctgaacagatcccgcatgttgggctctgaaggggaggaaaggaga
ggcggggcccgccagagggactgagaggggagcccccagctctgcctcgggggtggtcaggggaggcttccggggcgagttaggccagagtgaagagatgg
gaggagggtttcgggaagggacacgaacaggatgtggacacaaggttggtaactagagcaacttccaaatgttgacaggtcaaccccagagccctggtcagccc
gcagccttctgctttgagatctgggaagggctcctgtgctggtgttggtgggagatgggaggcaggaggacggctgggtcactgttcatgtggcaggggggtgggggtg
ttgagccagggcactcaccccacagccagctcttagcttttgagcccttctgtggcgttcccactgtgccaactcaccccacagccagctcttagcttttgagcccttttctg
tggcgttcccactgtgccacagaggtttaggattctgactgcaggggttcccgcggtggcaaaacagcacgggtagcatctccaatgtgccaggttgcaggttcaatc
cccagcccagcaccgtggattaaggatgcggcattgtcccagctgcggcacaggtcacaaatgcagctgggatctgattcctggtgccactgggagacaaaaaac
cgagggtgctgtggtggcccagagcactgggtcaaaggctctggcgttgccaccgccgtgcagtcagccagctgtggcttggaagagcattgaaccccccccaccc
aaccaaaaacccttttcttgcactgttgtccctggaggtacctgaatgaccactggtgatacacacctttattcagagccccccgcacctgctcttattactctagaatcac
catcctggtaaatagagggtttgtgcccaggaagaaagtgaatcctgagacgcgtcttaaaggccaggtaagggacgggcaacagcgcccccttcagccgccag
ccagcccttgccggccggagacagcatctcctgctttcttttcgtagattgagggagaggtggacctcgtggggatggtgaggctgacagagacccggaagccctttg
tcccggagaataatccagagaggaatcactggcattatcgggacctggaggccatggccaggctcacgggggcagagcccattttcatagatgccgacttcagtac
gtggtgcccagcctgccccctaagacccaggagctggtgtaaatgcccgcttctctctcccctaaccctgggcgcctcccagtgactcgccattcacactctaccctg
tgctgtgctggcgtgggagggagttaggcctgaccttgctcagcagatgctgagaagagagagcaccaggggctggctgatgccaggacagctctgggagagg
ctgcccctgtggacacccagcgccccgtctctgcagagagcacggtccctggaggccccgttggaggacagaccagagtcactctgaggaacgagcacctgcag
tacatcattacctggtgaggggcctggccacaccccgctcctcccctcctcccacccccagaccctgacgacggcccaccttccaaccgaaggtatggact
gtgcgcagccacgtcgtatctgtggtgtaagaaattcctgaggcggcctcctgcggtgtga3’.

5. Discussion

Mouse models are valuable tools to unravel the molecular and biochemical mechanisms underpinning mitochondrial diseases, but they often fail to develop the qualitative and/or quantitative clinical features of the human pathology. Significant examples stem from both our own experience and that of other investigators interested in genetic neurodegenerative disorders, including mitochondrial disease. For instance, we already mentioned that the Surf1 KO mouse displays mild but significant isolated COX deficiency in all tissues, but hardly any pathological phenotype, and, if anything, a prolongation of the lifespan and protection from Ca^{2+}-induced neurotoxicity. Conversely, in LS patients, the lack of Surf1 protein causes a devastating, early-onset, invariably fatal encephalopathy associated with an isolated COX deficiency and a typical pattern of MRI findings. The reasons for such a discrepancy in the clinical manifestations between mice and men could be partially attributed to intrinsic differences between the two species, including size, lifespan, metabolic rate, diet, and functional anatomy of target organs, notably the brain. Generally, the mouse phenotype is either absent or much less severe than the human one, sometimes even targeting different organs or displaying apparently paradoxical effects, as in the Surf1 KO mouse, due probably to the trigger of compensatory mechanisms. To investigate LS pathology from a theoretically less distant evolutionary point, we decided to generate the first Surf1 KO pig model, with the aim to characterize from a phenotypical and a biochemical point of view the pathological phenotype associated with Surf1 protein ablation in pigs and therefore attempt to unravel LS pathogenesis. Since the accurate and complete sequence of the swine Surf1 gene and its genomic organization were not available, we managed to obtain the precise annotation of swine Surf1 gene in order to precisely setup the genetic engineering protocol necessary for the definitive knockout of Surf1gene expression. The swine Surf1 gene, as the human, is characterized by 9 exons. We decided to target swine exon 3 of the Surf1 gene in order to disrupt the N-terminal transmembrane domain of the protein and thus generate a biallelic null mutation, therefore mimicking the complete absence of Surf1 protein found in the great majority of LS patients. Moreover, mutations in exon 3 have also been reported in LS patients (Lee *et al.*, 2012). For the precise editing of the genomic region of interest of swine Surf1 gene, we exploited the most recent genetic engineering technology in terms of site-specific nucleases, in particular TALENs and CRISPR/Cas9, in combination with a specific homologous recombination vector, to knockout Surf1 expression in selected primary porcine fibroblast cell lines. After a deep genotyping analysis of cell clones generated, we identified suitable nuclear donor clones carrying the mutations of interest and animals were then generated through high efficiency SCNT procedure. Using both

TALENs and CRISPR/Cas9 system, we obtained a high number of fibroblast colonies suitable for SCNT. TALENs proved to be more effective (55% to 67% of targeted colonies in presence of the targeting vector) and this difference could be attributable to the efficacy of the preliminary screening we performed to identify the most effective TALEN pair. On the other hand, the CRISPR/Cas9 sgRNA guides were selected only based on the software prediction. After SCNT using few selected cell clones as nuclear donor cells, we managed to obtain two compound heterozygous KO male lines, one through TALENs technology and one using CRISPR/Cas9 system. The KO male lines generated through TALENs technology (ID6639 and subsequent 487 re-cloning) is characterized by the monoallelic integration of the HR vector, therefore substituting wild type exon 3 with a 106 bp-deleted version together with a loxable puromycin cassette useful for colony selection and eventually removable by Cre-Lox recombinase system, and the deletion of 5bp in the other allele. From this genetic background, we generated the great majority of Surf1 KO piglets described in our study. On the other hand, the KO male line modified through CRISPR/Cas9 technology is characterized by the integration of the same HR vector as above on one allele and the insertion of one bp (+A) in the other allele. We managed to observe and analyze one male animal for each TALENs and CRISPR/Cas9 Surf1 KO lines that survived more than three weeks. Interestingly, the severe pathological phenotype observed in the two longer-lived Surf1 KO pigs was the same, excluding the interference of nuclease-specific off-target effect in the phenotype generation. Considering the unpredictability of the pathological phenotype in pigs, in addition to Surf1 KO pig model, we generated in parallel both male and female Surf1 heterozygous animals. Surf1 heterozygous individuals have been used as controls for the Surf1 KO animals, together with wild type controls, and will be used for breeding to obtain Surf1 KO individuals by conventional breeding, therefore free from possible SCNT side effects (Kurome *et al.*, 2013). The genetic engineering of Surf1 heterozygous animals was performed with the same reagents as for Surf1 KO animals (same TALENs pair associated with the same HR vector and same CRISPR sgRNA). Surf1 heterozygous animals did not show any pathological sign and were totally comparable to wild type controls. The absence of monoallelic Surf1 silencing-related symptoms excluded a possible influence of the genetic engineering procedure (e.g. nuclease-associated off target effects, severe disturbance of surfeit cluster due to HR vector integration, mutation-specific phenotype) on the establishment of the severe phenotype observed in Surf1 KO animals and, at the same time, confirmed the autosomal recessive nature of LS. In particular, the female Surf1 heterozygous line was generated through TALENs technology and was characterized by the monoallelic integration of the HR vector and one wild type allele. The male Surf1 heterozygous line, on the other hand, was generated through CRISPR/Cas9 technology without

the HR vector, and presented a monoallelic single base-pair insertion (+A) and a wild type allele. The extremely severe phenotype observed in our Surf1 KO animals, invariably leading to death of the animals within the first 10 days of life under normal feeding and housing conditions, is therefore entirely attributable to the biallelic disruption of swine Surf1 gene and the consequent complete ablation of Surf1 protein. The two longer-lived piglets were raised with an artificial feeder in an designated housing room, which is a normal precaution when the litter size is very small (1-2 piglets) because they are unable to keep the sow sufficiently stimulated to produce milk. Moreover, the artificial feeder allowed Surf1 KO piglets to feed more easily as they were not supposed to actively suck the milk. On the other hand, when a large litter was obtained and the piglets were allowed to feed in natural condition under the sow no piglet survived more than 9 days because of the insufficient milk intake due to improper suckling and lack of appetite, and also because of the poor energy conversion efficiency.

The animals considered in this study, independently from the genotype (wild type, Surf1 KO and heterozygous), were generated through SCNT procedure. The SCNT efficiency obtained throughout the study, in terms of live offspring per number of reconstructed embryos transferred to the recipient, ranges from 1% to 10%, being comparable, and in some cases even higher, than the 1%-to-5% range presented in (Kurome *et al.*, 2013). Nonetheless, a slight decrease in live offspring rates is observed in association with the Surf1 KO in comparison with the Surf1 heterozygous and wild type (data not shown) condition. It is well known that SCNT-derived individuals can be weaker than natural breeding-derived animals (Loi *et al.*, 2016), therefore the perinatal period in particular could be extremely challenging for genome-edited cloned piglets. Moreover, although we edited a nuclear-encoded mitochondrial protein, it is fundamental to consider the interactions between nuclear DNA (of a transfected somatic cell) and mitochondrial DNA (of the enucleated oocyte) at the basis of the overall functioning of the MRC. Different studies on mtDNA in porcine SCNT embryos, fetuses and offspring revealed the presence of varying levels of nuclear donor mtDNA, giving rise to heteroplasmy phenomenon, which is thought to be at least in part responsible for the high death rates associated with nuclear transfer (Sutovsky *et al.*, 1999; Zhong *et al.*, 2008). Nevertheless, the majority of SCNT-derived individuals appeared to be homoplasmic or displayed only mild heteroplasmy (St John *et al.*, 2005; Takeda *et al.*, 2006). Besides, SCNT itself is sometimes described as a challenging procedure as it deprives an oocytes' mtDNA of the corresponding maternal nuclear DNA, forcing it to interact with a foreign nucleus. This can result in various degrees of nuclear-mitochondrial incompatibility with consequent impairment of mitochondrial functions (Sutovsky Peter, 2007; Lagutina *et al.*, 2013). Interestingly, the recently discussed issue of three-parents IVF babies has highlighted the

potentiality and reliability of SCNT procedure (Amato *et al.*, 2014), overcoming the controversial issue of nuclear-mitochondrial incompatibility. It is fundamental to consider the high complexity of SCNT procedure and the possible consequences of its application to the generation of genome-edited animals, therefore this study was designed to use the same SCNT procedure to generate Surf1 KO as well as Surf1 heterozygous and wild type control animals. Therefore, the lethal phenotype observed in our Surf1 KO piglets could only be exacerbated by the SCNT procedure, but not caused by it. In conclusion, SCNT is considered a unique tool both for research purposes and for animal reproduction, and efforts to improve the procedure are constantly been done. Recent small technical improvements in SCNT procedure have been made in order to obtain high-efficiency production of ESCs from SCNT-derived human embryos, making SCNT a promising therapeutic tool (Loi *et al.*, 2016).

The absence of Surf1 protein in our Surf1 KO pigs, confirmed through western blot (WB) analysis on all animals, affects piglets immediately after birth and mainly in the perinatal period, with the early onset of an extremely and progressive pathological phenotype inevitably ending in death of animals in a matter of days. The direct effect of Surf1 protein ablation on survival rate of our pig model is evident comparing Kaplan-Meier survival curve of Surf1 KO individuals with the curves of wild type controls and Surf1 heterozygous, and no differences were detected between controls' curve and heterozygous one.

Therefore, our Surf1 KO piglets already show a typical pattern of pathological signs at birth (e.g. lack of appetite, lethargy, tremors, low muscle tone). Conversely, in LS patients, the onset of the pathological phenotype is generally after a period of normal development in which the infants acquire normal neuro-muscular skills in line with the age and, in the great majority of cases, the trigger of first LS-related symptoms is related to a stimulation of immune system activation. The difference in the pathology onset timing could be related to the intrinsic differences between human and pig development at birth. Babies are completely helpless at birth, the growth rate inside of the womb is far greater than the one in the months after birth. Conversely, the piglets have a lesser intensive *in utero* growth compared to humans, due to the limited time of pregnancy (114 days vs. 280 days on average, respectively) and to the nature of the swine species itself, which is notably characterized by multiple offsprings and very fast growth after birth. The timing of the pathology onset could be directly related to the achievement of specific metabolic and/or physiologic cutoffs, which are already present in newborn piglets, and therefore the birth is enough to trigger immediately the pathological symptoms cascade, whereas it needs at least a few months of post-natal development in humans. From each animal generated by SCNT we have established a biobank containing primary fibroblast cell lines to be used for future SCNT and for *in vitro*

mitochondria analysis as well as different tissue specimens for the current biochemical, molecular and morphological characterization of the animal model. Since we still not fully understand our Surf1 swine model, we plan to further extend our investigation to the transcriptome analysis of the 3 groups of animals studied (Surf1 KO, Surf1 heterozygous and wild type controls) to unveil the molecular and metabolic pathways affected, leading inevitably to the death of Surf1 KO animals. Analyzing our Surf1 KO pig model from a biochemical point of view, in spite of the severity of the pathological phenotype observed, we did not detect the typical isolated COX deficiency reported in LS patients neither in analyzed tissues (quadriceps, liver and brain specimens) nor in fibroblast, and no significant alteration of other MRC complexes was detected. Importantly, skeletal muscle is one of the most targeted tissues of OXPHOS-defect-related pathologies because of its high-energy requirements. Commercial breeds of pigs, which is the genetic background used for our LS model, are characterized by a postnatal growth of muscular tissue, directly related to the number of fibres and satellite cells (myoblasts). The number of myoblasts, therefore the final growth potential of the muscle, is determined by prenatally-operating factors still not fully known (Wigmore e Stickland, 1983). In particular, myogenesis of swine striated skeletal muscle is completed on the third day of postnatal life. At birth, multi-nuclei muscular fibrils and myotubes (immature fibres with central nucleus) are largely interspersed in interstitial tissue, which tends to decrease in the three days after birth, with a proportional increment of fibrils. Moreover, from birth to the 18th day of post-natal life, only red muscle fibres (primary oxidative fibres) are detectable, whereas white muscle fibres (secondary glycolytic fibres) can be found from day 48 on (P. Makovický *et al.*, 2009). In this thesis we analysed mainly newborn muscular tissue, because of the postnatal severity of the pathological phenotype observed in our Surf1 KO pigs and our morphological findings agree with the myogenesis process described by Makovicky et al (2009), as we observe a profound infiltration of interstitial tissue in quadriceps muscle specimens of newborn piglets. Moreover, an important variability factor to consider is the number of fibres between and within litters of pigs. It has been demonstrated that primary oxidative muscle fibres vary significantly between litters and this variation is responsible for the difference in total muscle fibre. The same phenomenon, to a lesser extent, is detected also within litters (Dwyer e Stickland, 1991). Different factors influencing this variability were identified, most importantly the sow parity was highlighted. Young sows (parity 1-2) are still growing during their first two pregnancy, therefore the distribution of nutrients and oxygen between the sow and the embryos/foetuses is not sufficient to guarantee the fulfilment of embryos/foetuses requirements and thus to reach the optimal muscle development (Da Silva *et al.*, 2013). Interestingly, we used only 1 parity recipient sows for the generation of all piglets of this study (Surf1 KO and heterozygous and wild type

controls), therefore the hypothetical sub-optimal *in utero* conditions of embryo development has only to be considered as a general statement. Besides, the high variability within muscular fibrils population (e.g. multi-nuclei fibrils and myotubes, fibrils with centrally-located nucleus, etc) in the period of life considered in our study (newborn 0 to 1 day after birth), due to the gradual transition between the immature state and the completion of myogenesis, made it difficult to detect potential variations in quadriceps morphology of Surf1 KO piglets compared to age-matched controls. It is well known that COX is characterized by developmentally regulated isoforms that change between foetal- to adult-ones as an adaptation response to the exposure to higher partial oxygen concentrations after birth, which require an increase in oxygen metabolism and in cellular respiration (Minai *et al.*, 2008). In particular, the time-depending subunit substitution has been reported to be substantial during myogenesis (Lomax *et al.*, 1990). Since the completion of myogenesis in the pig occurs during the first days of post-natal life, it is plausible that muscles of newborn piglets could present more or less advanced state of transition between the foetal and the adult COX assembly status, therefore that COX activity could result extremely variable between individuals, even considering clones and even if no genome editing was performed (e.g. wild type controls). Therefore, individual variability (described in biochemical analysis) and intrinsic tissue variability (observed in morphological findings), potentially due to the species of interest and the delicate period of life considered, made it hazardous to interpret in a definitive way our biochemical results on Surf1 KO piglet skeletal muscle analysis. Anyway, no gross MRC activity defects and COX assembly alterations were detected in our Surf1 KO swine model compared to wild type controls, suggesting the trigger of compensatory mechanisms with protective effects on OXPHOS enzymes and functioning, but failing to suppress the severe pathological phenotype probably caused by different metabolic and/or physiologic pathway impairments.

Another frequent symptom used as an LS pathological sign in patients is a remarkable increase of blood lactate, sometimes leading to severe metabolic acidosis, consequent to a block in aerobic energy metabolism following MRC activity impairment (Zeviani *et al.*, 1996). Blood lactate levels in our newborn Surf1 KO piglets were slightly but significantly elevated in comparison with Surf1 heterozygous and wild type controls. Nonetheless, the blood lactate level of piglets in the first days of life can be altered by stress and birth-related factors, and a slight alteration can therefore be attributable rather to post-natal adaptation than to OXPHOS impairment, supporting our previous findings of normal MRC enzymes activity.

The clinical phenotype observed in our Surf1 KO piglets suggested an energy metabolism impairment that was not supported by our biochemical findings. Therefore we analyzed the intra-muscular lipid content and, interestingly, in a significant number of cases histological preparations

of quadriceps muscle of Surf1 KO newborn piglets showed a reduction of intramuscular fat deposit compared to controls, confirming a remarkable alteration of energy storage and/or distribution pathways. Over the years, energy metabolism pathways in commercial pig breeds have been forced towards the achievements of high feed conversion ratio in order to lower meat production costs. Different studies demonstrated how pigs with a low residual feed intake (RFI), a measure of feed efficiency and energy use (Cai *et al.*, 2008; Herd e Arthur, 2009; Boddicker *et al.*, 2011), are more efficient in the conversion of feed-to-body mass than animals with a high RFI, maintaining similar growth performance. Recently, it was demonstrated that the genetic selection for low RFI in pigs affects tissue metabolism and mitochondrial protein profile, resulting in a reduction of oxidative stress and a consequent improved efficiency of the MRC. Considering the commercial genetic background of our swine Surf1 KO model, it can be hypothesized that the inevitable genetic selection contributed to the enhancing of the MRC efficiency, partially or completely compensating for potential respiratory enzyme deficiency caused by Surf1 protein ablation. A comparable strict genetic selection is lacking in other Surf1 KO animal models generated so far (Drosophila, zebrafish, mouse) and obviously in LS patients, therefore this could help explaining why we observe a normal COX activity especially in muscle, while expecting for the reported isolated COX deficiency. Moreover, muscular tissue, genetically busted towards a rapid growth, suffers the lack of nutrients therefore depleting intramuscular fat, which is known to be located inside skeletal muscle fibers in lipid droplets that exist in close proximity to the mitochondria.

To further investigate the nature of the perinatal lethal phenotype observed in our Surf1 KO animals, we analyzed the histochemical COX and SDH reactions in jejunum villi, as small intestine is known to have the highest expression of Surf1 protein amongst human organs, together with endocrine tissue and liver (http://www.proteinatlas.org/ENSG00000148290-SURF1/tissue), although small intestine has not been biochemically and morphologically analysed in LS patients. High individual variability was detected also in this analysis but, interestingly, a significant number of Surf1 KO newborn piglets showed a strikingly reduced COX activity associated with an increased SDH reaction. Due to the multiple tissue and cellular types characterizing the intestinal tissue, we managed to investigate the COX deficiency in villi only through histochemical reaction, as the separation of villous cells from other populations for the biochemical measurements of MRC enzymes activity was not feasible. Similar to muscular tissue, the intestinal tissue in pigs undergo a substantial remodeling of the epithelium immediately after birth due to post-natal development. In particular, it has been demonstrated that in newborn animals the jejunum villi are thin and heterogeneous in length and shape, without extrusion zones and with plenty packets of apoptotic enterocytes, suggesting a fast and deep remodeling of mucosa leading

to functional maturation (Skrzypek *et al.*, 2007). The transition between the fetal-type enterocytes, characterized by the presence of wide vacuoles for the uptake of large colostrum molecules, and the adult-type occurs within the first three days after birth. During this period, the swine small intestine is subject to high stress levels because of the dramatic swift from parenteral to enteral nutrition and the first assumptions of milk and colostrum (Francois Blachier *et al.*, 2013). Therefore, in the first three days after birth piglets' small intestine undergo dramatic changes that can definitely result in the observed variability in COX reaction samples from newborn Surf1 KO piglets and controls. Moreover, especially in the post-natal period, the high demand of energy of intestinal tissue, together with its delicate functional balance, could be impaired by lesser MRC efficiency alterations not significant for the correct functioning of other tissues, influencing the proper assumption of colostrum and nutrients and prompting failure to thrive and general infections susceptibility.

The severe pathological phenotype observed in central nervous system of LS patients is largely attributed to the presence of typical microscopic lesions, characterized by vacuolation associated with demyelination, gliosis and vascular proliferation. Regarding our Surf1 KO swine model, vacuolation, demyelination and vascular proliferation were not observed. A consistent feature reported was the presence of microgliosis especially within the cerebral and cerebellar cortex in the older KO animal (80 days of age). The presence of microgliosis and hypertrophy of microglia is reported in LS associated pathology (Gogus *et al.*, 1994; Topcu *et al.*, 2000), however we cannot exclude it could be related to secondary general infections that caused the premature death of the animal.

Moreover, differences in cortical architecture associated to the presence of immature still migrating DCX positive neurons and numerous astroglial cells were observed at early postnatal ages. Although an inter-individual heterogeneity should be considered, a delayed or an altered cortical development of Surf 1 KO swine could not be excluded.

Finally, an important consideration needs to be made as premise for the interpretation of the wide range of results obtained from our animal model, and, in general, when an animal model is considered. It is in fact essential to evaluate the real nature of our Surf1 KO swine model, that is the generation of an exon-specific gene knockout, starting from a wild type genomic background, therefore from an healthy individual (ID6639). This approach, and the re-cloning procedure (starting from ID487) which guarantees the study of only one genetic background, allows the analysis of the phenotypic alterations induced by our specific mutations only, therefore excluding the theoretically infinite patterns of mutations occurring in LS human patients. This concept is deeply examined in a recent paper by Chen et al., in which the identification of healthy individuals

resilient to high penetrant forms of genetic childhood disorders is showed (Chen *et al.*, 2016). Therefore, the information coming from the study of each animal model of the same pathology (e.g. LS) can be useful to investigate different metabolic and/or physiologic pathways involved in the onset of the pathology of interest. Nonetheless, it is fundamental to keep the focus on the different genetic variability that can possibly contribute to the onset of the pathology in humans and the hypothetical limited number of cases reported (e.g. only born child presenting symptoms matching with the pathology of interest), versus the necessarily precise editing of genomes that occurs in the generation of animal models and the deep analysis of all the animal model phenotypes. This could explain, at least partially, the difficulties in the generation of an animal model that can perfectly replicate both the biochemical and the pathological phenotypes reported in human patients.

6. Conclusions and future perspective

In conclusion, we obtained a viable Surf1 KO pig model with a severe and progressive pathological phenotype, highlighting the fundamental roles of Surf1 protein presence/absence in pig survival. This finding is comparable to the typical pathological phenotype of LS patients, contrary to what observed in mouse models generated so far. The large animal model presented in this thesis was generated and characterize with a limited number of animals (n° 67), which makes the precise genetic engineering of large animals combined with SCNT important tools for the reduction (3R) of the number of animals required for modelling of human pathologies. The limited survival observed in out model, thus, prevents its use for diagnostic and therapeutic purposes, but could provide useful information on the understanding of the precise functions, pathways and interactions of Surf1 protein on a defined genetic background to pave the way for the discover of more complex genetic interactions in human patients. Considering our Surf1 KO pig model and the previously described animal models of LS, the different severity of the phenotype associated with the depletion of Surf1 protein may depend on the presence and efficiency of compensatory genetic and/or epigenetic mechanisms acting in different organisms. Further experiments based on a compared (pig-mouse-human) transcriptomic-proteomic approach could elucidate the compensatory mechanisms that allow the correct assembly of complex IV in the absence of Surf1 protein. As a future plan, we will breed our Surf1 heterozygous animals produced in this project to generate SCNT-free KO animals. A conditional Surf1 KO model could be generated to overcome the perinatal lethality in order to switch on the onset of pathological phenotype cascade on individuals of required ages to be comparable to human patients, and at the same time, to maintain healthy individuals to be used as founders of a breeding line.

7. Bibliography

AGOSTINO, A. et al. Constitutive knockout of Surf1 is associated with high embryonic lethality, mitochondrial disease and cytochrome c oxidase deficiency in mice. **Hum Mol Genet,** v. 12, n. 4, p. 399-413, Feb 15 2003. ISSN 0964-6906 (Print)

0964-6906.

AMATO, P. et al. Three-parent in vitro fertilization: gene replacement for the prevention of inherited mitochondrial diseases. **Fertil Steril,** v. 101, n. 1, p. 31-5, Jan 2014. ISSN 0015-0282.

ARCHIBONG, A. E. et al. Influence of sexual maturity of donor on in vivo survival of transferred porcine embryos. **Biol Reprod,** v. 47, n. 6, p. 1026-30, Dec 1992. ISSN 0006-3363 (Print)

0006-3363.

BADEN, K. N. et al. Early developmental pathology due to cytochrome c oxidase deficiency is revealed by a new zebrafish model. **J Biol Chem,** v. 282, n. 48, p. 34839-49, Nov 30 2007. ISSN 0021-9258 (Print)

0021-9258.

BARRIENTOS, A.; KORR, D.; TZAGOLOFF, A. Shy1p is necessary for full expression of mitochondrial COX1 in the yeast model of Leigh's syndrome. **The EMBO Journal**, Oxford, UK**,** v. 21, n. 1-2, p. 43-52, 08/29/received

11/05/revised

11/08/accepted 2002. ISSN 0261-4189

1460-2075. Disponível em: < http://www.ncbi.nlm.nih.gov/pmc/articles/PMC125806/ >.

BARRIENTOS, A. et al. Cytochrome c oxidase assembly in primates is sensitive to small evolutionary variations in amino acid sequence. **Mol Biol Evol,** v. 17, n. 10, p. 1508-19, Oct 2000. ISSN 0737-4038 (Print)

0737-4038.

BEAUJEAN, N. et al. The effect of interspecific oocytes on demethylation of sperm DNA. **Proc Natl Acad Sci U S A,** v. 101, n. 20, p. 7636-40, May 18 2004. ISSN 0027-8424 (Print)

0027-8424.

BODDICKER, N. et al. Effects of ad libitum and restricted feed intake on growth performance and body composition of Yorkshire pigs selected for reduced residual feed intake. **J Anim Sci,** v. 89, n. 1, p. 40-51, Jan 2011. ISSN 0021-8812.

BOYLE, J. Molecular biology of the cell, 5th edition by B. Alberts, A. Johnson, J. Lewis, M. Raff, K. Roberts, and P. Walter. **Biochemistry and Molecular Biology Education,** v. 36, n. 4, p. 317-318, 2008. ISSN 1539-3429. Disponível em: < http://dx.doi.org/10.1002/bmb.20192 >.

BRUNETTI, D. et al. Transgene expression of green fluorescent protein and germ line transmission in cloned pigs derived from in vitro transfected adult fibroblasts. **Cloning Stem Cells,** v. 10, n. 4, p. 409-19, Dec 2008. ISSN 1536-2302.

BURGSTALLER, J. P. et al. Mitochondrial DNA heteroplasmy in ovine fetuses and sheep cloned by somatic cell nuclear transfer. **BMC Dev Biol,** v. 7, p. 141, Dec 21 2007. ISSN 1471-213x.

CAI, W.; CASEY, D. S.; DEKKERS, J. C. Selection response and genetic parameters for residual feed intake in Yorkshire swine. **J Anim Sci,** v. 86, n. 2, p. 287-98, Feb 2008. ISSN 0021-8812.

CALVARUSO, M. A.; SMEITINK, J.; NIJTMANS, L. Electrophoresis techniques to investigate defects in oxidative phosphorylation. **Methods,** v. 46, n. 4, p. 281-7, Dec 2008. ISSN 1046-2023.

CAPECCHI, M. R. Gene targeting in mice: functional analysis of the mammalian genome for the twenty-first century. **Nat Rev Genet,** v. 6, n. 6, p. 507-12, Jun 2005. ISSN 1471-0056 (Print)

1471-0056.

CHEN, L. Y. et al. Changes in synaptic morphology accompany actin signaling during LTP. **J Neurosci,** v. 27, n. 20, p. 5363-72, May 16 2007. ISSN 0270-6474.

CHEN, R. et al. Analysis of 589,306 genomes identifies individuals resilient to severe Mendelian childhood diseases. **Nat Biotech,** v. 34, n. 5, p. 531-538, 05//print 2016. ISSN 1087-0156. Disponível em: < http://dx.doi.org/10.1038/nbt.3514 >.

CHENG, W. T. K.; MOOR, R. M.; POLGE, C. In vitro fertilization of pig and sheep oocytes matured in vivo and in vitro. **Theriogenology,** v. 25, n. 1, p. 146, 1986. ISSN 0093-691X. Disponível em: < http://dx.doi.org/10.1016/0093-691X(86)90200-1 >. Acesso em: 2017/03/11.

CHOMCZYNSKI, P.; SACCHI, N. Single-step method of RNA isolation by acid guanidinium thiocyanate-phenol-chloroform extraction. **Anal Biochem,** v. 162, n. 1, p. 156-9, Apr 1987. ISSN 0003-2697 (Print)

0003-2697.

COY, P. et al. Oviduct-specific glycoprotein and heparin modulate sperm-zona pellucida interaction during fertilization and contribute to the control of polyspermy. **Proc Natl Acad Sci U S A,** v. 105, n. 41, p. 15809-14, Oct 14 2008. ISSN 0027-8424.

DA SILVA, A. et al. Differences in muscle characteristics of piglets related to the sow parity. **Canadian Journal of Animal Science,** v. 93, n. 4, p. 471-475, 2013/12/01 2013. ISSN 0008-3984. Disponível em: < http://dx.doi.org/10.4141/cjas2013-049 >. Acesso em: 2017/03/06.

DA-RE, C. et al. Leigh syndrome in Drosophila melanogaster: morphological and biochemical characterization of Surf1 post-transcriptional silencing. **J Biol Chem,** v. 289, n. 42, p. 29235-46, Oct 17 2014. ISSN 0021-9258.

DARIN, N. et al. Genotypes and clinical phenotypes in children with cytochrome-c oxidase deficiency. **Neuropediatrics,** v. 34, n. 6, p. 311-7, Dec 2003. ISSN 0174-304X (Print)

0174-304x.

DAVIS, D. L.; STEVENSON, J. S.; SCHMIDT, W. E. Scheduled breeding of gilts after estrous synchronization with altrenogest. **J Anim Sci,** v. 60, n. 3, p. 599-602, Mar 1985. ISSN 0021-8812 (Print)

0021-8812.

DELL'AGNELLO, C. et al. Increased longevity and refractoriness to Ca(2+)-dependent neurodegeneration in Surf1 knockout mice. **Hum Mol Genet,** v. 16, n. 4, p. 431-44, Feb 15 2007. ISSN 0964-6906 (Print)

0964-6906.

DEY, R.; BARRIENTOS, A.; MORAES, C. T. Functional constraints of nuclear-mitochondrial DNA interactions in xenomitochondrial rodent cell lines. **J Biol Chem,** v. 275, n. 40, p. 31520-7, Oct 06 2000. ISSN 0021-9258 (Print)

0021-9258.

DIVIDICH, J. L.; PLUSKE, J. R.; VERSTEGEN, M. W. A., Eds. **Weaning the pig**: Wageningen Academic Publishers, p.432ed. 2003.

DUHIG, T. et al. The Human Surfeit Locus. **Genomics,** v. 52, n. 1, p. 72-78, 8/15/ 1998. ISSN 0888-7543. Disponível em: < http://www.sciencedirect.com/science/article/pii/S0888754398953721 >.

DURAI, S. et al. Zinc finger nucleases: custom-designed molecular scissors for genome engineering of plant and mammalian cells. **Nucleic Acids Res,** v. 33, n. 18, p. 5978-90, 2005. ISSN 0305-1048.

DWYER, C. M.; STICKLAND, N. C. Sources of variation in myofibre number within and between litters of pigs. **Animal Science**, Cambridge, UK**,** v. 52, n. 3, p. 527-533, 1991/006/001 1991. Disponível em: < https://www.cambridge.org/core/article/div-class-title-sources-of-variation-in-myofibre-number-within-and-between-litters-of-pigs-div/4711648AB6E814F7D95A6A6FDE8B14C4 >.

ECHANIZ-LAGUNA, A. et al. SURF1 deficiency causes demyelinating Charcot-Marie-Tooth disease. **Neurology,** v. 81, n. 17, p. 1523-30, Oct 22 2013. ISSN 0028-3878.

ENGLISH, P. R.; WILKINSON, V. 23 - MANAGEMENT OF THE SOW AND LITTER IN LATE PREGNANCY AND LACTATION IN RELATION TO PIGLET SURVIVAL AND GROWTH. In: (Ed.). **Control of Pig Reproduction**: Butterworth-Heinemann, 1982. p.479-506. ISBN 978-0-408-10768-6.

FERNANDEZ-VIZARRA, E.; LOPEZ-PEREZ, M. J.; ENRIQUEZ, J. A. Isolation of biogenetically competent mitochondria from mammalian tissues and cultured cells. **Methods,** v. 26, n. 4, p. 292-7, Apr 2002. ISSN 1046-2023 (Print)

1046-2023.

FRANCOIS BLACHIER; GUOYAO WU; YIN, Y. **Nutritional and Physiological Functions of Amino Acids in Pigs**. Springer Vienna, 2013. ISBN 978-3-7091-1327-1.

FUNAHASHI, H.; CANTLEY, T. C.; DAY, B. N. Synchronization of meiosis in porcine oocytes by exposure to dibutyryl cyclic adenosine monophosphate improves developmental competence following in vitro fertilization. **Biol Reprod,** v. 57, n. 1, p. 49-53, Jul 1997. ISSN 0006-3363 (Print)

0006-3363.

GALLI, C. et al. Pregnancy: a cloned horse born to its dam twin. **Nature,** v. 424, n. 6949, p. 635, Aug 07 2003. ISSN 0028-0836.

GALLI, C.; LAGUTINA, I.; LAZZARI, G. Introduction to cloning by nuclear transplantation. **Cloning Stem Cells,** v. 5, n. 4, p. 223-32, 2003. ISSN 1536-2302 (Print)

1536-2302.

GERARDS, M.; SALLEVELT, S. C.; SMEETS, H. J. Leigh syndrome: Resolving the clinical and genetic heterogeneity paves the way for treatment options. **Mol Genet Metab,** v. 117, n. 3, p. 300-12, Mar 2016. ISSN 1096-7192.

GOGUS, S. et al. Subacute necrotizing encephalopathy (Leigh syndrome): report of two juvenile cases with fatal outcome. **Turk J Pediatr,** v. 36, n. 1, p. 57-65, Jan-Mar 1994. ISSN 0041-4301 (Print)

0041-4301.

GRUPEN, C. G. The evolution of porcine embryo in vitro production. **Theriogenology,** v. 81, n. 1, p. 24-37, Jan 1 2014. ISSN 0093-691x.

GRUPEN, C. G.; NAGASHIMA, H.; NOTTLE, M. B. Cysteamine enhances in vitro development of porcine oocytes matured and fertilized in vitro. **Biol Reprod,** v. 53, n. 1, p. 173-8, Jul 1995. ISSN 0006-3363 (Print)

0006-3363.

_____. Asynchronous meiotic progression in porcine oocytes matured in vitro: a cause of polyspermic fertilization? **Reprod Fertil Dev,** v. 9, n. 2, p. 187-91, 1997. ISSN 1031-3613 (Print)

1031-3613.

GUIROUILH-BARBAT, J. et al. Impact of the KU80 pathway on NHEJ-induced genome rearrangements in mammalian cells. **Mol Cell,** v. 14, n. 5, p. 611-23, Jun 04 2004. ISSN 1097-2765 (Print)

1097-2765.

GUTIERREZ, K. et al. Efficacy of the porcine species in biomedical research. **Frontiers in Genetics,** v. 6, p. 293, 09/16

06/30/received

09/04/accepted 2015. ISSN 1664-8021. Disponível em: < http://www.ncbi.nlm.nih.gov/pmc/articles/PMC4584988/ >.

HATADA, I.; HORII, T. Genome editing: A breakthrough in life science and medicine. **Endocr J,** v. 63, n. 2, p. 105-10, 2016. ISSN 0918-8959.

HERD, R. M.; ARTHUR, P. F. Physiological basis for residual feed intake. **J Anim Sci,** v. 87, n. 14 Suppl, p. E64-71, Apr 2009. ISSN 0021-8812.

HIENDLEDER, S. et al. Heteroplasmy in bovine fetuses produced by intra- and inter-subspecific somatic cell nuclear transfer: neutral segregation of nuclear donor mitochondrial DNA in various tissues and evidence for recipient cow mitochondria in fetal blood. **Biol Reprod,** v. 68, n. 1, p. 159-66, Jan 2003. ISSN 0006-3363 (Print)

0006-3363.

HOLM, I. E.; ALSTRUP, A. K. O.; LUO, Y. Genetically modified pig models for neurodegenerative disorders. **The Journal of Pathology,** v. 238, n. 2, p. 267-287, 2016. ISSN 1096-9896. Disponível em: < http://dx.doi.org/10.1002/path.4654 >.

HUA, S. et al. High levels of mitochondrial heteroplasmy modify the development of ovine-bovine interspecies nuclear transferred embryos. **Reprod Fertil Dev,** v. 24, n. 3, p. 501-9, 2012. ISSN 1031-3613 (Print)

1031-3613.

HYTTEL, P.; NIEMANN, H. Ultrastructure of porcine embryos following development in vitro versus in vivo. **Mol Reprod Dev,** v. 27, n. 2, p. 136-44, Oct 1990. ISSN 1040-452X (Print)

1040-452x.

JOLLIFF, W. J.; PRATHER, R. S. Parthenogenic development of in vitro-matured, in vivo-cultured porcine oocytes beyond blastocyst. **Biol Reprod,** v. 56, n. 2, p. 544-8, Feb 1997. ISSN 0006-3363 (Print)

0006-3363.

KAEOKET, K. Study on the oestrous synchronization in gilts by using progestin altrenogest and hCG: its effect on the follicular development, ovulation time and subsequent reproductive performance. **Reprod Domest Anim,** v. 43, n. 1, p. 127-9, Feb 2008. ISSN 0936-6768 (Print)

0936-6768.

KATAYAMA, M. et al. Mitochondrial distribution and microtubule organization in fertilized and cloned porcine embryos: Implications for developmental potential. **Developmental Biology,** v. 299, n. 1, p. 206-220, 11/1/ 2006. ISSN 0012-1606. Disponível em: < http://www.sciencedirect.com/science/article/pii/S001216060601027X >.

KENYON, L.; MORAES, C. T. Expanding the functional human mitochondrial DNA database by the establishment of primate xenomitochondrial cybrids. **Proc Natl Acad Sci U S A,** v. 94, n. 17, p. 9131-5, Aug 19 1997. ISSN 0027-8424 (Print)

0027-8424.

KIM, H. J. et al. Targeted genome editing in human cells with zinc finger nucleases constructed via modular assembly. **Genome Res,** v. 19, n. 7, p. 1279-88, Jul 2009. ISSN 1088-9051 (Print)

1088-9051.

KIM, J. S. Genome editing comes of age. **Nat Protoc,** v. 11, n. 9, p. 1573-8, Sep 2016. ISSN 1750-2799.

KOOPMAN, W. J. H. et al. OXPHOS mutations and neurodegeneration. **The EMBO Journal,** v. 32, n. 1, p. 9-29, 11/13

08/21/received

10/09/accepted 2013. ISSN 0261-4189

1460-2075. Disponível em: < http://www.ncbi.nlm.nih.gov/pmc/articles/PMC3545297/ >.

KOVAROVA, N. et al. Tissue- and species-specific differences in cytochrome c oxidase assembly induced by SURF1 defects. **Biochim Biophys Acta,** v. 1862, n. 4, p. 705-15, Apr 2016. ISSN 0006-3002 (Print)

0006-3002.

KRAYTSBERG, Y. et al. Recombination of human mitochondrial DNA. **Science,** v. 304, n. 5673, p. 981, May 14 2004. ISSN 0036-8075.

KREINER, G. Compensatory mechanisms in genetic models of neurodegeneration: are the mice better than humans? **Frontiers in Cellular Neuroscience,** v. 9, p. 56, 03/06

10/06/received

02/06/accepted 2015. ISSN 1662-5102. Disponível em: < http://www.ncbi.nlm.nih.gov/pmc/articles/PMC4351629/ >.

KUROME, M. et al. Factors influencing the efficiency of generating genetically engineered pigs by nuclear transfer: multi-factorial analysis of a large data set. **BMC Biotechnol,** v. 13, p. 43, May 20 2013. ISSN 1472-6750.

LAGUTINA, I. et al. Interspecies somatic cell nuclear transfer: advancements and problems. **Cell Reprogram,** v. 15, n. 5, p. 374-84, Oct 2013. ISSN 2152-4971.

LAGUTINA, I.; LAZZARI, G.; GALLI, C. Birth of cloned pigs from zona-free nuclear transfer blastocysts developed in vitro before transfer. **Cloning Stem Cells,** v. 8, n. 4, p. 283-93, Winter 2006. ISSN 1536-2302 (Print)

1536-2302.

LAKE, N. J. et al. Leigh Syndrome: Neuropathology and Pathogenesis. **Journal of Neuropathology & Experimental Neurology,** v. 74, n. 6, p. 482-492, 2015. Disponível em: < http://jnen.oxfordjournals.org/content/74/6/482.abstract >.

LAMPERTI, C.; ZEVIANI, M. Encephalomyopathies caused by abnormal nuclear-mitochondrial intergenomic cross-talk. **Acta Myologica**, Ospedaletto (Pisa), Italy**,** v. 28, n. 1, p. 2-11, 2009. ISSN 1128-2460. Disponível em: < http://www.ncbi.nlm.nih.gov/pmc/articles/PMC2859628/ >.

LEE, I. C. et al. SURF1-associated Leigh syndrome: a case series and novel mutations. **Hum Mutat,** v. 33, n. 8, p. 1192-200, Aug 2012. ISSN 1059-7794.

LEE, J. et al. Designed nucleases for targeted genome editing. **Plant Biotechnol J,** v. 14, n. 2, p. 448-62, Feb 2016. ISSN 1467-7644.

LEIGH, D. Subacute necrotizing encephalomyelopathy in an infant. **Biochem. J. Neurol. Neurosurg. Psychiat.,** v. 14, p. 216-221, // 1951.

_____. SUBACUTE NECROTIZING ENCEPHALOMYELOPATHY IN AN INFANT. **Journal of Neurology, Neurosurgery, and Psychiatry,** v. 14, n. 3, p. 216-221, 1951. ISSN 0022-3050

1468-330X. Disponível em: < http://www.ncbi.nlm.nih.gov/pmc/articles/PMC499520/ >.

LIN, A. L. et al. Decreased in vitro mitochondrial function is associated with enhanced brain metabolism, blood flow, and memory in Surf1-deficient mice. **J Cereb Blood Flow Metab,** v. 33, n. 10, p. 1605-11, Oct 2013. ISSN 0271-678x.

LIN, B. et al. Theta stimulation polymerizes actin in dendritic spines of hippocampus. **J Neurosci,** v. 25, n. 8, p. 2062-9, Feb 23 2005. ISSN 0270-6474.

LIND, N. M. et al. The use of pigs in neuroscience: Modeling brain disorders. **Neuroscience & Biobehavioral Reviews,** v. 31, n. 5, p. 728-751, // 2007. ISSN 0149-7634. Disponível em: < http://www.sciencedirect.com/science/article/pii/S014976340700019X >.

LOI, P. et al. A New, Dynamic Era for Somatic Cell Nuclear Transfer? **Trends Biotechnol,** v. 34, n. 10, p. 791-7, Oct 2016. ISSN 0167-7799.

LOMAX, M. I. et al. Differential expression of nuclear genes for cytochrome c oxidase during myogenesis. **Muscle Nerve,** v. 13, n. 4, p. 330-7, Apr 1990. ISSN 0148-639X (Print)

0148-639x.

MATTHEWS, P. M. et al. Molecular genetic characterization of an X-linked form of Leigh's syndrome. **Ann Neurol,** v. 33, n. 6, p. 652-5, Jun 1993. ISSN 0364-5134 (Print)

0364-5134.

MCKENZIE, M.; TROUNCE, I. Expression of Rattus norvegicus mtDNA in Mus musculus cells results in multiple respiratory chain defects. **J Biol Chem,** v. 275, n. 40, p. 31514-9, Oct 06 2000. ISSN 0021-9258 (Print)

0021-9258.

MINAI, L. et al. Mitochondrial respiratory chain complex assembly and function during human fetal development. **Mol Genet Metab,** v. 94, n. 1, p. 120-6, May 2008. ISSN 1096-7192.

NICHOL, R. et al. Concentrations of energy substrates in oviductal fluid and blood plasma of pigs during the peri-ovulatory period. **J Reprod Fertil,** v. 96, n. 2, p. 699-707, Nov 1992. ISSN 0022-4251 (Print)

0022-4251.

_____. Concentrations of energy substrates in oviduct fluid in unilaterally ovariectomised pigs. **Res Vet Sci,** v. 65, n. 3, p. 263-4, Nov-Dec 1998. ISSN 0034-5288 (Print)

0034-5288.

NIJTMANS, L. G.; HENDERSON, N. S.; HOLT, I. J. Blue Native electrophoresis to study mitochondrial and other protein complexes. **Methods,** v. 26, n. 4, p. 327-34, Apr 2002. ISSN 1046-2023 (Print)

1046-2023.

OZIL, J. P.; HUNEAU, D. Activation of rabbit oocytes: the impact of the Ca2+ signal regime on development. **Development,** v. 128, n. 6, p. 917-28, Mar 2001. ISSN 0950-1991 (Print)

0950-1991.

OZIL, J. P. et al. Egg activation events are regulated by the duration of a sustained [Ca2+]cyt signal in the mouse. **Dev Biol,** v. 282, n. 1, p. 39-54, Jun 01 2005. ISSN 0012-1606 (Print)

0012-1606.

P. MAKOVICKÝ et al. MORPHOMETRICAL AND HISTOCHEMICAL STUDY OF THE CROSS

STRIATED SKELETAL MUSCLES OF PIGS. **Slovak Journal of Animal Science,** v. 42, n. 9, p. 174-179, 2009. ISSN 1337-9984.

POYAU, A. et al. Missense mutations in SURF1 associated with deficient cytochrome c oxidase assembly in Leigh syndrome patients. **Hum Genet,** v. 106, n. 2, p. 194-205, Feb 2000. ISSN 0340-6717 (Print)

0340-6717.

PULLIAM, D. A. et al. Complex IV-deficient Surf1(-/-) mice initiate mitochondrial stress responses. **Biochem J,** v. 462, n. 2, p. 359-71, Sep 1 2014. ISSN 0264-6021.

RAHMAN, S. et al. Leigh syndrome: clinical features and biochemical and DNA abnormalities. **Ann Neurol,** v. 39, n. 3, p. 343-51, Mar 1996. ISSN 0364-5134 (Print)

0364-5134.

_____. A SURF1 gene mutation presenting as isolated leukodystrophy. **Ann Neurol,** v. 49, n. 6, p. 797-800, Jun 2001. ISSN 0364-5134 (Print)

0364-5134.

ROCHA, L. M. et al. Hand-held lactate analyzer as a tool for the real-time measurement of physical fatigue before slaughter and pork quality prediction. **Animal,** v. 9, n. 4, p. 707-14, Apr 2015. ISSN 1751-7311.

ROUET, P.; SMIH, F.; JASIN, M. Introduction of double-strand breaks into the genome of mouse cells by expression of a rare-cutting endonuclease. **Mol Cell Biol,** v. 14, n. 12, p. 8096-106, Dec 1994. ISSN 0270-7306 (Print)

0270-7306.

RUDIN, N.; HABER, J. E. Efficient repair of HO-induced chromosomal breaks in Saccharomyces cerevisiae by recombination between flanking homologous sequences. **Mol Cell Biol,** v. 8, n. 9, p. 3918-28, Sep 1988. ISSN 0270-7306 (Print)

0270-7306.

SACCONI, S. et al. Mutation screening in patients with isolated cytochrome c oxidase deficiency. **Pediatr Res,** v. 53, n. 2, p. 224-30, Feb 2003. ISSN 0031-3998 (Print)

0031-3998.

SAMBROOK, J.; FRITSCH, E. F.; MANIATIS, T. **Molecular cloning**. Cold spring harbor laboratory press New York, 1989.

SANTORO, L. et al. A novel SURF1 mutation results in Leigh syndrome with peripheral neuropathy caused by cytochrome c oxidase deficiency. **Neuromuscul Disord,** v. 10, n. 6, p. 450-3, Aug 2000. ISSN 0960-8966 (Print)

0960-8966.

SCHWARTZ, M.; VISSING, J. Paternal inheritance of mitochondrial DNA. **N Engl J Med,** v. 347, n. 8, p. 576-80, Aug 22 2002. ISSN 0028-4793.

SCIACCO, M.; BONILLA, E. Cytochemistry and immunocytochemistry of mitochondria in tissue sections. **Methods Enzymol,** v. 264, p. 509-21, 1996. ISSN 0076-6879 (Print)

0076-6879.

SKRZYPEK, T. et al. Intestinal villi structure during the development of pig and wild boar crossbreed neonates. **Livestock Science,** v. 109, n. 1, p. 38-41, 2007. ISSN 1871-1413. Disponível em: < http://dx.doi.org/10.1016/j.livsci.2007.01.040 >. Acesso em: 2017/03/09.

SMEITINK, J.; VAN DEN HEUVEL, L.; DIMAURO, S. The genetics and pathology of oxidative phosphorylation. **Nat Rev Genet,** v. 2, n. 5, p. 342-352, 05//print 2001. ISSN 1471-0056. Disponível em: < http://dx.doi.org/10.1038/35072063 >.

ST JOHN, J. C.; MOFFATT, O.; D'SOUZA, N. Aberrant heteroplasmic transmission of mtDNA in cloned pigs arising from double nuclear transfer. **Mol Reprod Dev,** v. 72, n. 4, p. 450-60, Dec 2005. ISSN 1040-452X (Print)

1040-452x.

STEVENSON, J. S.; DAVIS, D. L. Estrous synchronization and fertility in gilts after 14- or 18-day feeding of altrenogest beginning at estrus or diestrus. **J Anim Sci,** v. 55, n. 1, p. 119-23, Jul 1982. ISSN 0021-8812 (Print)

0021-8812.

SUTOVSKY, P. et al. Ubiquitin tag for sperm mitochondria. **Nature,** v. 402, n. 6760, p. 371-2, Nov 25 1999. ISSN 0028-0836 (Print)

0028-0836.

_____. Degradation of paternal mitochondria after fertilization: implications for heteroplasmy, assisted reproductive technologies and mtDNA inheritance. **Reprod Biomed Online,** v. 8, n. 1, p. 24-33, Jan 2004. ISSN 1472-6483 (Print)

1472-6483.

SUTOVSKY PETER, P. D. **Somatic Cell Nuclear Transfer**. Springer New York, 2007. 135 ISBN 978-0-387-37753-7.

SWINDLE, M. M. et al. Swine as Models in Biomedical Research and Toxicology Testing. **Veterinary Pathology Online,** v. 49, n. 2, p. 344-356, March 1, 2012 2012. Disponível em: < http://vet.sagepub.com/content/49/2/344.abstract >.

SWINDLE, M. M.; SMITH, A. C. **Swine in the Laboratory: Surgery, Anesthesia, Imaging, and Experimental Techniques**. Third Edition. CRC Press, 2015. ISBN ISBN 9781466553477.

_____. **Swine in the Laboratory: Surgery, Anesthesia, Imaging, and Experimental Techniques, Third Edition**. Third edition. 2015. ISBN 9781466553477.

TAKATA, M. et al. Homologous recombination and non-homologous end-joining pathways of DNA double-strand break repair have overlapping roles in the maintenance of chromosomal integrity in vertebrate cells. **Embo j,** v. 17, n. 18, p. 5497-508, Sep 15 1998. ISSN 0261-4189 (Print)

0261-4189.

TAKEDA, K. et al. Transmission of mitochondrial DNA in pigs and progeny derived from nuclear transfer of Meishan pig fibroblast cells. **Mol Reprod Dev,** v. 73, n. 3, p. 306-12, Mar 2006. ISSN 1040-452X (Print)

1040-452x.

TAY, S. K. H. et al. Unusual Clinical Presentations in Four Cases of Leigh Disease, Cytochrome C Oxidase Deficiency, and SURF1 Gene Mutations. **Journal of Child Neurology,** v. 20, n. 8, p. 670-674, 2005. Disponível em: < http://jcn.sagepub.com/content/20/8/670.abstract >.

TERVIT, H. R.; WHITTINGHAM, D. G.; ROWSON, L. E. Successful culture in vitro of sheep and cattle ova. **J Reprod Fertil,** v. 30, n. 3, p. 493-7, Sep 1972. ISSN 0022-4251 (Print)

0022-4251.

TIRANTI, V. et al. Loss-of-function mutations of SURF-1 are specifically associated with Leigh syndrome with cytochrome c oxidase deficiency. **Annals of Neurology,** v. 46, n. 2, p. 161-166, 1999. ISSN 1531-8249. Disponível em: < http://dx.doi.org/10.1002/1531-8249(199908)46:2<161::AID-ANA4>3.0.CO >.

_____. Nuclear DNA origin of cytochrome c oxidase deficiency in Leigh's syndrome: genetic evidence based on patient's-derived rho degrees transformants. **Hum Mol Genet,** v. 4, n. 11, p. 2017-23, Nov 1995. ISSN 0964-6906 (Print)

0964-6906.

TOPCU, M. et al. Leigh syndrome in a 3-year-old boy with unusual brain MR imaging and pathologic findings. **AJNR Am J Neuroradiol,** v. 21, n. 1, p. 224-7, Jan 2000. ISSN 0195-6108 (Print)

0195-6108.

VAJTA, G. et al. New method for culture of zona-included or zona-free embryos: the Well of the Well (WOW) system. **Mol Reprod Dev,** v. 55, n. 3, p. 256-64, Mar 2000. ISSN 1040-452X (Print)

1040-452x.

VAJTA, G.; RIENZI, L.; BAVISTER, B. D. Zona-free embryo culture: is it a viable option to improve pregnancy rates? **Reprod Biomed Online,** v. 21, n. 1, p. 17-25, Jul 2010. ISSN 1472-6483.

VON KLEIST-RETZOW, J. C. et al. Mutations in SURF1 are not specifically associated with Leigh syndrome. **J Med Genet,** v. 38, n. 2, p. 109-13, Feb 2001. ISSN 0022-2593.

WEKSBERG, R. et al. Beckwith-Wiedemann syndrome demonstrates a role for epigenetic control of normal development. **Hum Mol Genet,** v. 12 Spec No 1, p. R61-8, Apr 01 2003. ISSN 0964-6906 (Print)

0964-6906.

WEST, J.; GILL, W. W. Genome Editing in Large Animals. **Journal of Equine Veterinary Science,** v. 41, p. 1-6, 2016. ISSN 0737-0806. Disponível em: < http://dx.doi.org/10.1016/j.jevs.2016.03.008 >. Acesso em: 2016/10/14.

WIGMORE, P. M.; STICKLAND, N. C. Muscle development in large and small pig fetuses. **J Anat,** v. 137 (Pt 2), p. 235-45, Sep 1983. ISSN 0021-8782 (Print)

0021-8782.

WILMUT, I. et al. Viable offspring derived from fetal and adult mammalian cells. **Nature,** v. 385, n. 6619, p. 810-3, Feb 27 1997. ISSN 0028-0836 (Print)

0028-0836.

WOOD, C. M.; KORNEGAY, E. T.; SHIPLEY, C. F. Efficacy of altrenogest in synchronizing estrus in two swine breeding programs and effects on subsequent reproductive performance of sows. **J Anim Sci,** v. 70, n. 5, p. 1357-64, May 1992. ISSN 0021-8812 (Print)

0021-8812.

YAO, J.; SHOUBRIDGE, E. A. Expression and functional analysis of SURF1 in Leigh syndrome patients with cytochrome c oxidase deficiency. **Hum Mol Genet,** v. 8, n. 13, p. 2541-9, Dec 1999. ISSN 0964-6906 (Print)

0964-6906.

YOSHIOKA, K.; SUZUKI, C.; ONISHI, A. Defined system for in vitro production of porcine embryos using a single basic medium. **J Reprod Dev,** v. 54, n. 3, p. 208-13, Jun 2008. ISSN 0916-8818 (Print)

0916-8818.

YOUNG, L. E.; SINCLAIR, K. D.; WILMUT, I. Large offspring syndrome in cattle and sheep. **Rev Reprod,** v. 3, n. 3, p. 155-63, Sep 1998. ISSN 1359-6004 (Print)

1359-6004.

ZEVIANI, M.; BERTAGNOLIO, B.; UZIEL, G. Neurological presentations of mitochondrial diseases. **Journal of Inherited Metabolic Disease,** v. 19, n. 4, p. 504-520, 1996// 1996. ISSN 1573-2665. Disponível em: < http://dx.doi.org/10.1007/BF01799111 >.

ZHONG, Z. et al. Analysis of Heterogeneous Mitochondria Distribution in Somatic Cell Nuclear Transfer Porcine Embryos. **Microscopy and Microanalysis**, New York, USA**,** v. 14, n. 5, p. 418-432, 2008/10/001 2008. Disponível em: < https://www.cambridge.org/core/article/div-class-title-analysis-of-heterogeneous-mitochondria-distribution-in-somatic-cell-nuclear-transfer-porcine-embryos-div/2680E7DDA6A141080775857D33689F58 >.

ZORDAN, M. A. et al. Post-transcriptional silencing and functional characterization of the Drosophila melanogaster homolog of human Surf1. **Genetics,** v. 172, n. 1, p. 229-41, Jan 2006. ISSN 0016-6731 (Print)

0016-6731.

ZSURKA, G. et al. Recombination of mitochondrial DNA in skeletal muscle of individuals with multiple mitochondrial DNA heteroplasmy. **Nat Genet,** v. 37, n. 8, p. 873-7, Aug 2005. ISSN 1061-4036 (Print)

1061-4036.